

# **Metal Surface area**

**Dr.K.R.Krishnamurthy**

**NCCR,IITM, Chennai**

**February-2017**

# Types of Catalysts

Type	Examples	Applications
Supported metal catalysts	Pt/Al <sub>2</sub> O <sub>3</sub> , Pd/Al <sub>2</sub> O <sub>3</sub> Ni/Al <sub>2</sub> O <sub>3</sub> Fe/Co	Dehydrogenation Hydrogenation Oxidation, FTS
Metal oxide /sulfide/ chloride catalysts	V <sub>2</sub> O <sub>5</sub> , Ag/Al <sub>2</sub> O <sub>3</sub> Bi-Mo Oxide Co-Mo/Al <sub>2</sub> O <sub>3</sub> CuCl <sub>2</sub> -KCl/Al <sub>2</sub> O <sub>3</sub>	Oxidation, Epoxidation Ammonoxidation HDS, HDN, HDC Oxychlorination
Zeolite catalysts	Zeolite Y, REY, USY, ZSM-5 Mordenite	FCC, MTG, MTO, Alkylation, Aromatization Isomerization



Wide Spectrum of Applications

# Catalysts- Characteristics

- **Chemical composition**
- **Phase composition, Crystalline/Amorphous**
- **Structural features, Phase transformations**
- **Surface composition, Co-ordination, Structure**
- **Dispersion& distribution of active phases**
- **Electronic properties**
- **Textural properties-Surface area, Pore-size**
- **Physical properties-Size, Shape, Strength**
- **Chemical properties- Surface reactivity/Acidity**

**Enabling Structure-Activity correlations**

# Catalysis & Analytical Chemistry

<b>Preparation</b>	<b>Characterization</b>	<b>Evaluation</b>	<b>Ageing</b>	<b>Spent</b>
Concn. of active elements	Phase composition	In-situ Spectroscopy	Solid state transformations	Inactive phases
Species in Solution phase	Electronic state	Transient surface species	Structural transformations	Poisons
Solid state transformations	Structural features	Reactants & Products	Surface composition	Analysis of coke
Preparation techniques	Dispersion & Distribution	Kinetics & mechanism		
	Surface composition			
<b><i>Evolve active phase</i></b>	<b><i>Ensure desired characteristics</i></b>	<b><i>Surface reactions</i></b>	<b><i>Catalyst life</i></b>	<b><i>Deactivation</i></b>

Application of Analytical Techniques- **From Cradle to Coffin**



# Supported metal catalysts

## Characteristics

- Metal dispersion/Crystallite size (XRD, XPS)
- Metals distribution / Profile ( EDXA)
- Metal support interactions ( XPS)
- Metal-Promoter interactions (XPS)
- Nature of coke deposits ( HPLC, TGA, NMR)

# Metal surface area

- What do we mean by metal surface area ?
- How it is related to catalytic activity?
- How do we measure metal surface area?

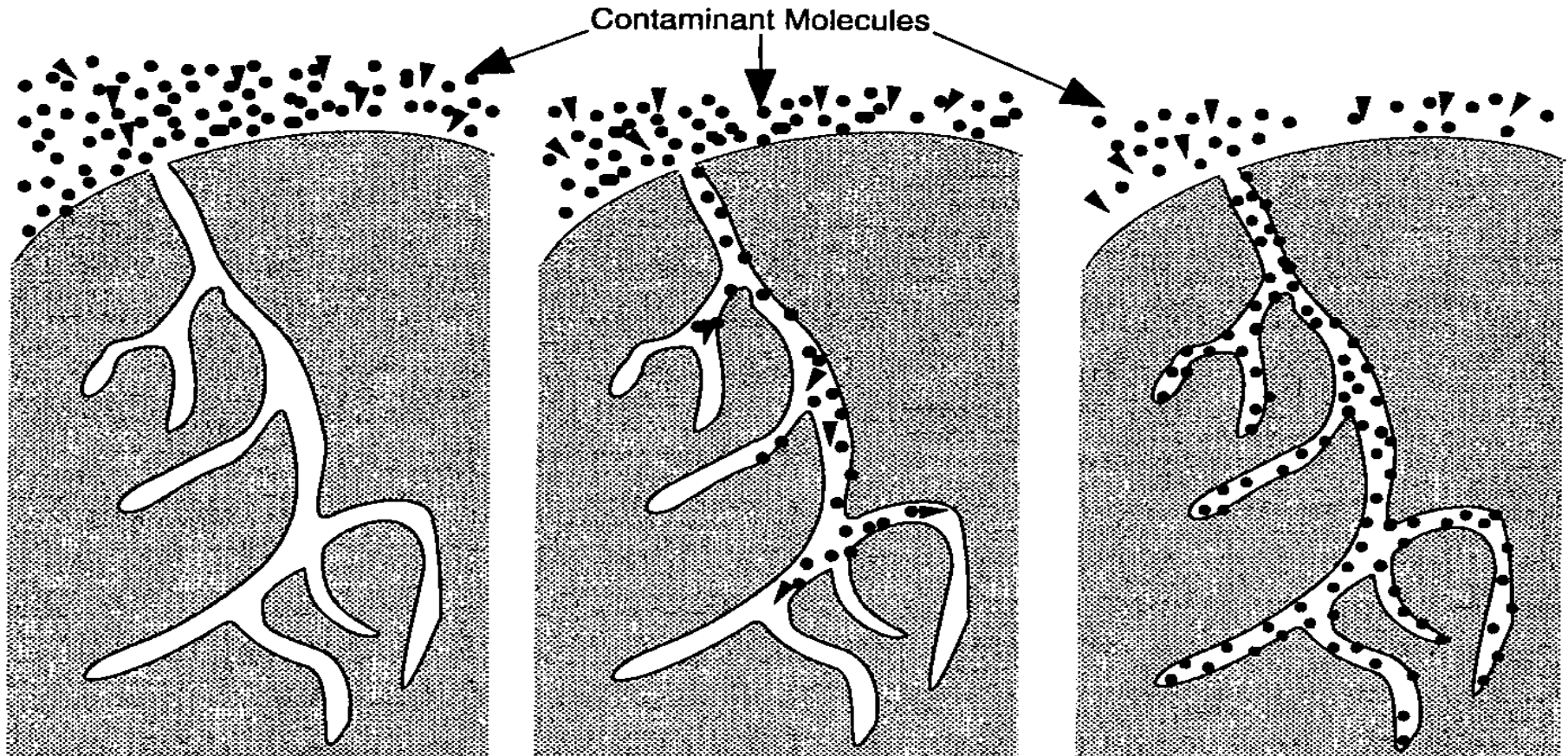


# Adsorption Mechanism

Step 1: Diffusion to Adsorbent Surface

Step 2: Migration into Pores of Adsorbent

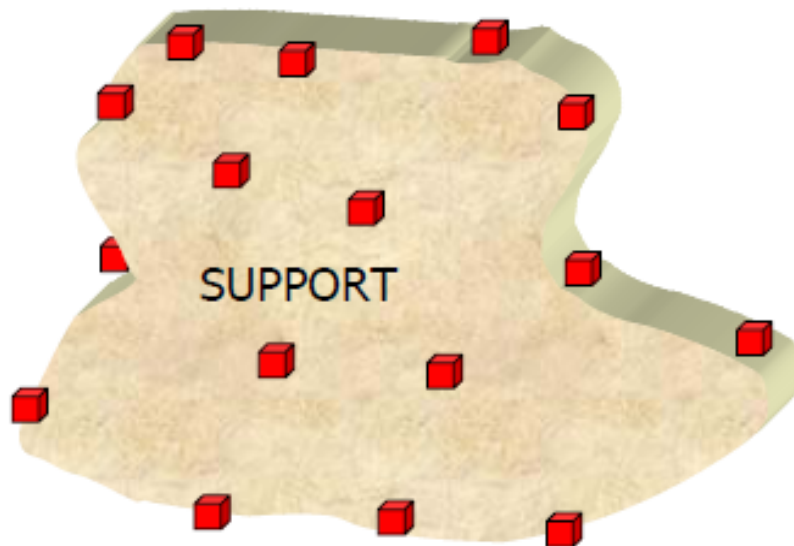
Step 3: Monolayer Buildup of Adsorbate



The above adsorption process represents the diffusion of metal salt/impregnation solution into the pores of the support

## Supports

- ❖ High surface area oxidic compounds: zeolites,  $\text{SiO}_2$ ,  $\text{Al}_2\text{O}_3$ ,  $\text{TiO}_2$ ,  $\text{ZrO}_2$ ,  $\text{CeO}_2$ ,  $\text{ZnO}$
- ❖ Carbon materials



## Dispersed phase

- ❖ Increased surface area
- ❖ Stabilized

- ❖ Goal: disperse an *active phase* on an inexpensive and inert (?) *support*

*Area occupied by metal crystallites is responsible for activity*

# Metal Crystallites - Features

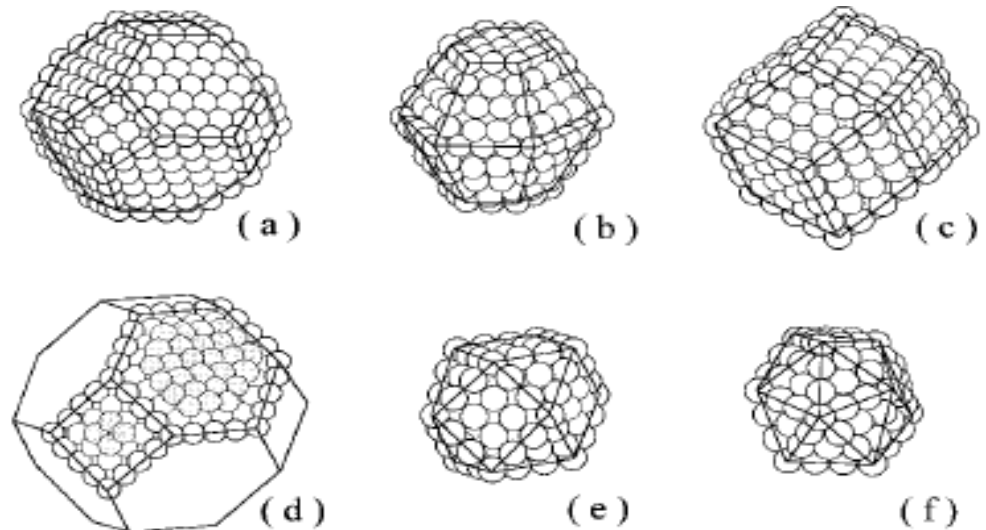
- **Crystal-** Specific arrangement of atoms/ions as per stoichiometry  
Long range order-fcc,bcc,hexagonal-Specific geometry, morphology, shape
- **Particles** – Primary/Secondary- Particle size- Measurement methods-  
Support particle size- Std. Test Sieves- Instrumental methods-Sedimentation
- **Crystallite-** Cluster of metal atoms- No stoichiometry-Specific shape – related to bulk metal structure, short range order, varying size & co-ordination No.-  
higher degree of co-ordinative unsaturation- active sites

- **Crystallite size control**

- Preparation methods
- Nature of support
- Metal loading
- Metal precursor

- **Parameters**

- Crystallite size-  $d$ - nm
- Metal area  $S$ - $m^2/g$
- Dispersion %  $D$



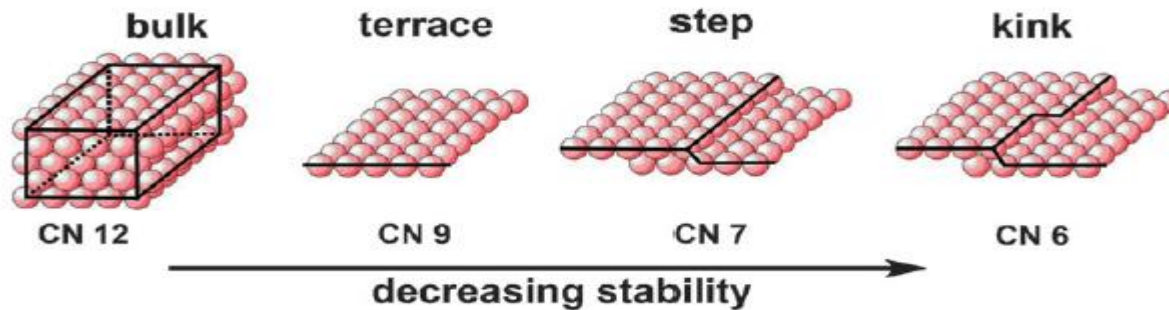
**Figure 2.** Types of crystallites considered in Figure 1: (a) VH cubooctahedron; (b) VH hcp truncated bipyramid; (c) VH bcc rhombic dodecahedron; (d) VH cubooctahedron max-B5; (e) MM cubooctahedron; and (f) MM icosahedron.



# Active sites on the surface

## Supported metal catalysts-guiding principles

Pt metal-Bulk Crystal-Crystal planes- Surface structure--active sites



- Bonding/Reactivity of reactants on terrace/step/kink sites is determined by the co-ordination numbers/co-ordinative unsaturation
- For cyclic hydrocarbon reactant
- C-H bond activation - step sites- Dehydrogenated product
- C-C- bond activation - kink sites- Ring opening

*Active phase composition-Structure-Size-Shape*  
*Surface structure-Selectivity*

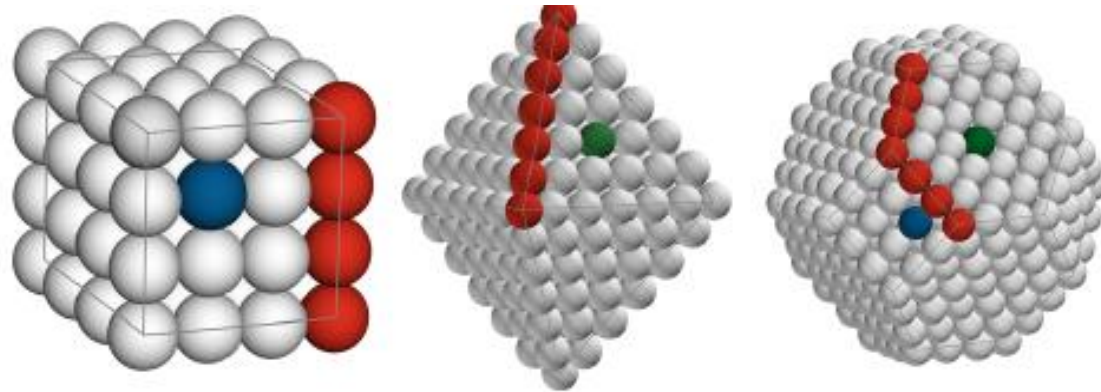
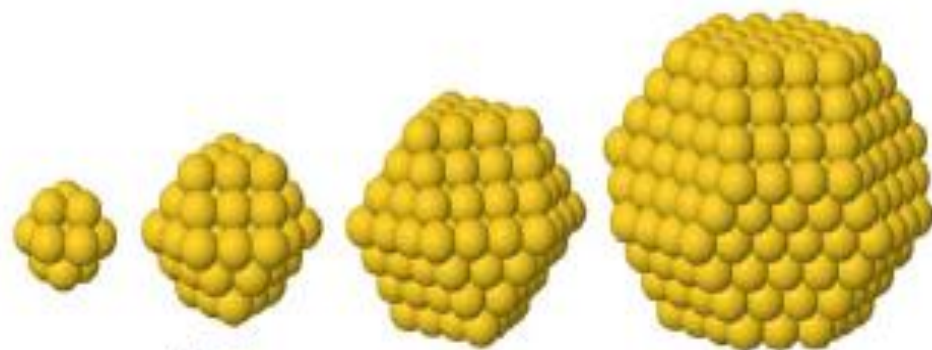


Figure 2.1: Schematic representation of the surface atoms found on three common *fcc* crystallites. ● low coordination number atoms, such as corner and edge atoms, ● (111) plane atoms and ● (100) plane atoms.



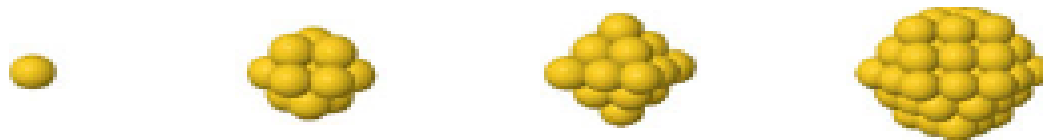


$N_S=12$   
 $N_T=13$   
 $d=0.86$  nm

$N_S=42$   
 $N_T=55$   
 $d=1.44$  nm

$N_S=92$   
 $N_T=147$   
 $d=2.02$  nm

$N_S=146$   
 $N_T=405$   
 $d=2.67$  nm



**1 atom**  
 $d=0.288$  nm

**13 atoms**  
 $d=0.86$  nm

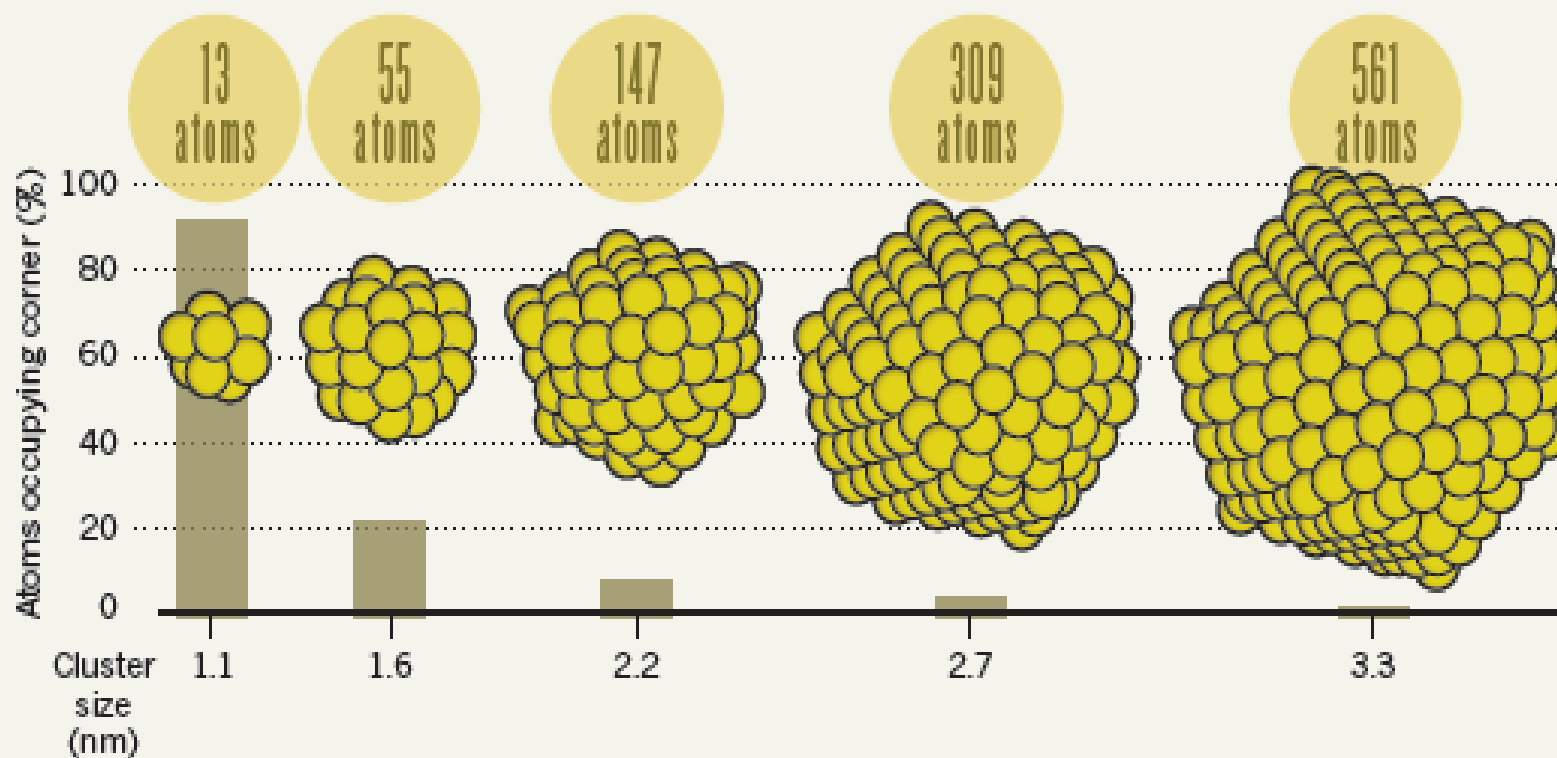
**19 atoms**  
 $d=1.10$  nm

**55 atoms**  
 $d=1.44$  nm

		Fractions of Surface Atoms ( $N_S$ ) that have low Coordination numbers (CN) situated at:					
$N_T$	$N_S$	Corners			Edges	Terraces	
		CN=4	CN=5	CN=6	CN=7	CN=8	CN=9
13	12	-	1.00	-	-	-	-
19	18	0.33	-	0.67	-	-	-
55	42	-	0.29	-	0.57	0.14	-
79	60	-	-	0.40	0.20	-	0.40



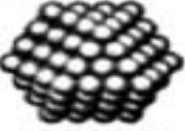

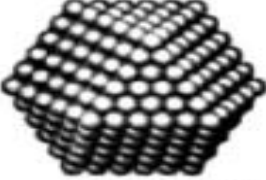
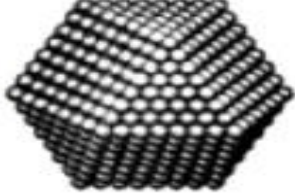
## CORNER CATALYSIS

Gold atoms sitting at the corners of catalyst particles are most able to participate in a chemical reaction. So using smaller clusters of gold atoms can maximize the number of these active atoms.



# Total Vs Exposed metal atoms

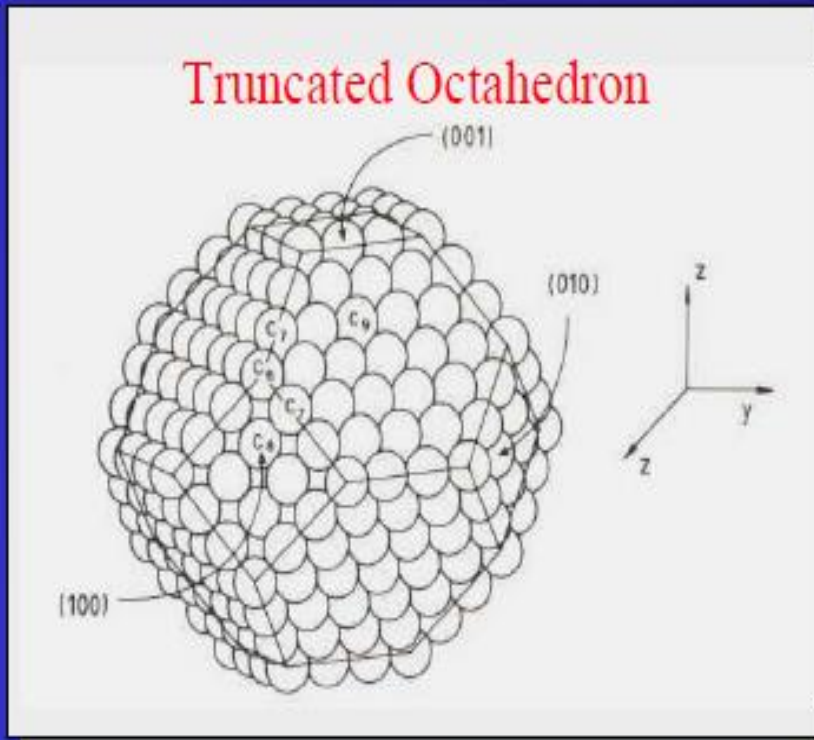
The relation between the total number of atoms in full shell clusters and the percentage of surface atoms (reprinted from [5] with permission from John Wiley & Sons)

Full shell clusters	Total number of atoms	Surface atoms (%)
One shell 	13	92
Two shells 	55	76
Three shells 	147	63
Four shells 	309	52
Five shells 	561	45
Seven shells 	1415	35

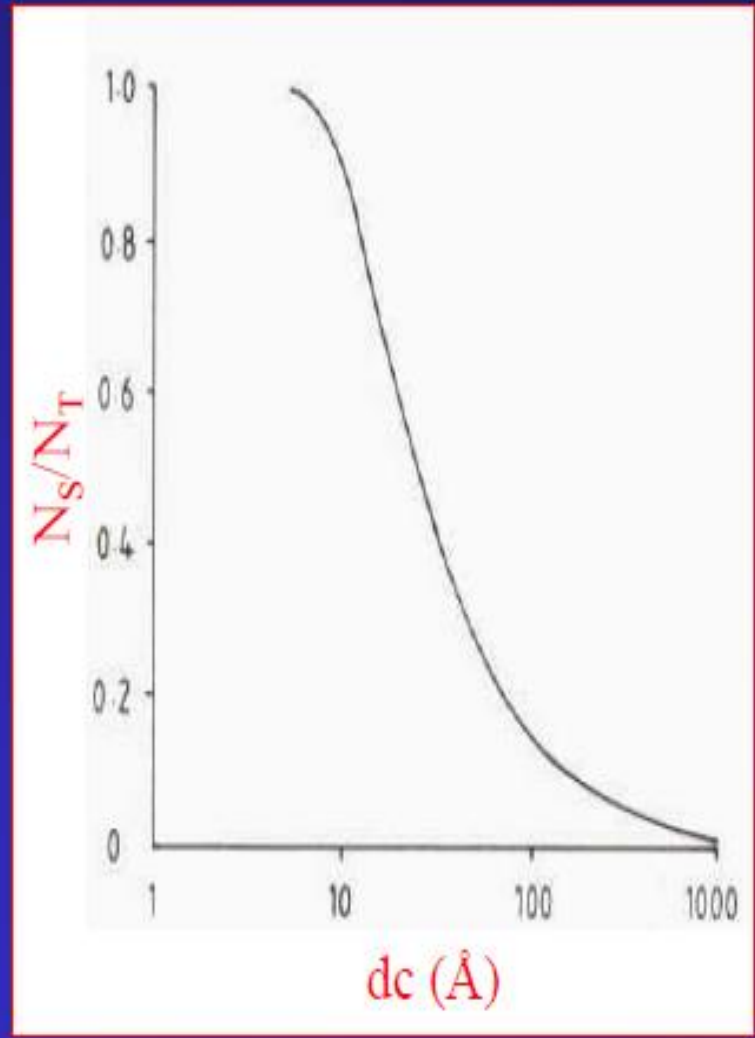
Aiken, J. D., III; Finke, R. G. *Journal of Molecular Catalysis A: Chemical* **1999**, *145*, 1-44.

***Dispersion decreases as crystallite size increases***

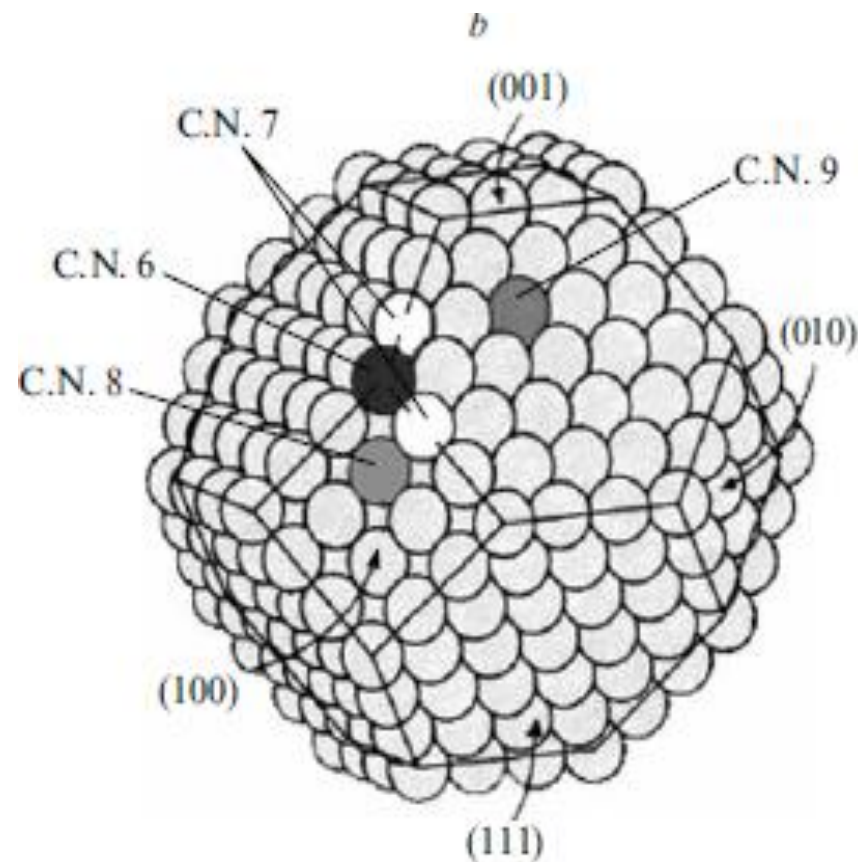
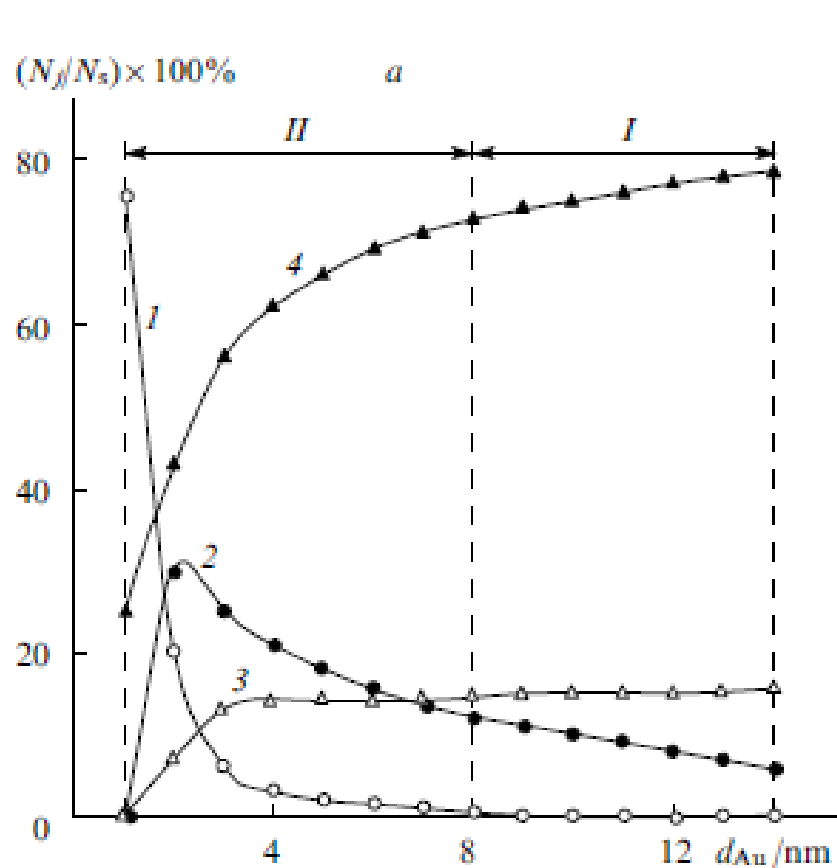
# Crystallite geometry, dispersion & co-ordination number



Crystal size  $\downarrow$  then  $N_S/N_T \uparrow$



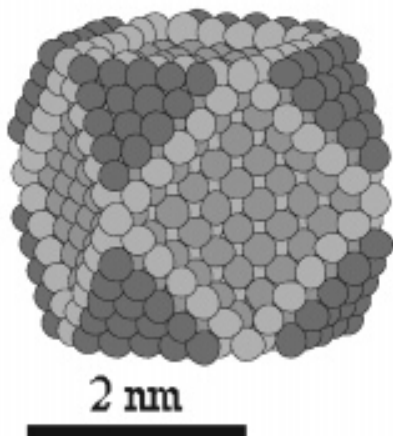
**Lower co-ordination number- higher unsaturation -Higher activity**



**Figure 7.** Relative concentrations of gold surface atoms  $N_j/N_s$  with coordination numbers of 6 (curve 1), 7 (curve 2), 8 (curve 3) and 9 (curve 4) vs. the diameter of gold nanoparticles  $d(Au)$  [(a) data of C Mohr, P Claus. *Sci. Progr.* **84** 311 (2001)]; the equilibrium cuboctahedral shape for Au particles was used in calculations (b) from Ref. 124).

$N_j$  is the number of atoms with C.N. of  $j$ ,  $N_s$  is the number of surface atoms.

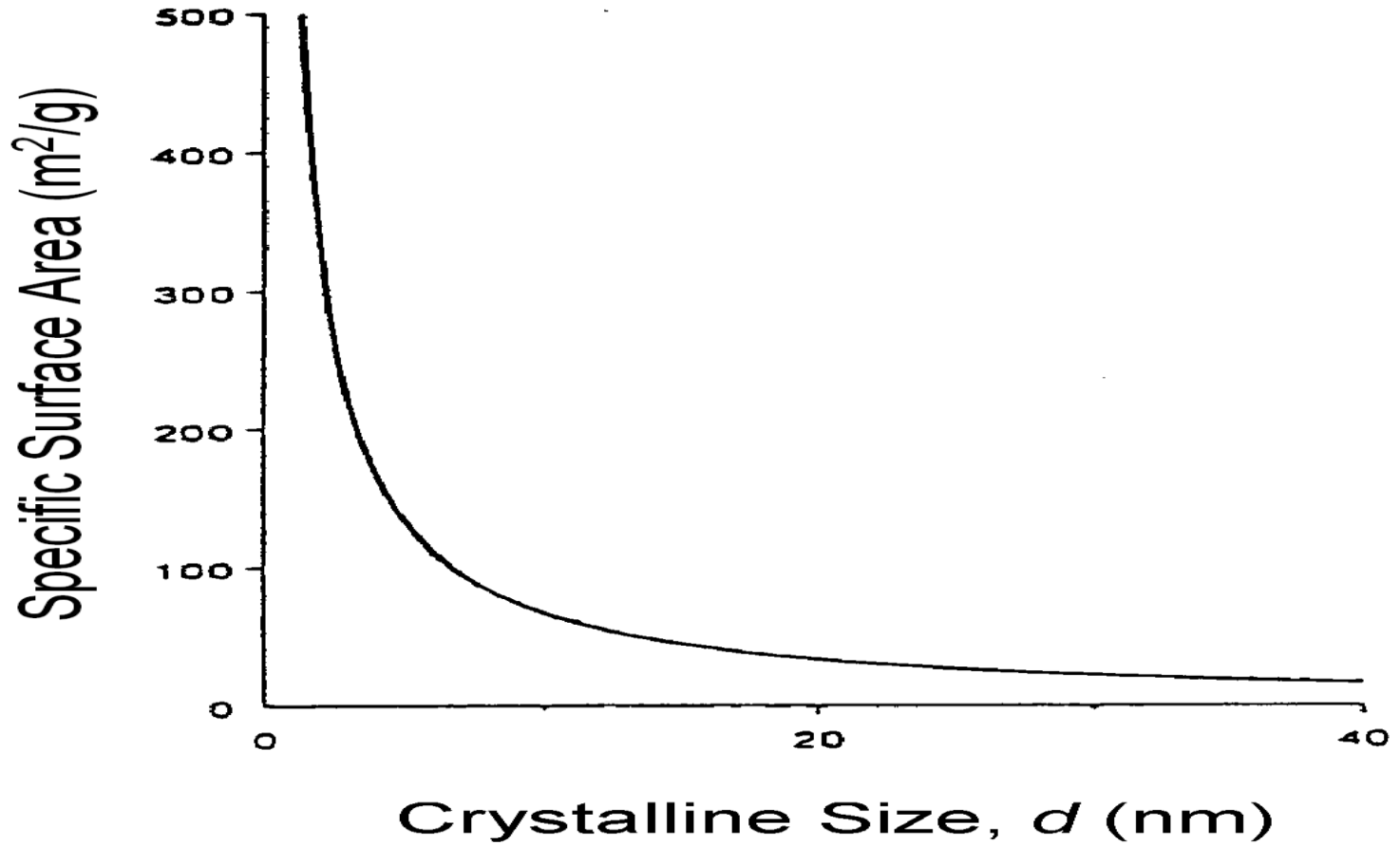
# Crystallite size data for Au/TiO<sub>2</sub>- Illustration



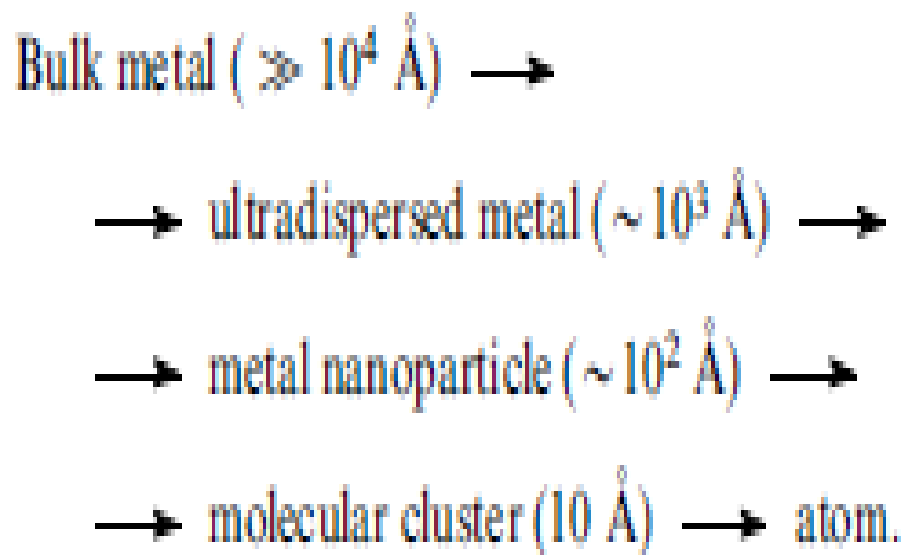
Crystallite size 3.41 nm  
Total no of Au atoms 893  
No of atoms on surface 468 –(Exposed atoms)  
Co ordination number- 5.7,11  
% Dispersion- 468/893 - 52  
No.of exposed atoms = No.of active sites

Crys.size nm	Surf.area m <sup>2</sup> /g	CO Oxidn %
3.41	108.2	99
4.09	87.7	93
3.79	84.8	63
5.21	56.1	14
5.63	53.5	1

# Crystallite size Vs. Activity- Supported Ni catalyst



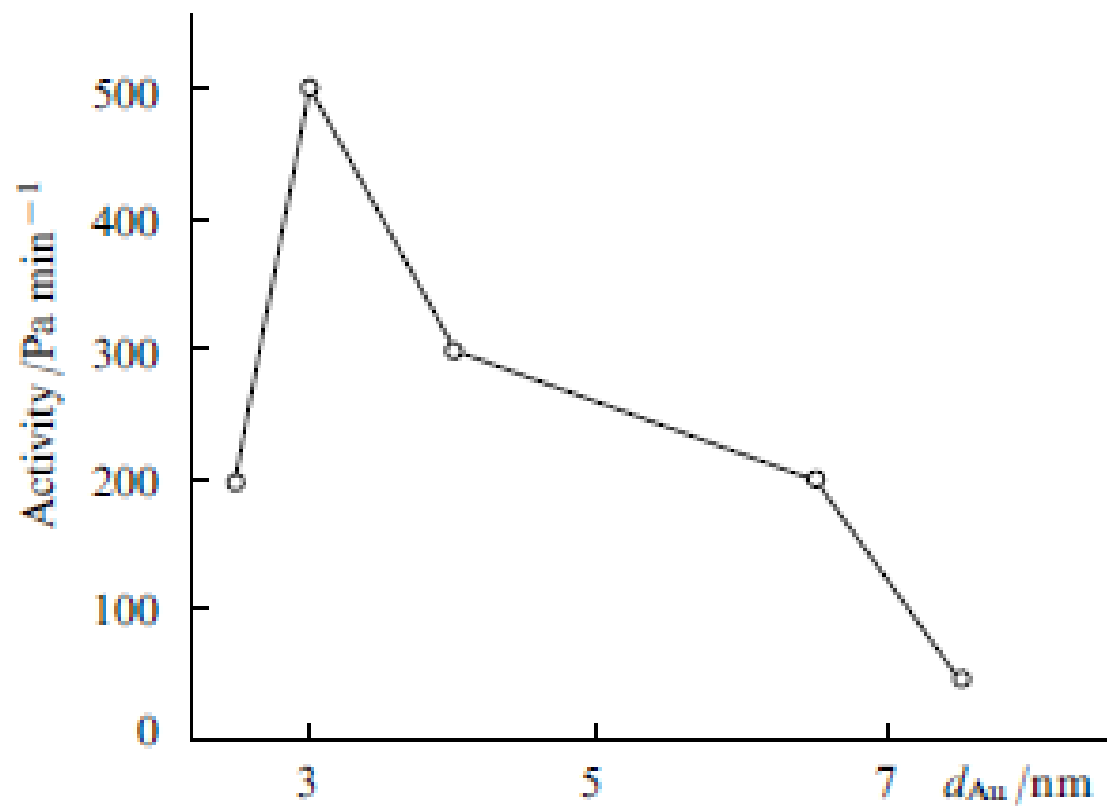
## Concept of size in metals



S A Nikolaev, L N Zhanavskii, V V Smirnov, V A Averyanov, K L Zhanavskii

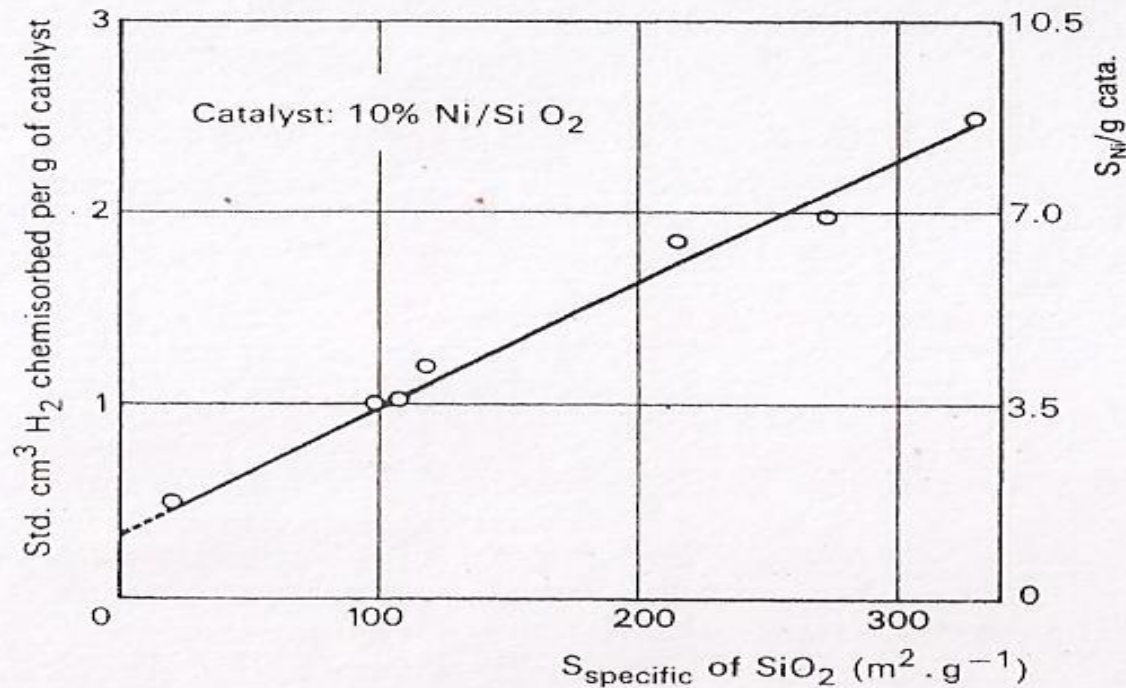
*Russian Chemical Reviews* **78** (3) 231–247 (2009)





**Figure 8.** Activity of gold nanoparticles in acetylene hydrogenation at 523 K vs. size of Au particles immobilized on alumina.<sup>152</sup>

# Support Surface Area Vs Dispersion



**FIG. 7.11** Influence of the support surface on the dispersion of the active agent (10% nickel on a silica support).

The supports are impregnated by a nickel nitrate solution with no excess. The impregnated catalysts are dried at 80° C, calcined at 500° C, and reduced. Tests plotted above show that the volume of hydrogen chemisorbed per gram of catalyst, i.e., the nickel surface accessible to the hydrogen, increases with the specific surface of the support. The plot suggests that the catalytic surface at zero support surface corresponds to the surface offered by solid nickel obtained from nitrate after the same treatments.

Rao, S., Cosyns, J., IFP unpublished results.

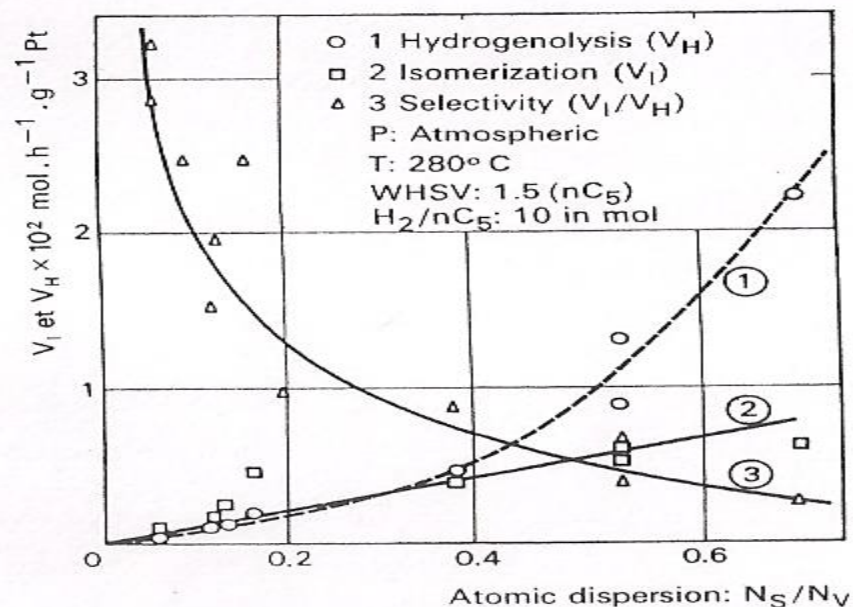


FIG. 7.12 Effects of atomic dispersion on activity and selectivity of platinum for the hydrogenolysis of *n*-pentane.

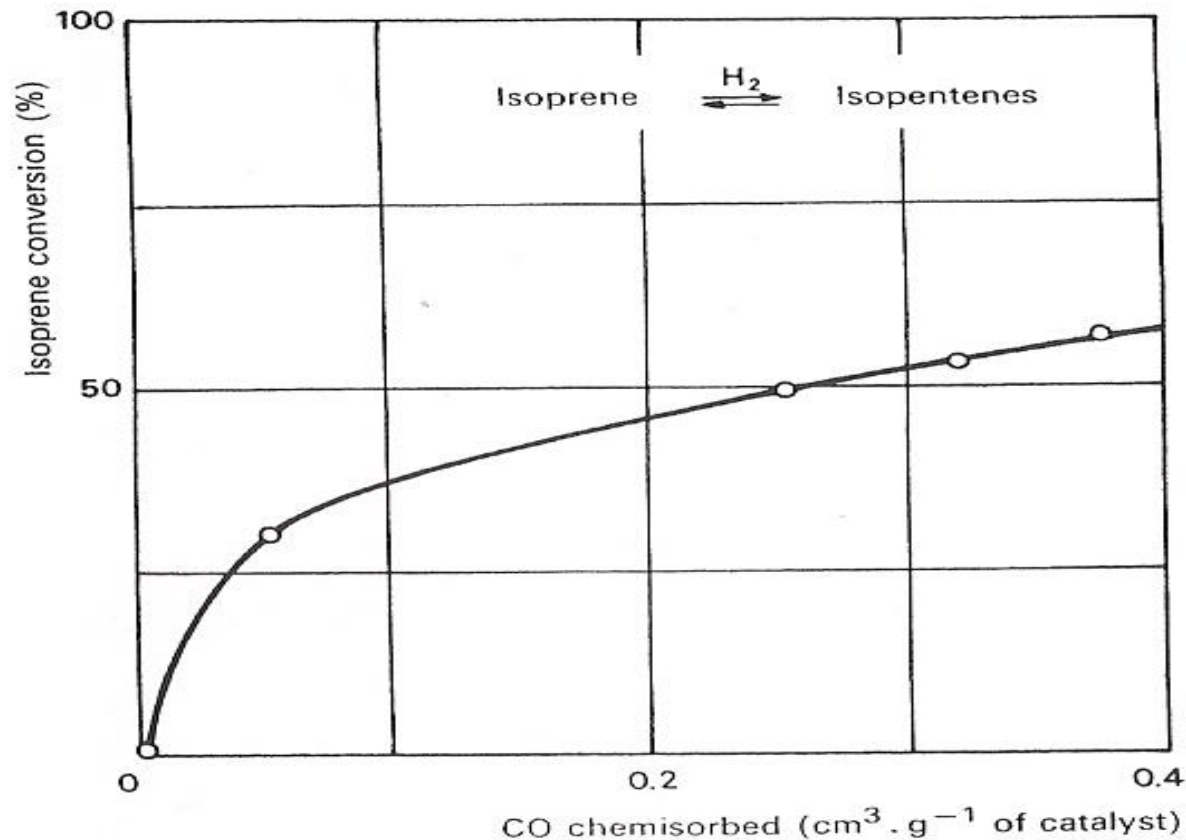
Normal pentane is treated with hydrogen in a differential fixed-bed reactor at low conversion rates, at the operating conditions shown in the figure, and the production of light products and isopentane is measured as indications of hydrogenolysis and isomerization respectively.

The rate of isomerization increases linearly with the dispersion of the metal, and the rate of hydrogenolysis increases much more rapidly. This can be interpreted by assuming the hydrogenolysis operates preferentially on atoms at the corners or edges of the crystallites, while the isomerization uses any of the surface atoms without discrimination:

$$\begin{aligned}
 V_I &= \text{rate of isomerization, mol} \cdot \text{h}^{-1} \cdot \text{g}^{-1} \text{Pt} \\
 V_H &= \text{rate of hydrogenolysis, mol} \cdot \text{h}^{-1} \cdot \text{g}^{-1} \text{Pt} \\
 V_I/V_H &= \text{selectivity} \\
 N_S/N_V &= \text{accessibility} = \text{atoms of surface/total atoms}
 \end{aligned}$$

$N_S$  is obtained from CO chemisorption by assuming an average stoichiometric ratio of (Pt atoms/molecule of CO) = 1.15 as valid for the range of aggregates studied in this example.

Brunelle, P., Sugier, A., Montarnal, R., *J. Catal.* Vol. 43 p. 273, 1976.



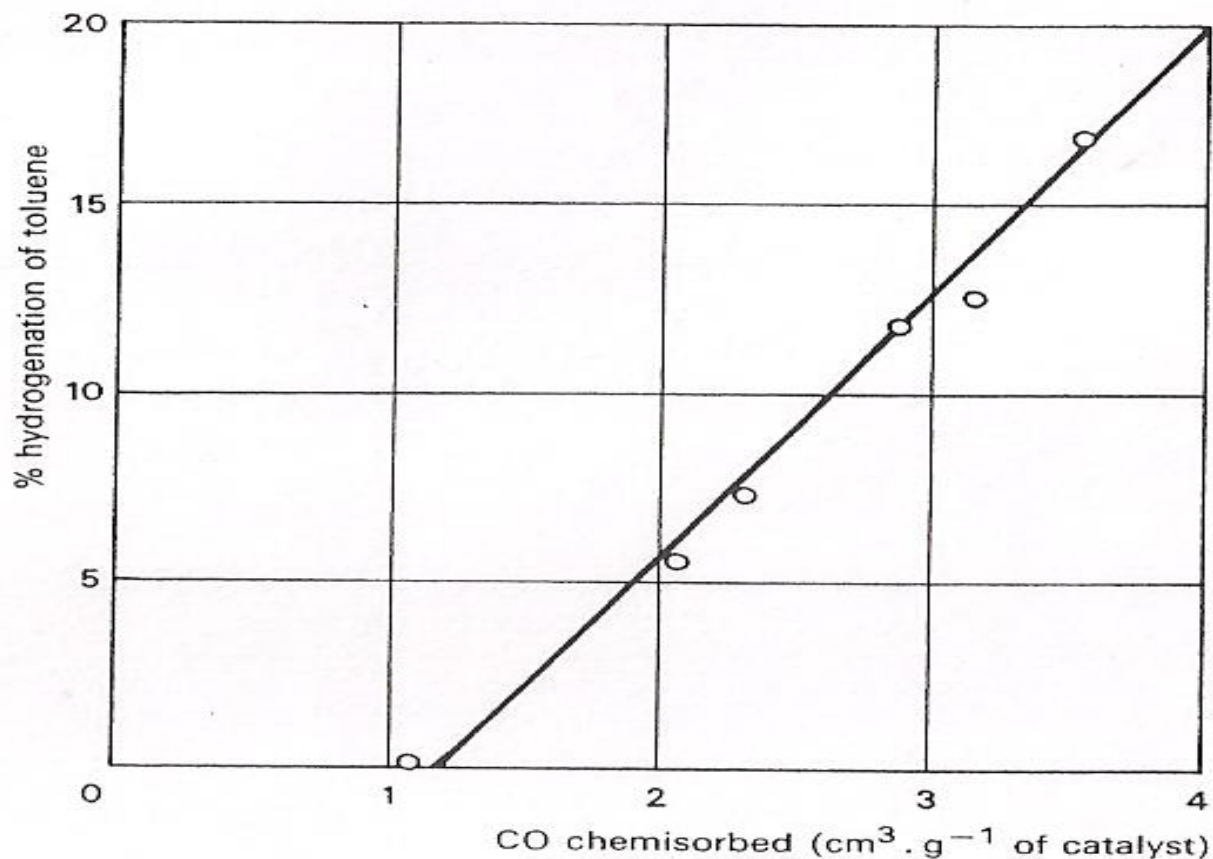
**FIG. 7.13** Effects of Pd dispersion on the selective hydrogenation of isoprene.

Operating conditions:  $P = 20$  bar;  $T = 60^\circ\text{C}$ ; LHSV = 10/h;  $H_2/HC$  in moles = 3; feed = 10 vol.% isoprene in 90% benzene; additive: 5,000 ppm thiophene added to feed by wt.

Each of the four data points represents a catalyst corresponding to a particular method of impregnation. The conversion increases with the amount of CO chemisorbed, but very moderately, because of the intervention of diffusional phenomena on the overall rate of hydrogenation.

Derrien, M., Cosyns, J., IFP results.





**FIG. 7.14** CO chemisorption as a measure of hydrogenating activity.

Toluene was hydrogenated over sulfided Co-Mo supported on alumina, under the following conditions: feed = 79.5% cyclohexane, 20% toluene, and 0.5% thiophene, all by wt; total pressure = 60 bar;  $T = 350^{\circ}\text{C}$ ;  $\text{H}_2/\text{HC} = 450$  by vol; LHSV = constant.

The CO chemisorbed was measured by a volumetric method at ambient temperature. The data obtained for the different catalysts show that the hydrogenating activity varies linearly with the CO chemisorbed at ambient temperature, when allowance is made for the chemisorption of the support.

Miquel, J., Franck, J. P., IFP results.

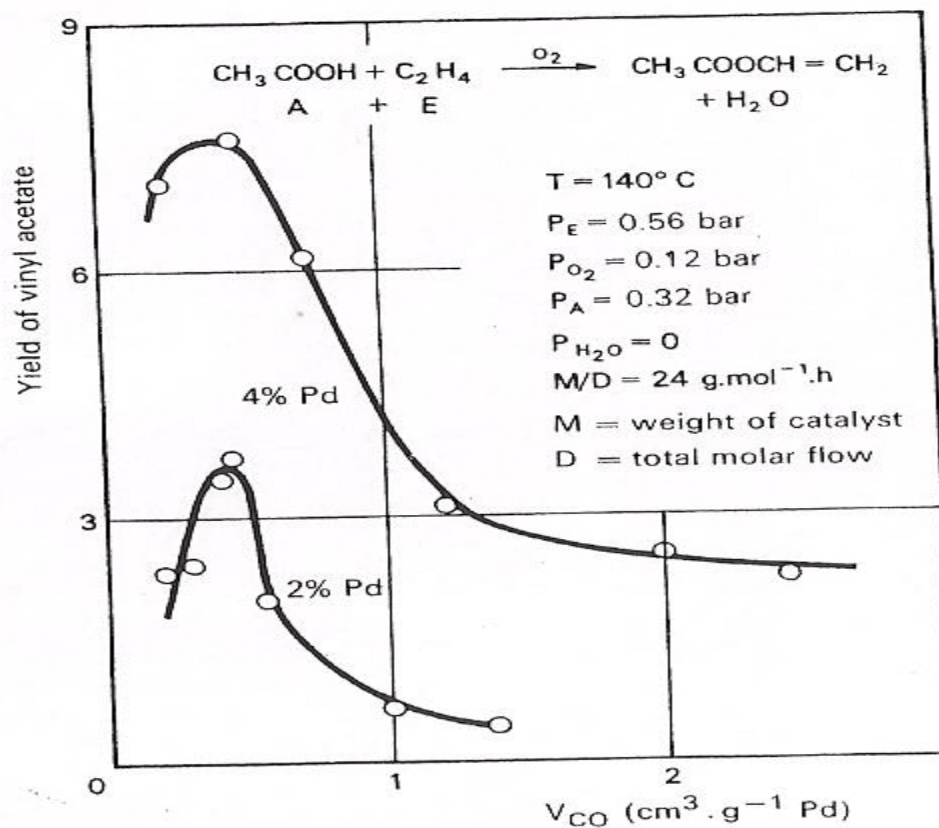
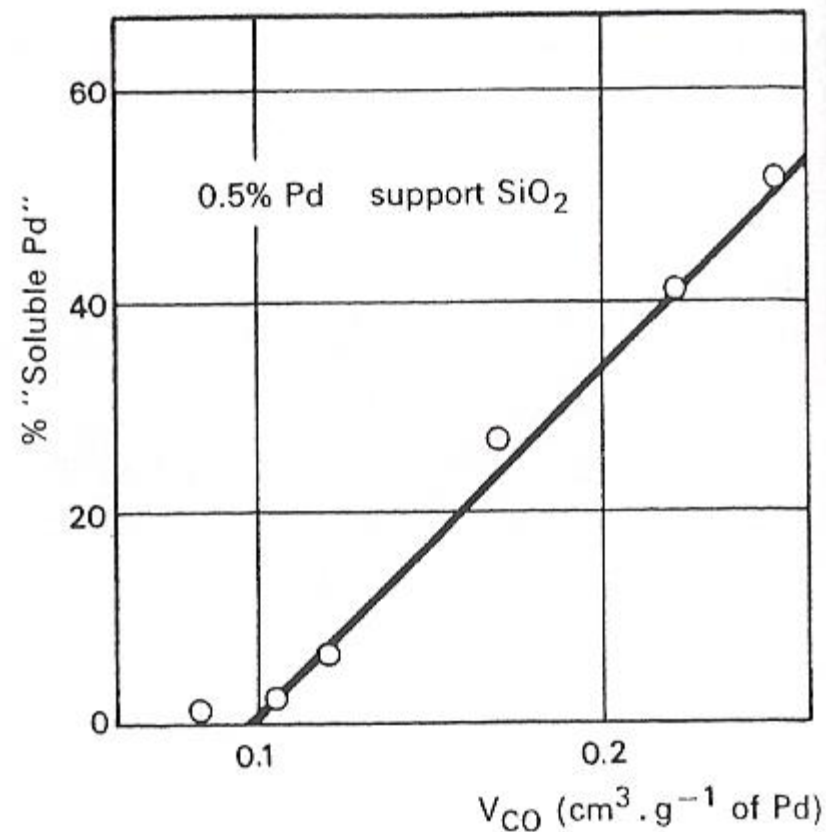
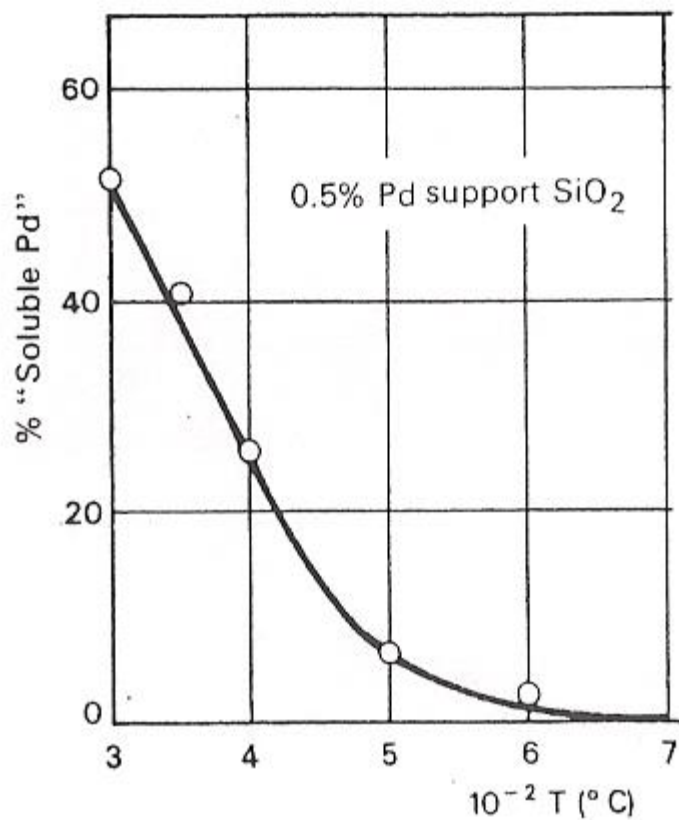


FIG. 7.18 Effect of crystallite dimensions on the synthesis of vinyl acetate by gas-phase acetoxidation of ethylene.

The catalysts were made by successive deposits on a  $220\text{ m}^2 \cdot \text{g}^{-1}$  silica, as follows: (a) deposit of palladium by cationic exchange followed by calcination at various temperatures, then reduction at  $150^\circ\text{C}$ ; (b) deposit of 15% by weight of  $\text{CH}_3\text{COONa}$  by impregnating without excess solution, followed by drying. The sodium acetate plays the role of activator in this reaction.

The curves connecting the data points show that the yield of vinyl acetate passes through a maximum for an optimum crystallite dimension expressed in terms of CO chemisorption.

Samanos, B., Thesis, Paris, 1971.



**FIGS 7.20 and 7.21** Correlation between the chemical solubility of deposited palladium and its dispersion.

Figure 7.20 shows that the solubility of palladium in a solution of 5% SnCl<sub>2</sub> decreases as the calcination temperature increases. The linear relation between the percentage of soluble Pd and the quantity of CO chemisorbed in Fig. 7.21 shows that solubility reflects the dimensions of the crystallites.

Samanos, B., Thesis, Paris, 1971.

# Crystallite size measurements - Experimental techniques

- X-ray line broadening Analysis –XLBA
- Transmission electron microscopy- TEM
- Chemisorption methods
- X-ray photo electron spectroscopy



# Crystallite size measurement- Methods

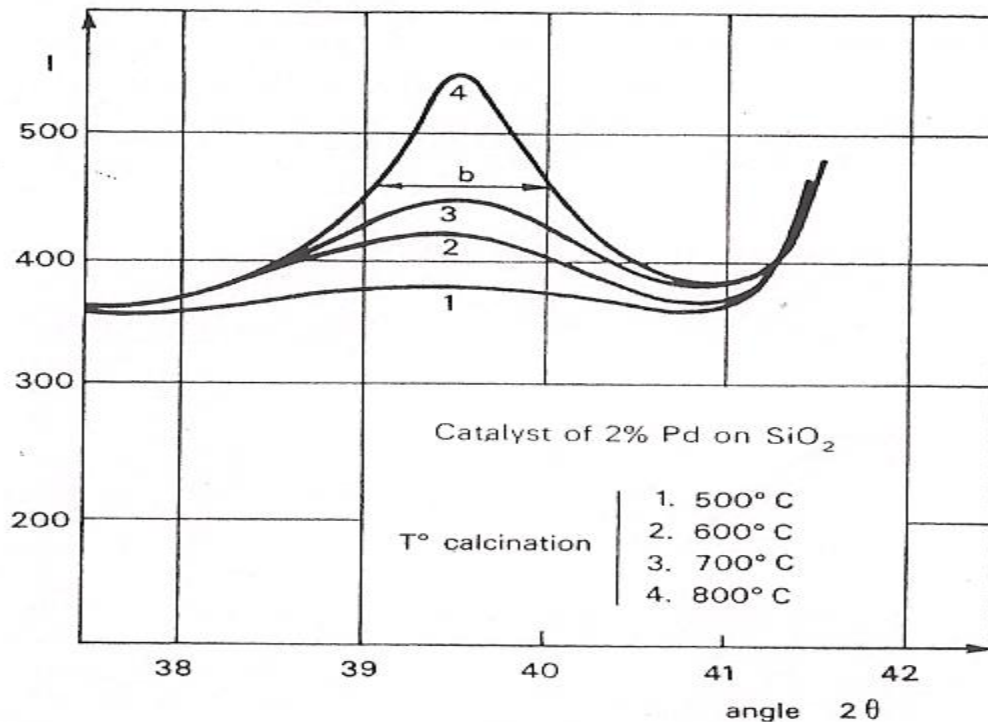
## X-ray line broadening analysis-XLBA

Crystallite/Particle size is inverse proportional to line width- FWHM

Debye- Sherrer formula- Size (d) =  $k\lambda / \beta \cos\theta$

- k- constant-0.94 or to 1;  $\beta$ - angular width at half-height,  $\lambda$ - X-ray wave length ,  $\beta = (B^2 - b^2)$  ; B- FWHM for sample & b-FWHM for standard
- Applicable range- 3-100 nm
- Not applicable for catalysts with low metal loading
- Only average value is obtained
- d- gives length; Shape/Geometry factor to be included
- $d_m = d \times g$
- Particle size/crystallite size could be measured
- Average value from different d-lines
- High temperature/in-situ studies
- Small angle X-ray diffraction

Crystal geometry	Factor <b>g</b>	Definition
Sphere	4/3	Diameter
Hemisphere	4	Diameter
Cube 100	1	Cube edge
110	1.061	Cube edge
111	1.155	Cube edge



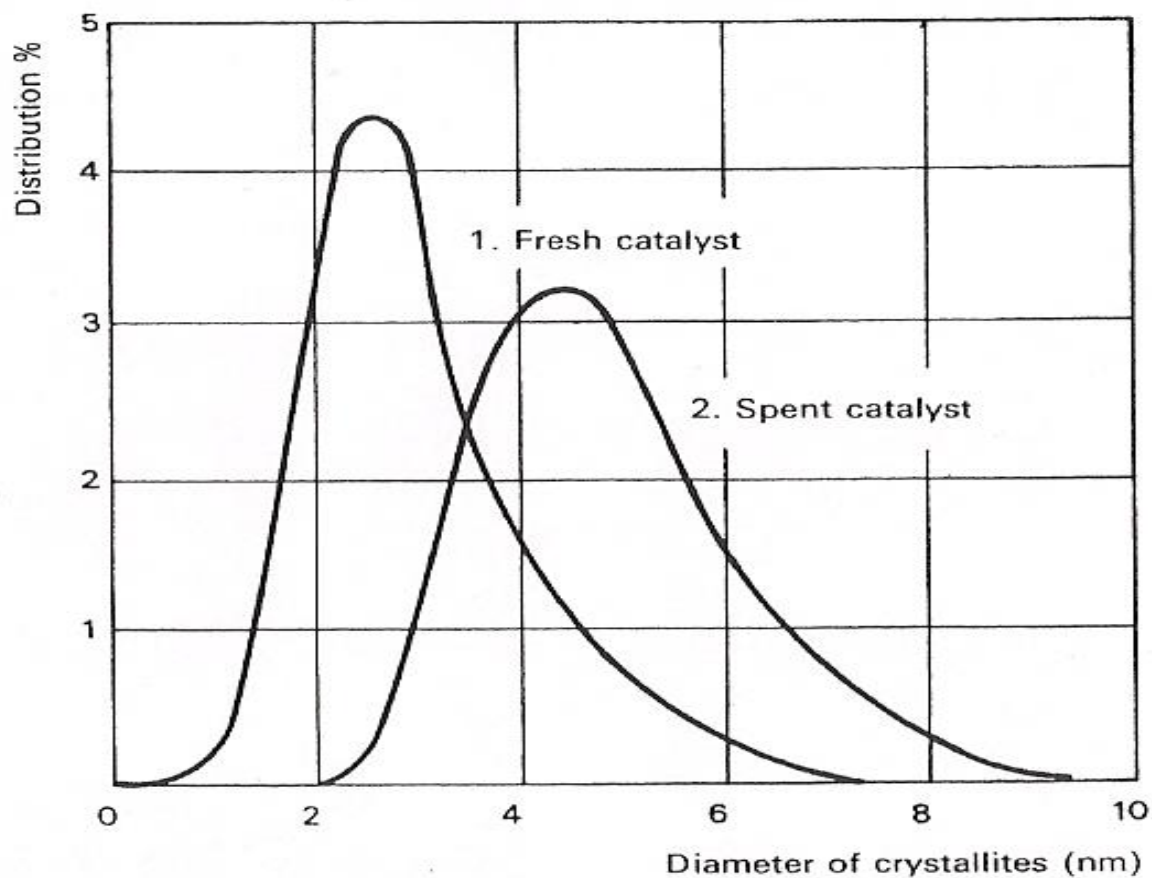
**Fig. 7.15** Determining the average size of palladium crystallites from the mid-height width ( $b$ ) of X-ray diffraction lines.

An estimate of the dimension of the crystallites,  $d$ , is first approximated by the Scherrer formula.

$$d = \frac{k\lambda}{b \cos \theta}$$

where  $b$  represents the angular width of the X-ray line at mid-height,  $\theta$ , the corresponding Bragg angle, and  $k$  is a constant close to one. This method applies particularly well for crystallite dimensions between 5 nm and 50 nm. The average dimensions of the crystallites of four catalysts of this figure appear in Table 7.6, which shows the importance of the calcining temperature on the enlargement of the palladium crystallites and hence on the surface that they offer for the access of the reactants.

Samanos, B., Thesis, Paris, 1971.



**FIG. 7.19** Dispersion of platinum on a reforming catalyst by the Small Angle X-ray Scattering (SAXS) method.

The figure shows the crystallite distribution according to dimension for both a fresh catalyst and a spent catalyst that has undergone six regenerations. The support is  $\eta$  alumina; and unwanted diffusion of the alumina pores is suppressed by previous adsorption of  $C_4H_9I$ , whose electronic density is close to that of alumina.

White, T. E., Kirklin, P. W., Gould, R. W., Heinemann, H., *J. Catalysis*, 25, 407, 1972.

# Transmission Electron Microscopy

Direct observation of crystallite size & shape; Sampling technique is critical

Size range upto 1 nm & below

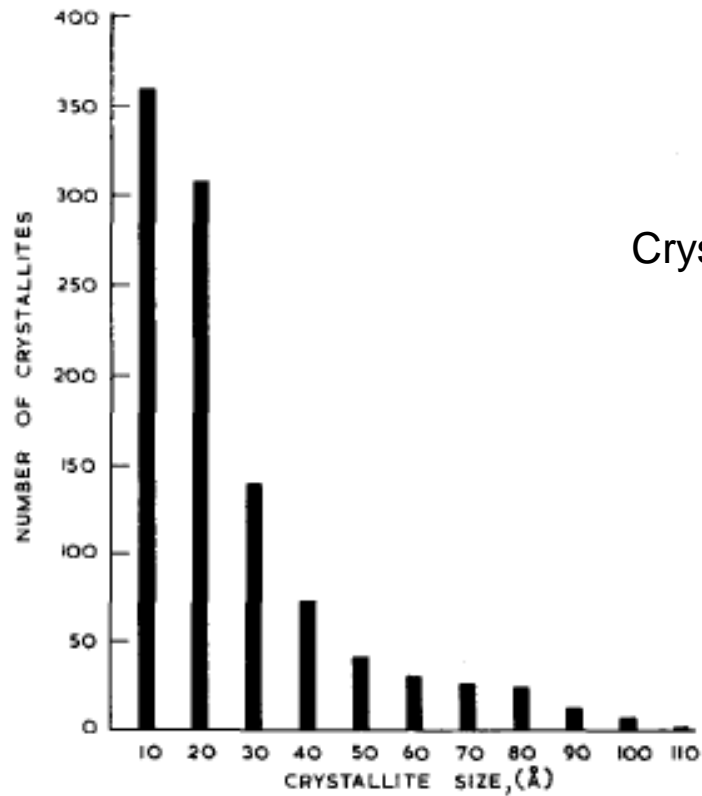
Small sample- May not be representative; in-situ studies possible



**FIG. 7.17** Electron microscope photograph of platinum deposits on zeolite (1 mm = 3.3 nm).

Gallezot, P., Dalmai-Imelik, G., Imelik, B., *Institut de recherche sur la catalyse, Lyon*, Unpublished results.

# Transmission Electron Microscopy



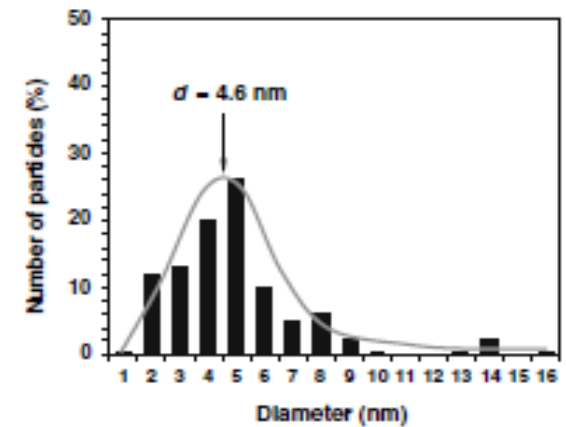
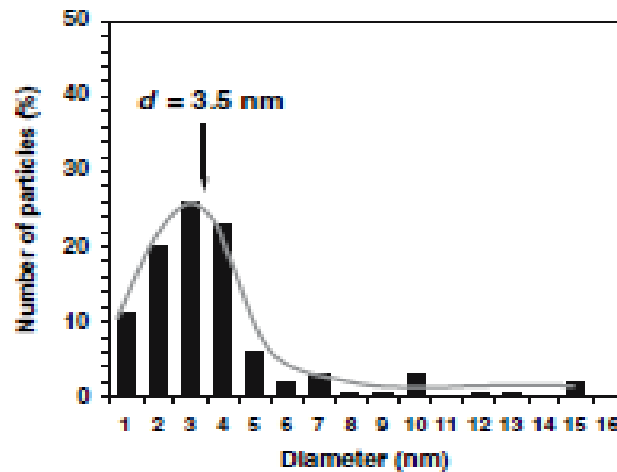
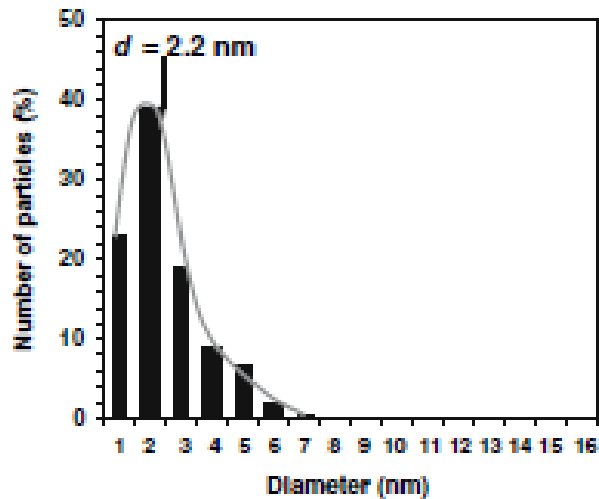
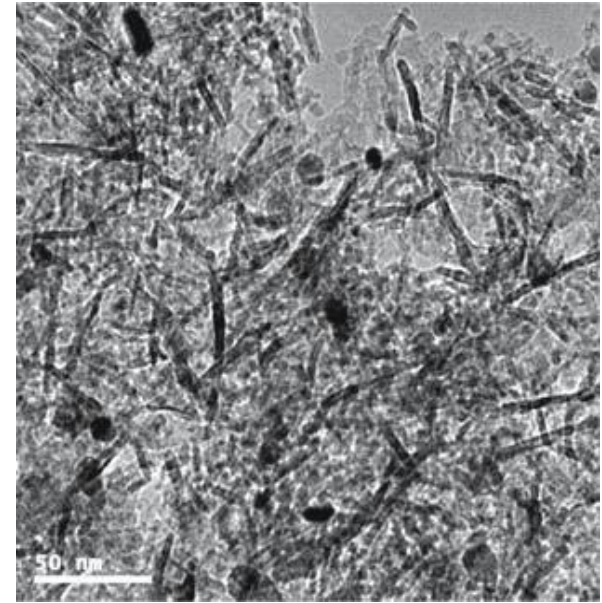
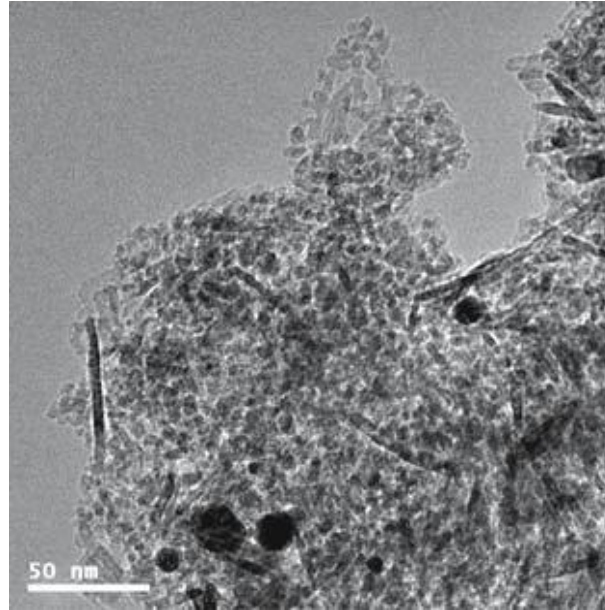
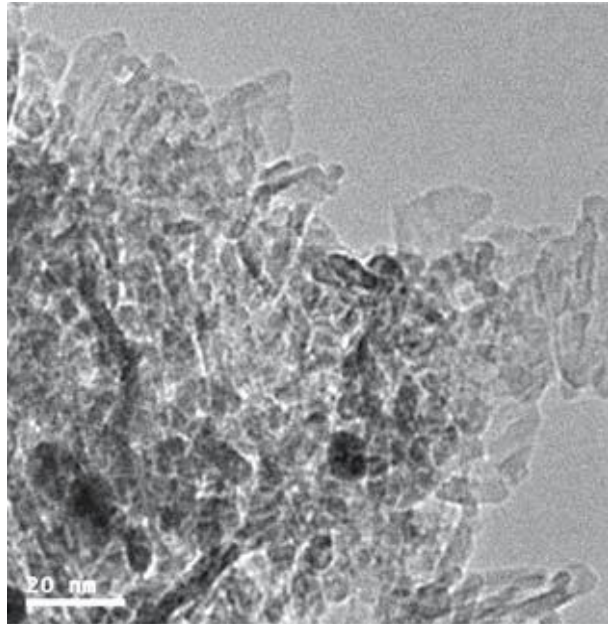
Crystallite size distribution-Histogram

FIG. 2. Size distribution of platinum crystallites in 3% Pt/silica catalyst derived from Fig. 1.

J.Catal.7,378,1967

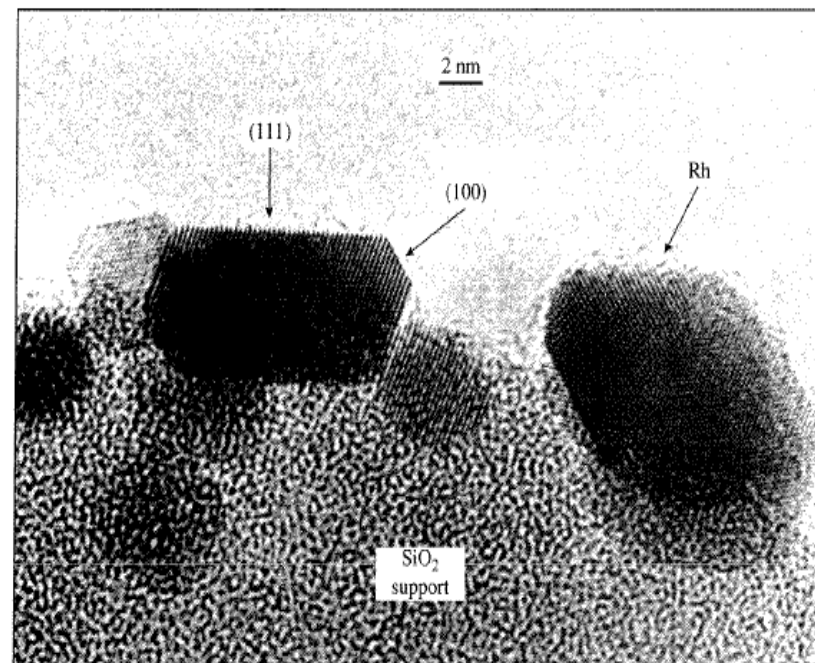
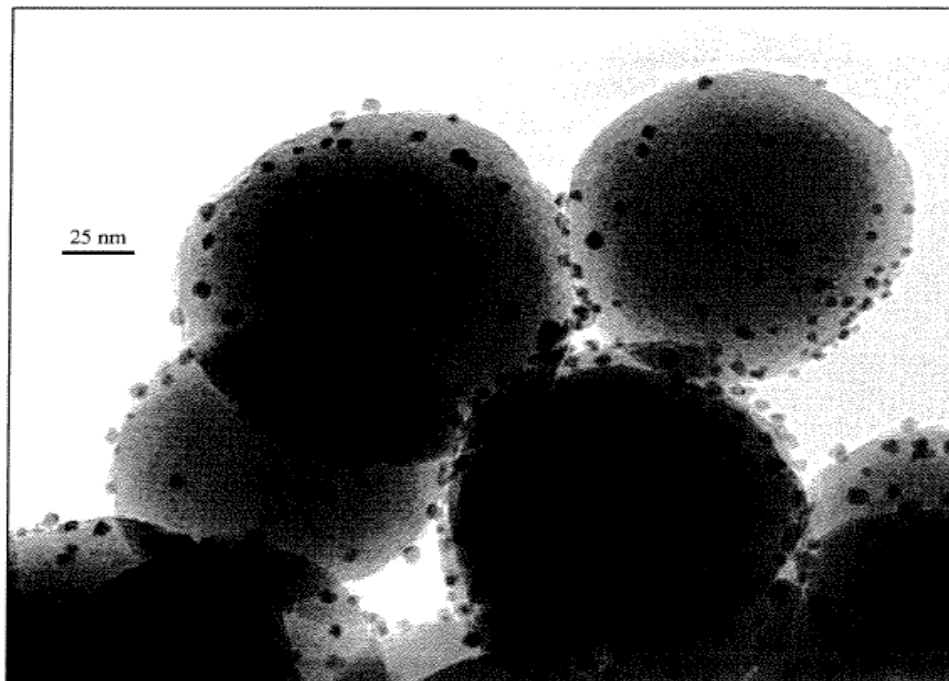


# Crystallite size analysis by TEM



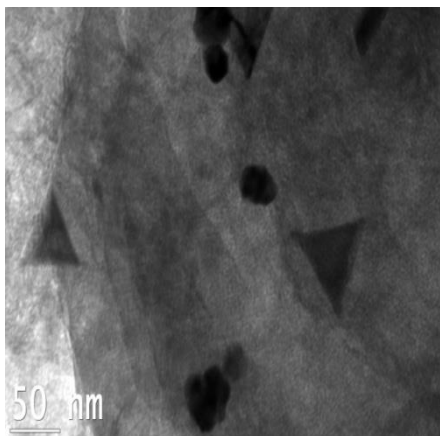
**Fig. 2** Selected TEM images and particle size distributions of the reduced samples. (a) 1.9 wt.% Ru (2.2 nm); (b) 4.7 wt.% Ru (3.5 nm); (c) 7.0 wt.% Ru (4.6 nm)

W.Zhang et.al,  
Catal.Lett., 119,311,2007

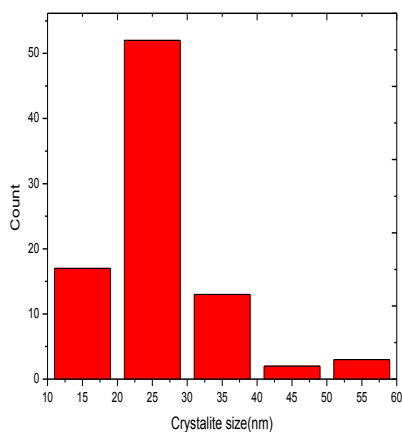


**(a)** Rhodium metal particles supported on silica carrier. **(b)** High-resolution electron micrograph shows how small supported Rh crystallites expose low-index faces. (Top photo courtesy of A. K. Datye. Bottom photo from “Modeling of heterogeneous catalysts using simple geometry supports” by A. K. Datye in *Topics in Catalysis*, vol. 13:131, copyright © 2000 by Kluwer Academic, reproduced by permission of the publisher and the author.)

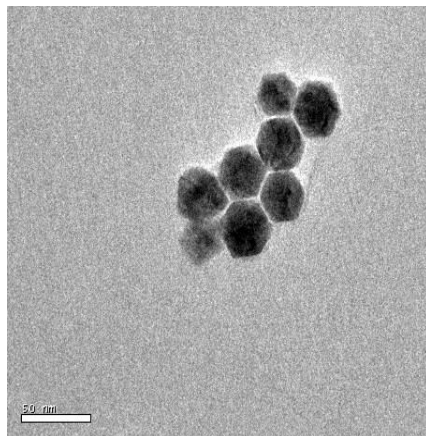
# Shape controlled Pd nano particles on Hydrotalcite & Titania



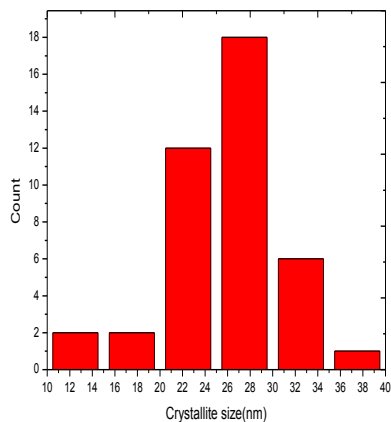
Tetrahedral  
Mean- 27.2 nm  
± 11.04 nm



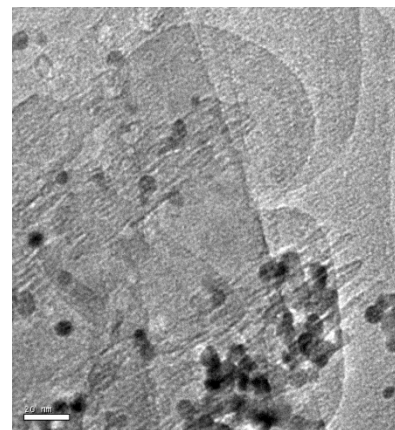
( 25-45 nm) \*



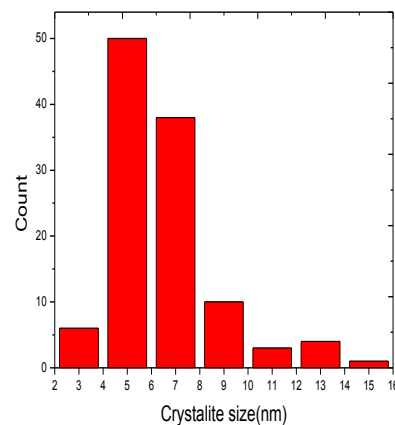
Octahedral  
Mean- 25.73 nm  
± 5.06 nm



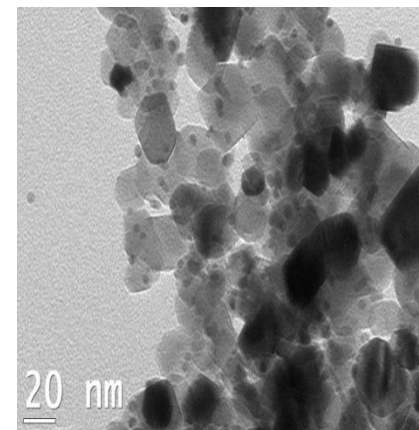
(30-50 nm)\*



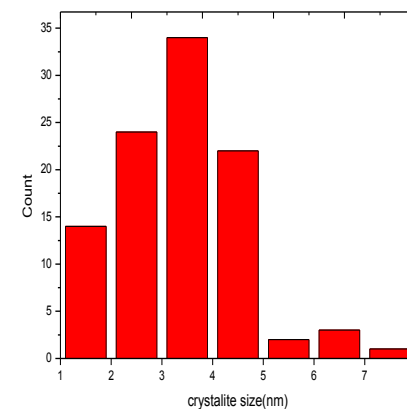
Spherical  
Mean- 6.4 nm  
± 2.24 nm



(8-40 nm)\*



Spherical-P-25  
Mean- 3.43 nm  
± 1.43 nm

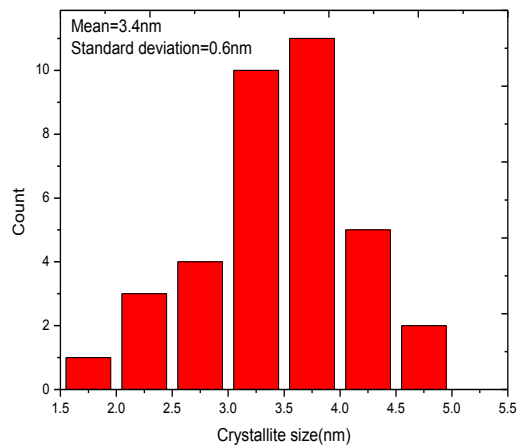
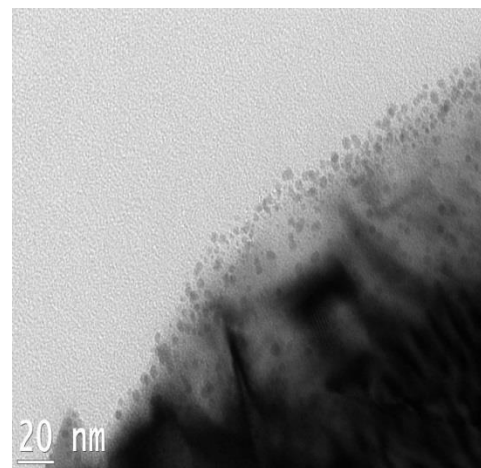
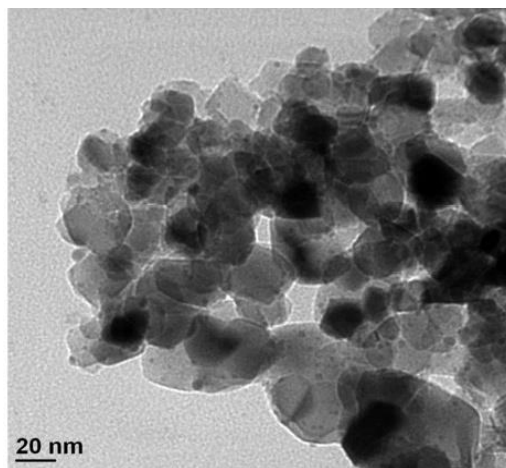
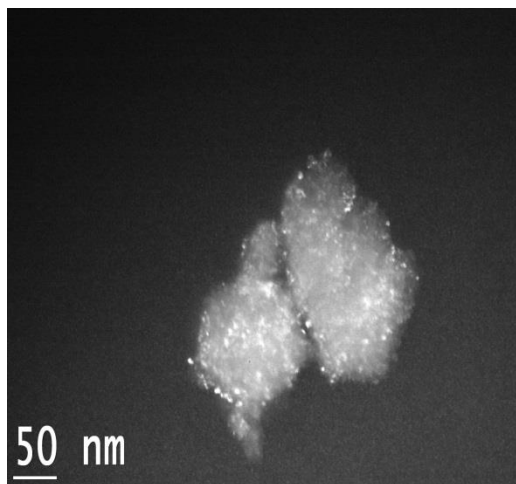


Pd loading  
HTC-3.6 %; P-25-1.5%

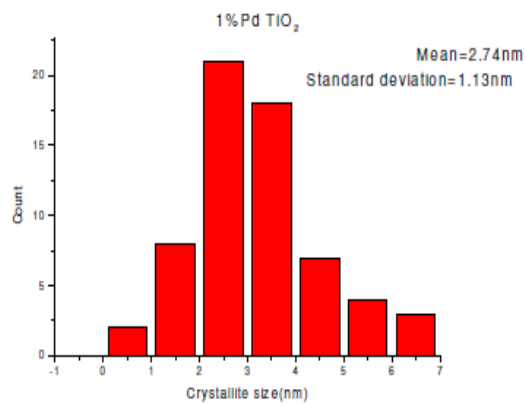
\* - Size values reported in Appl. Catal. A 413-414, 10,2012



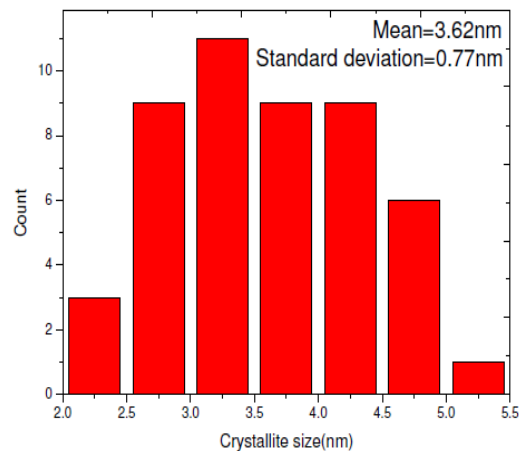
# TEM data for 1%Pd on polymorphs of TiO<sub>2</sub> as supports



Anatase  
3.4± 0.6 nm

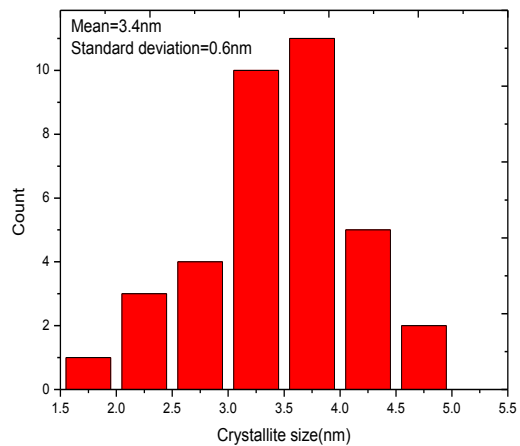
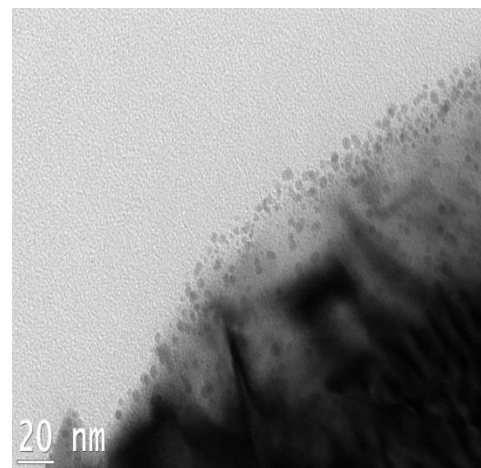
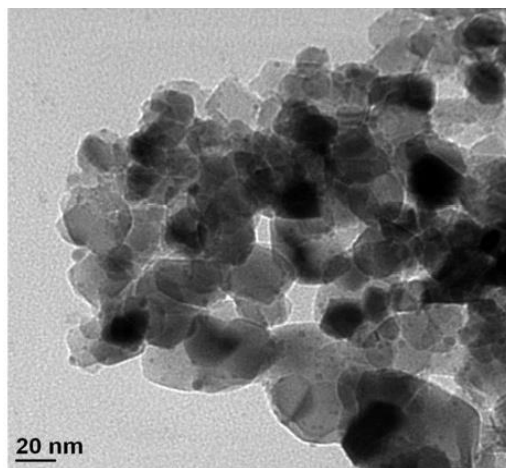
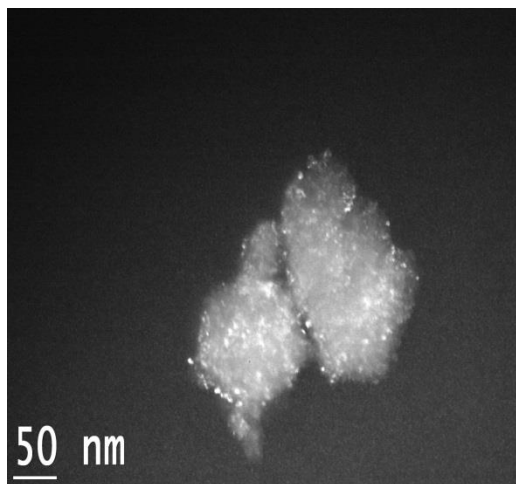


P-25  
2.74±1.13 nm

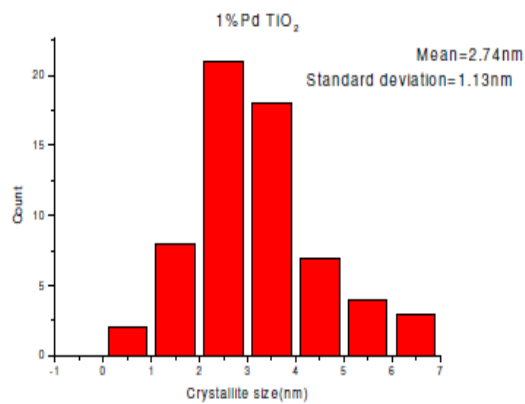


Rutile  
3.62±0.6 nm

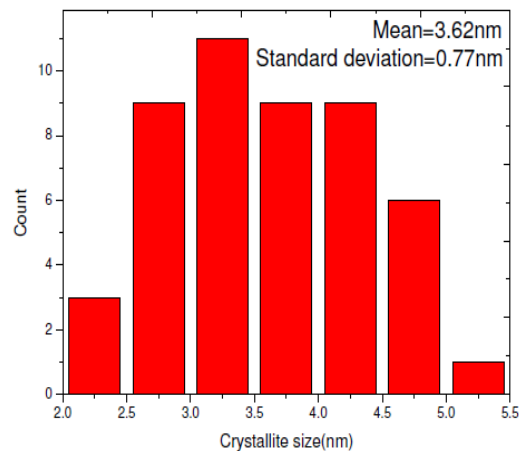
# TEM data for 1%Pd on polymorphs of TiO<sub>2</sub> as supports



Anatase  
3.4± 0.6 nm

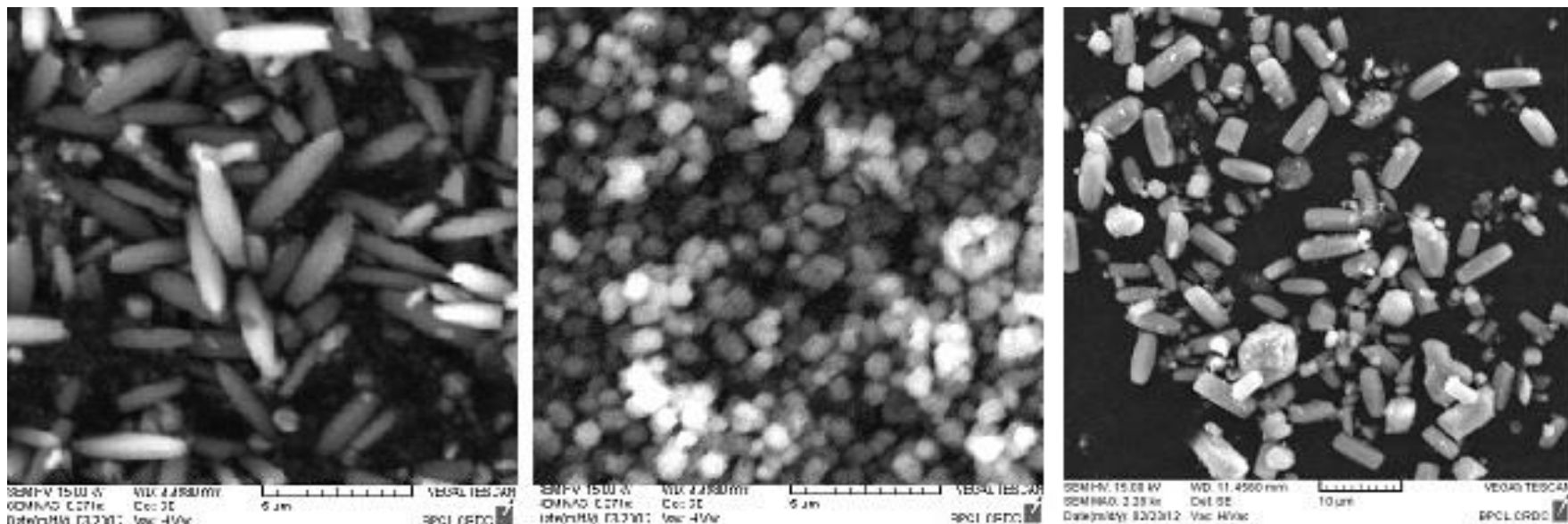


P-25  
2.74±1.13 nm



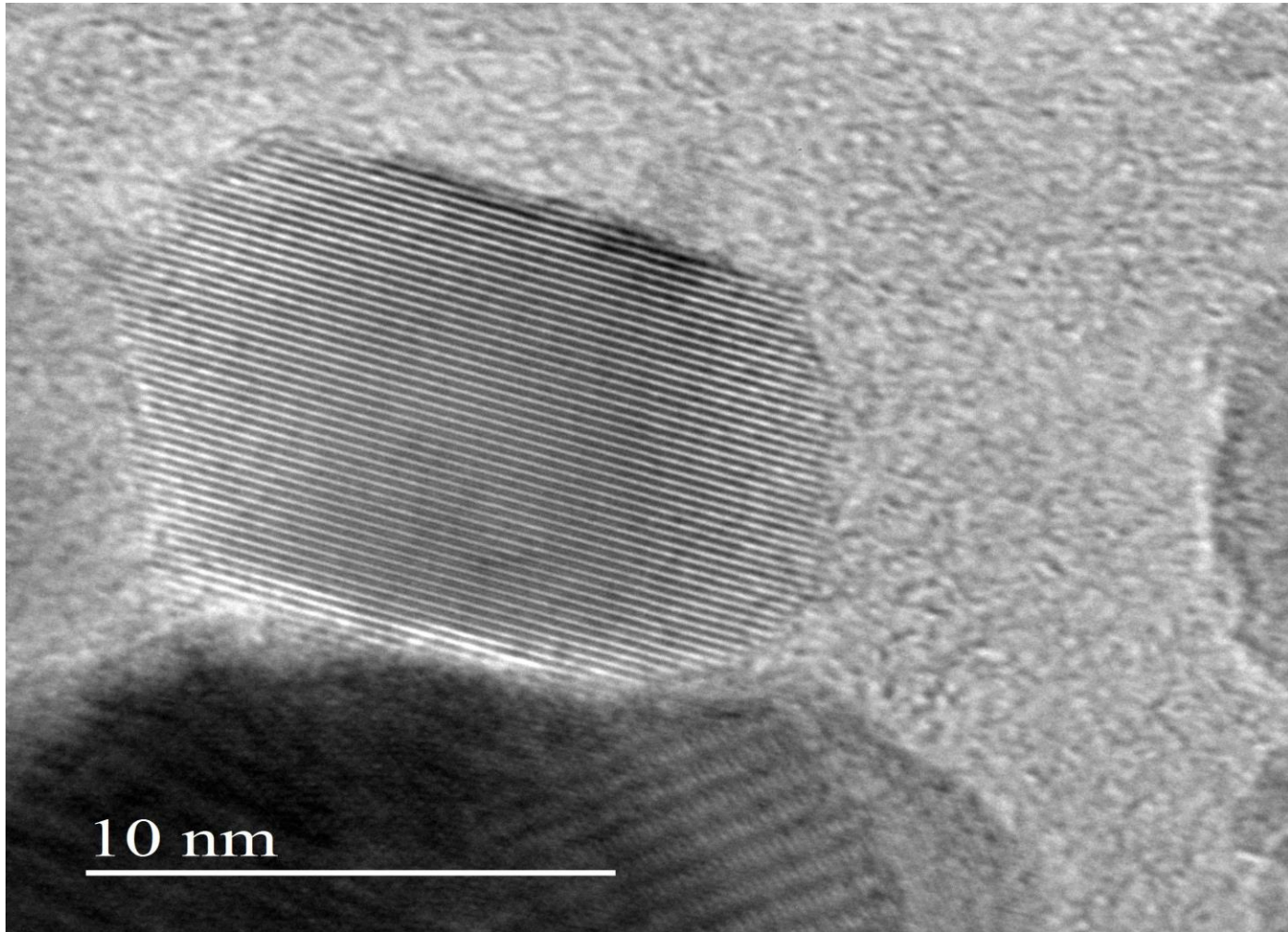
Rutile  
3.62±0.6 nm

# n-Hexadecane -Conversion & Selectivity on ZSM-12-Role of SDAs



Crystal morphologies of ZSM-12 (L to R)- BTMACl-ZSM-12: Rice shaped , TEABr-ZSM-12: Cuboidal shaped & MTEABr-ZSM-12: Elongated cuboidal shaped crystallites

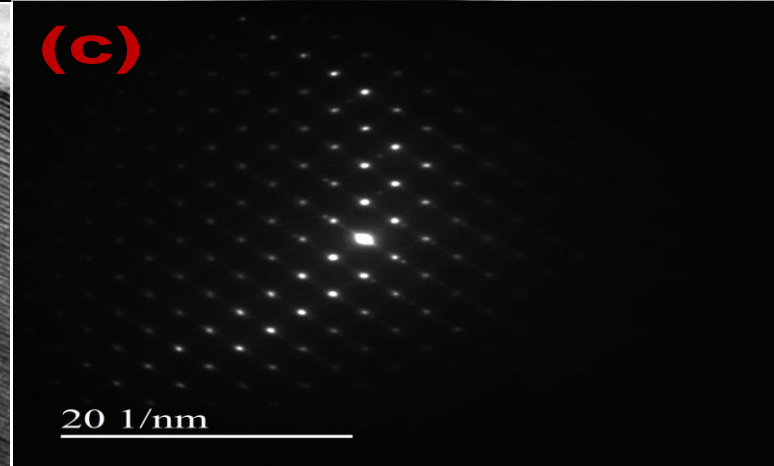
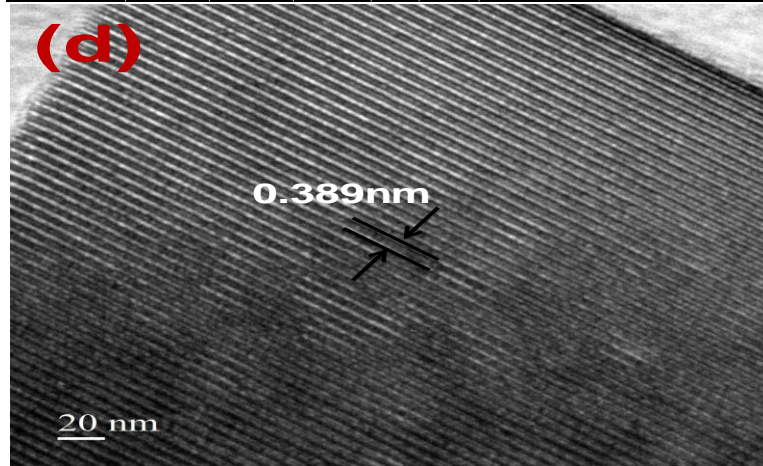
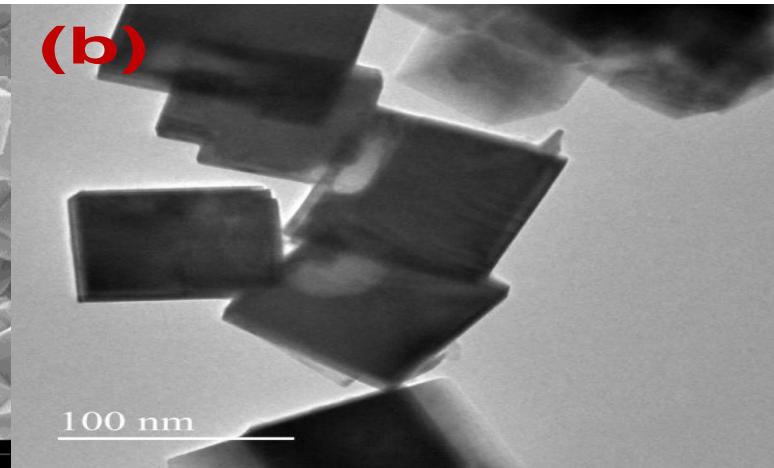
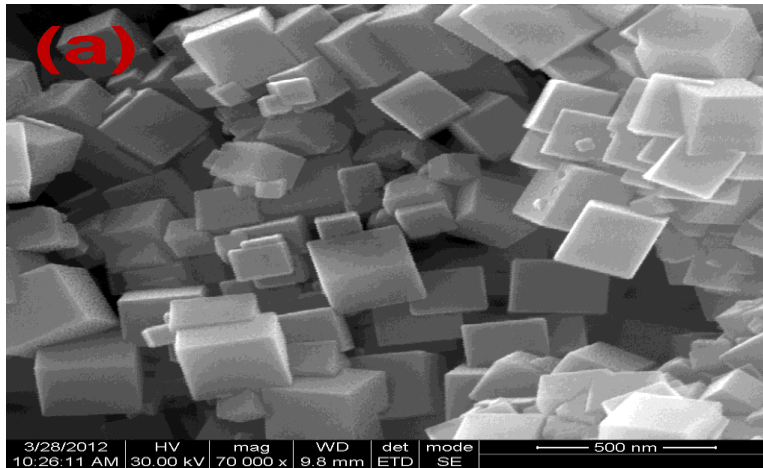
Catalyst	Template	Crystallite Size (μm)	Zeolite Acidity (μmol/g)	External SA (m <sup>2</sup> /g)	BET Total SA (m <sup>2</sup> /g)
CAT-1	BTMACl	3 – 4	107	40	260
CAT-2	TEABr	1 – 2	80	69	220
CAT-3	MTEABr	6 – 7	115	38	260

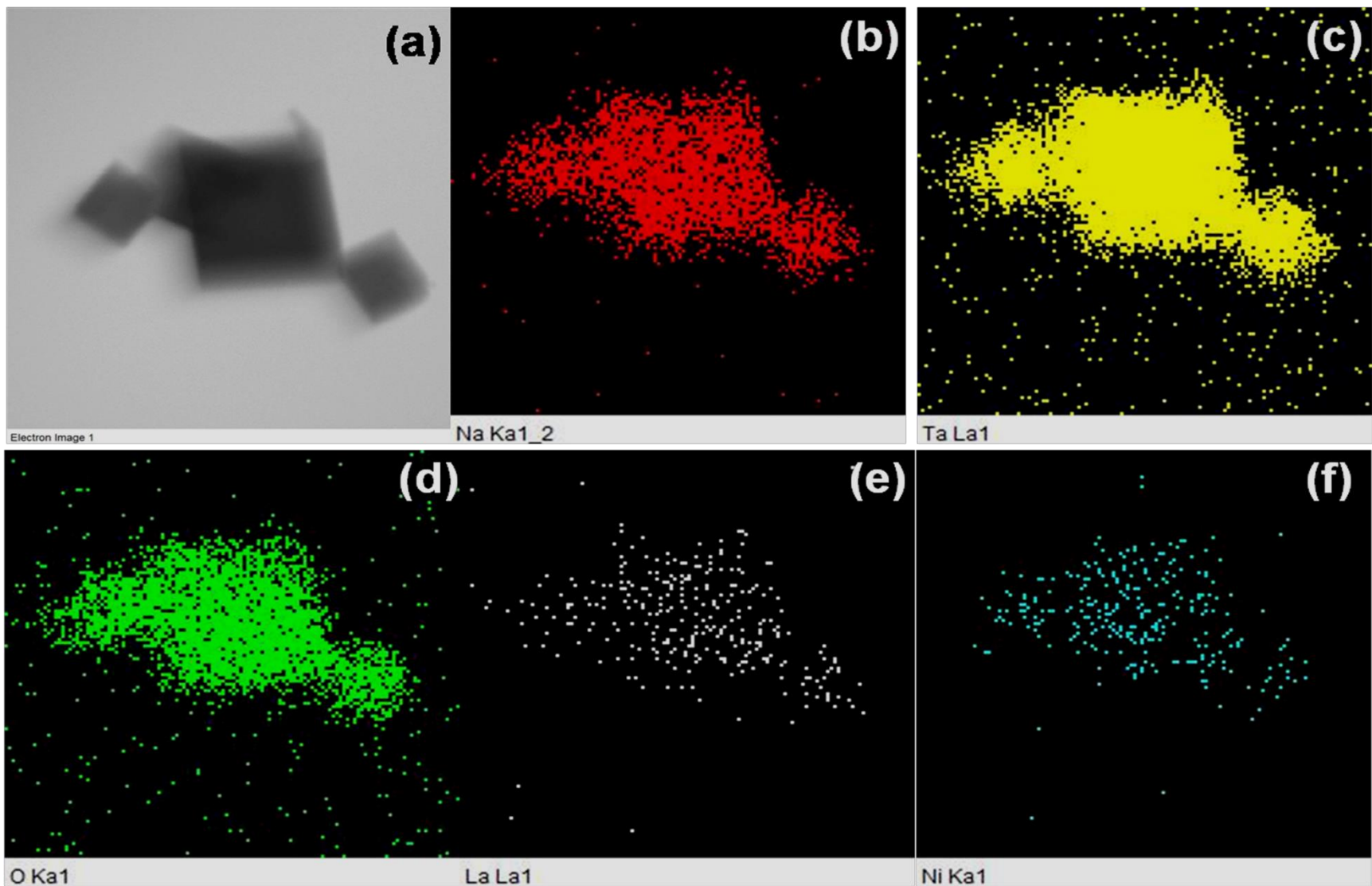


Nano size cobalt oxide prepared in the laboratory



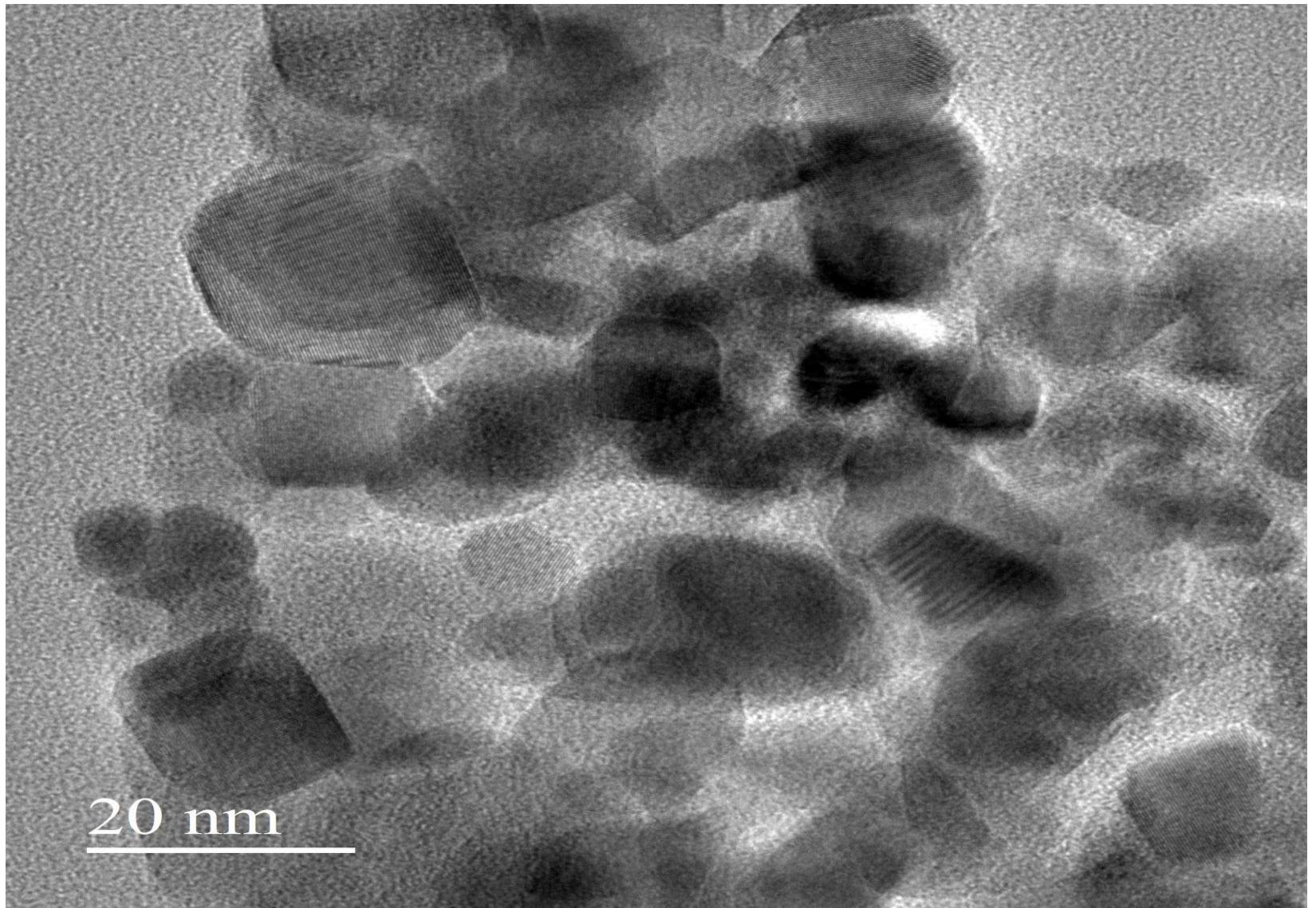
# Morphology of $\text{Na}_{(1-x)}\text{La}_x\text{TaO}_{(3+x)}$ (a) SEM image, (b) TEM image, (c) SAED (d) HRTEM





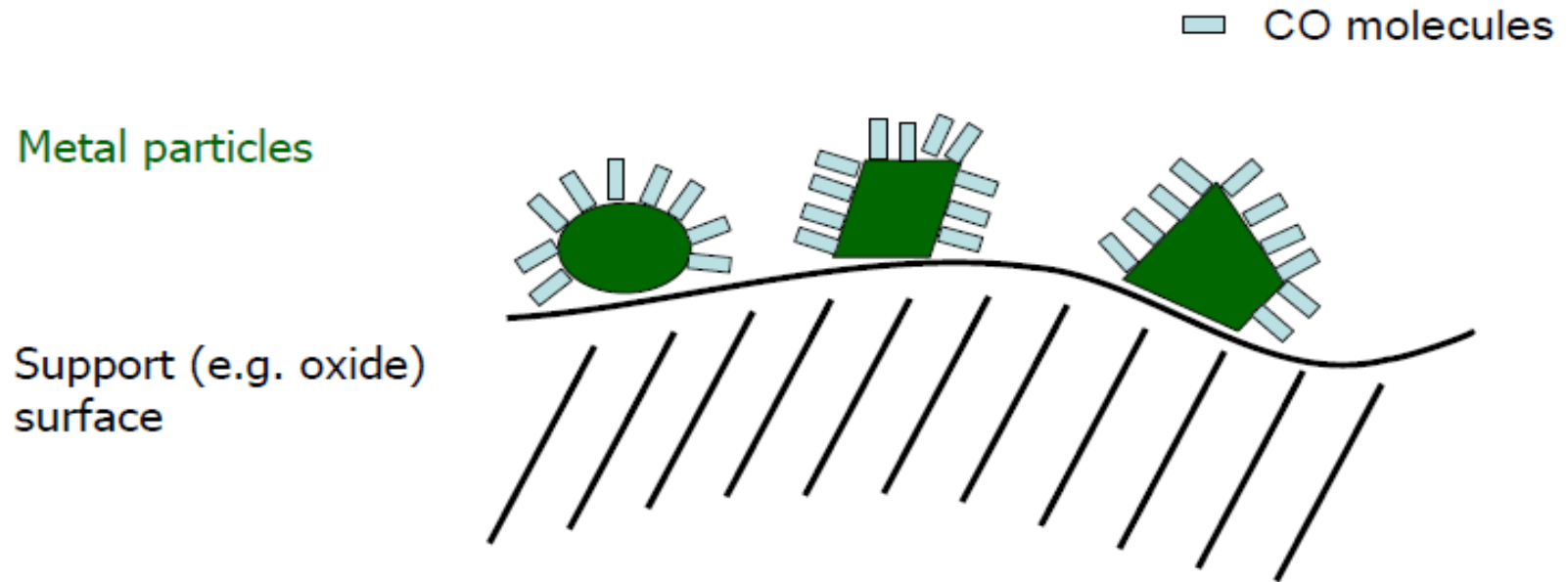
STEM (a) and Elemental mapping (b) Na-Kα (c) Ta-Lα (d) O-Kα (e) La-Lα (f) Ni-Kα for 0.2Wt% NiO/Na<sub>(1-x)</sub>La<sub>x</sub>TaO<sub>(3+x)</sub>.





Nano size cobalt oxide prepared in the laboratory

# Metal surface area by Chemisorption



- ❖ specific adsorption of probe on only one type of site (e.g. on metal and not on support): depends on strength of interaction of probe with metal/support sites, conditions (T, p) can be optimized

Physical adsorption - Non specific/selective

Chemisorption- Selective / specific w.r.t adsorbate/adsorbent

# Crystallite size by Chemisorption

- Volumetric (static) / Flow (dynamic) method/ Volume desorbed (TPD)
- Measurement of monolayer volume
- Adsorption specific to metal sites only
- Static method- Irreversibly adsorbed Hydrogen is measured by ASTM-D32 /ASTM D-3980-82,1998 method for H<sub>2</sub> adsn on supported Pt- Euro-Pt standard
- Adsorption isotherm- Total and after evacuation of physisorbed part
- Dynamic method- Pulse technique- Saturation of surface with adsorbate with repeated pulses
- Data for calculation-
  - Vol.of adsorbate consumed at specific pressure & temperature
  - Metal: Adsorbate- Stoichiometry at mono layer coverage-
  - No of metal atoms involved in adsorption for one molecule of adsorbate
  - $n_s$ - No.of metal atoms per unit area of surface
    - ❖ if adsorption is specific, number of sites can be derived from isotherm (no site heterogeneity, no spill-over)

# Adsorption isotherm- Static method

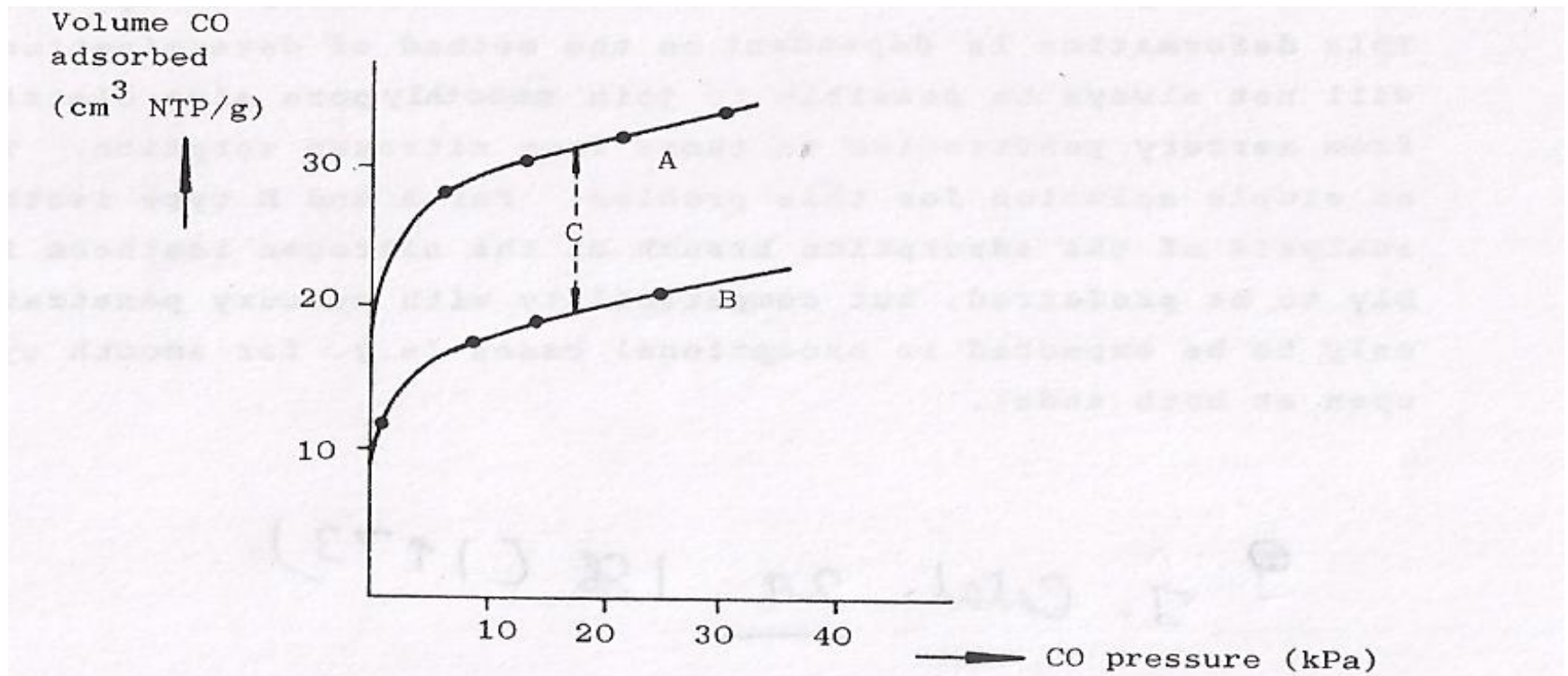


Fig. 1. Adsorption of carbon monoxide on a singly promoted ammonia synthesis catalyst. From lit. 3.

A. Total adsorption at 90 K.

C. Volume CO chemisorbed.

B. Physical adsorption, after evacuation at 195 K.



# Adsorption isotherm- Static method

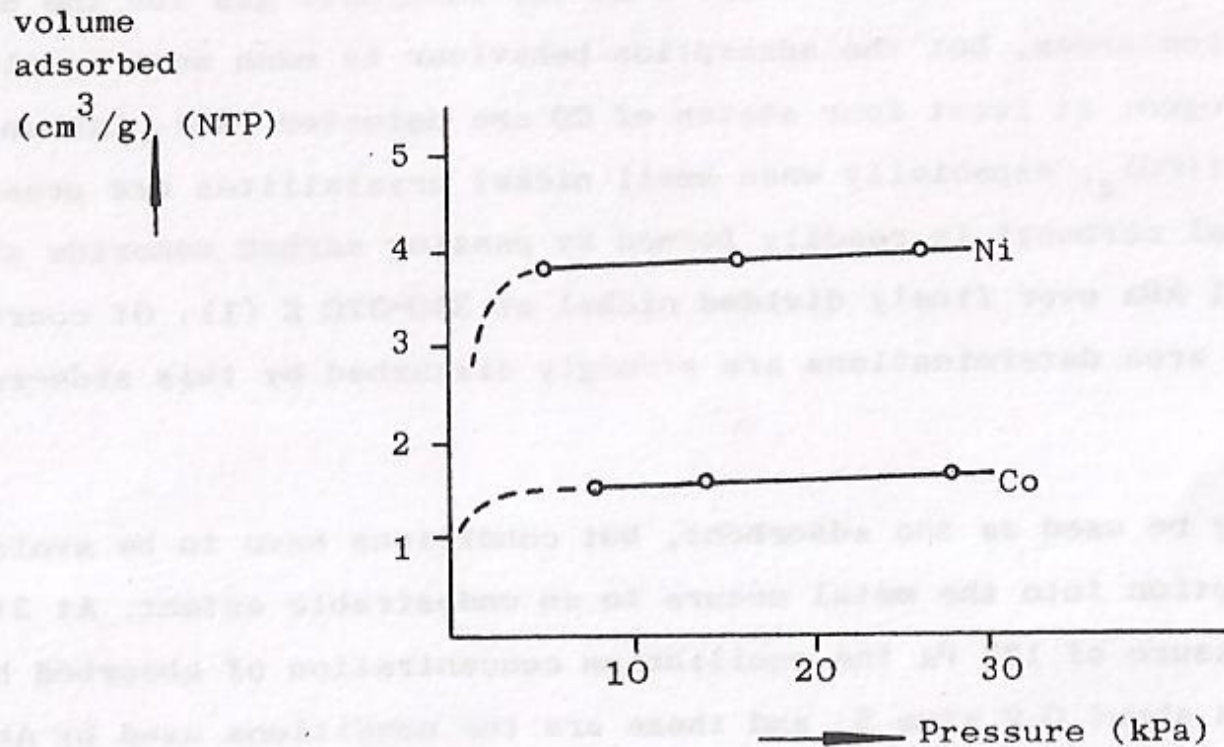


Fig. 6. Adsorption isotherms for hydrogen on silica-supported nickel and cobalt at 291 K. The samples are prerduced in flowing hydrogen, to 643 K. Evacuation at the same temperature (lit. 20).

# Measurement of chemisorption

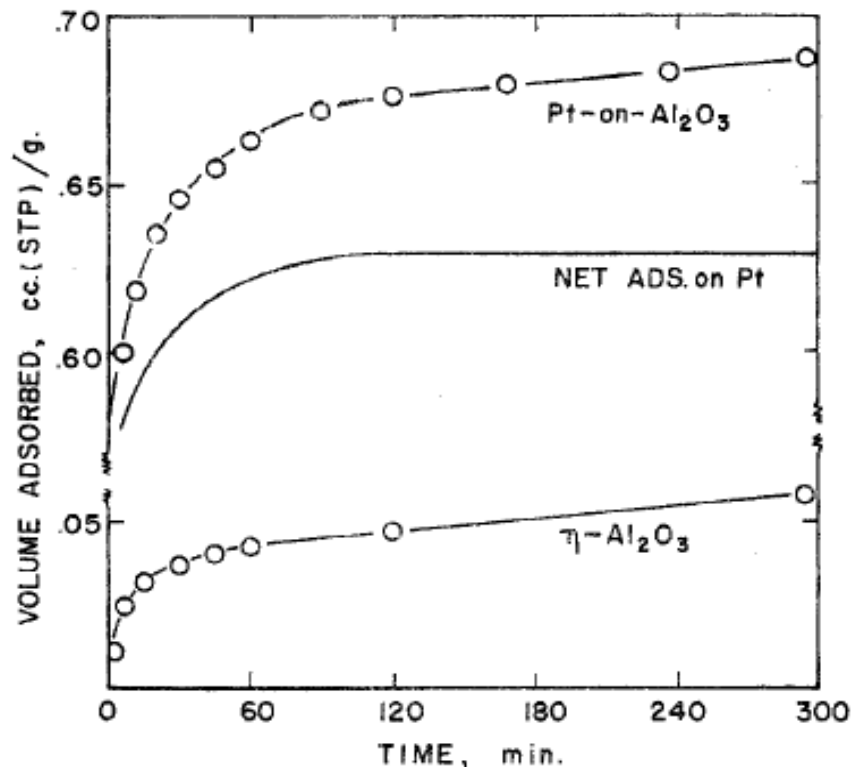


Fig. 3.—H<sub>2</sub> adsorption, 250°, 200 mm.

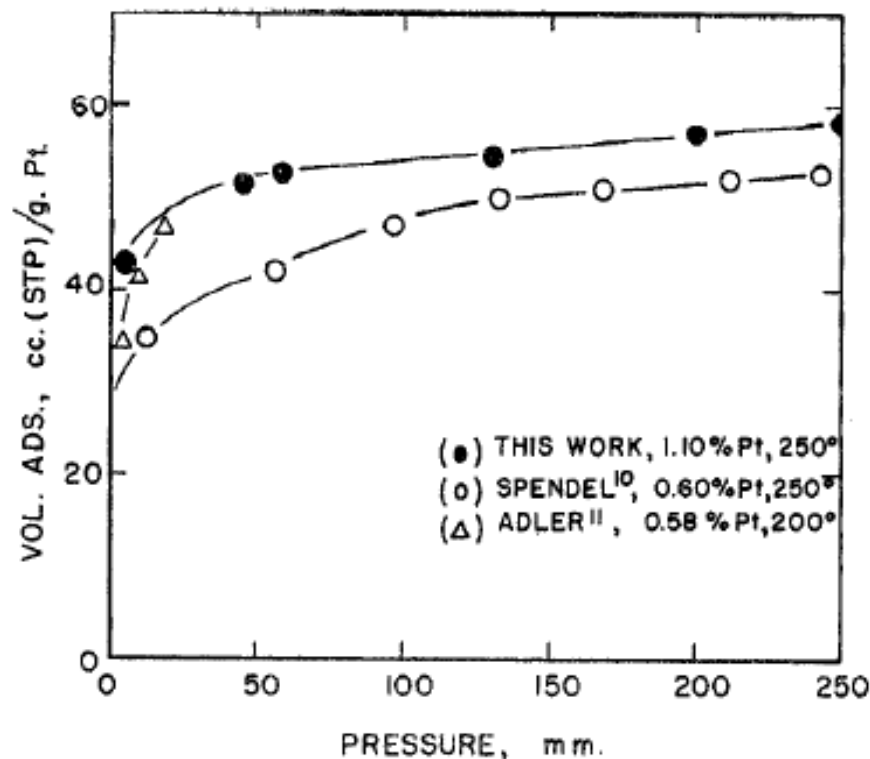


Fig. 2.—H<sub>2</sub> adsorption isotherms on platinum-on-alumina.

Extrapolation of linear region of isotherm to  $P_{eq}=0$  gives  $V_m$



# Stoichiometry for chemisorption

Metal	Gas	Operating conditions		Stoichiometry n
		T°C	Press torr	
Cu	CO	20	10	1-2
Ag	O <sub>2</sub>	200	10	2
Co	H <sub>2</sub>	20	10	2
Ni	H <sub>2</sub>	20	10	2
Ni	C <sub>2</sub> H <sub>4</sub>	0	100	2
Rh	CO	20	10	2
Pd	CO	20	10	1-2
Pt	H <sub>2</sub>	20	10	>2
Pt	H <sub>2</sub>	250	100	2
Pt	O <sub>2</sub>	25	100	2
Cu	N <sub>2</sub> O	Pulse mode		2

n- No of surface metal atoms per molecule of adsorbate

# No. of surface metal atoms

No. of surface metal atoms per unit area of Polycrystalline metals ( $n_s$ )  $\times 10^{15}$

Metal	Equal proportions of (100),(110 & 111)	25%(100),5% (110) 70% (111)*
Co	1.51	-
Ni	1.54	1.75
Pt	1.25	1.42
Pd	1.27	1.45
Ru	1.63	-
Ir	1.30	1.48
Rh	1.33	1.55
Cu	1.47	1.67
Os	1.59	-

\* Based on morphology of metal crystallites by TEM

Cross sectional area =  $1/n_s$

For Pt -  $1/(1.25 \times 10^{15}) = 8 \text{ \AA}^2$

For Ni -  $1/(1.54 \times 10^{15}) = 6.5 \text{ \AA}^2$

# Chemisorption method-Assumptions

- Surface metal atoms are free from any other adsorbates /poisons- Evacuation-Purging
- Suitable activation/pre-treatment/pre-reduction procedures to be adopted
- All metal atoms are in zero oxidn state/completely reduced- Check by TPR  
Noble metals Vs Base metals – Pt-Ni –Presence of Ni ions in supported Ni-
- Adsorption stoichiometry for specific adsorbate-metal system is known and is independent of crystallite size- CO chemisorption- stoichiometry dependence on size
- In the case of measurements on used/spent catalysts, proper pre-treatment procedure is to be evolved so that the dispersion is not affected
- Adsorption due to support, hydrogen spill over effects and metal support interactions are to be factored in
- Euro Pt standards could be used for calibrations.

# Pulse chemisorption set up

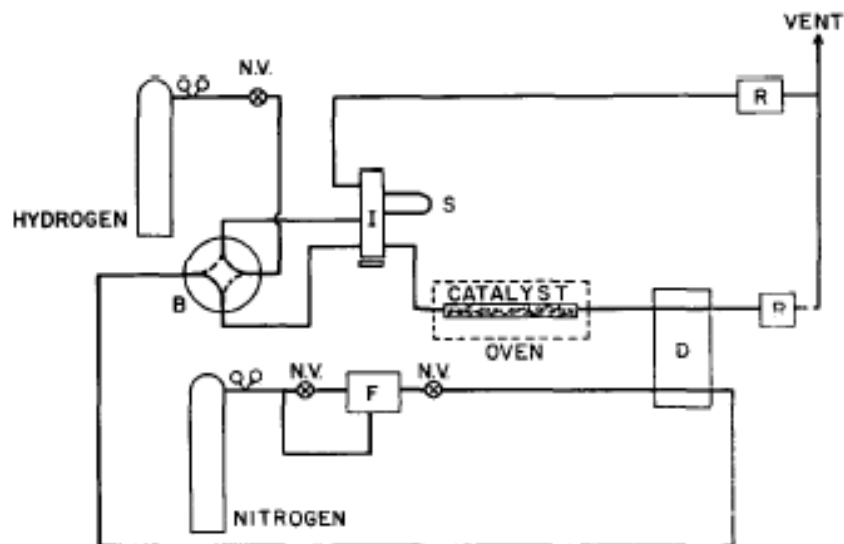
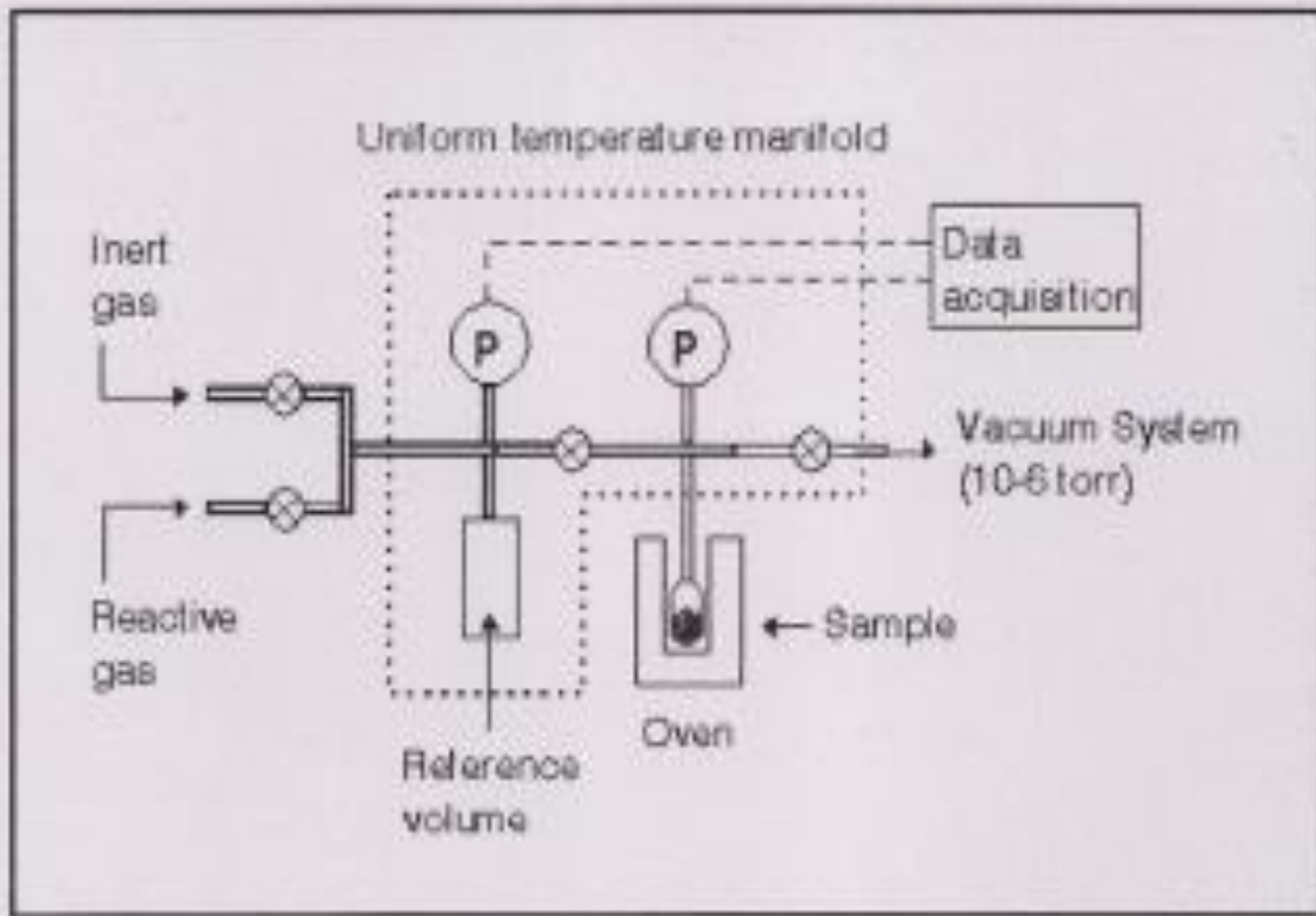


FIG. 1. Schematic of the flow system. F = "Moore" flow controller, N.V. = needle valve, D = thermal conductivity detector, B = glass backflush valve, I = 6-port "Varian" sample-injector, S = sample loop, R = rotameter. The setup for hydrogen adsorption is shown. Prereduction was carried out with the valve B in its alternate position. Oxygen chemisorption was studied by replacing the hydrogen source with oxygen.



Static chemisorption unit

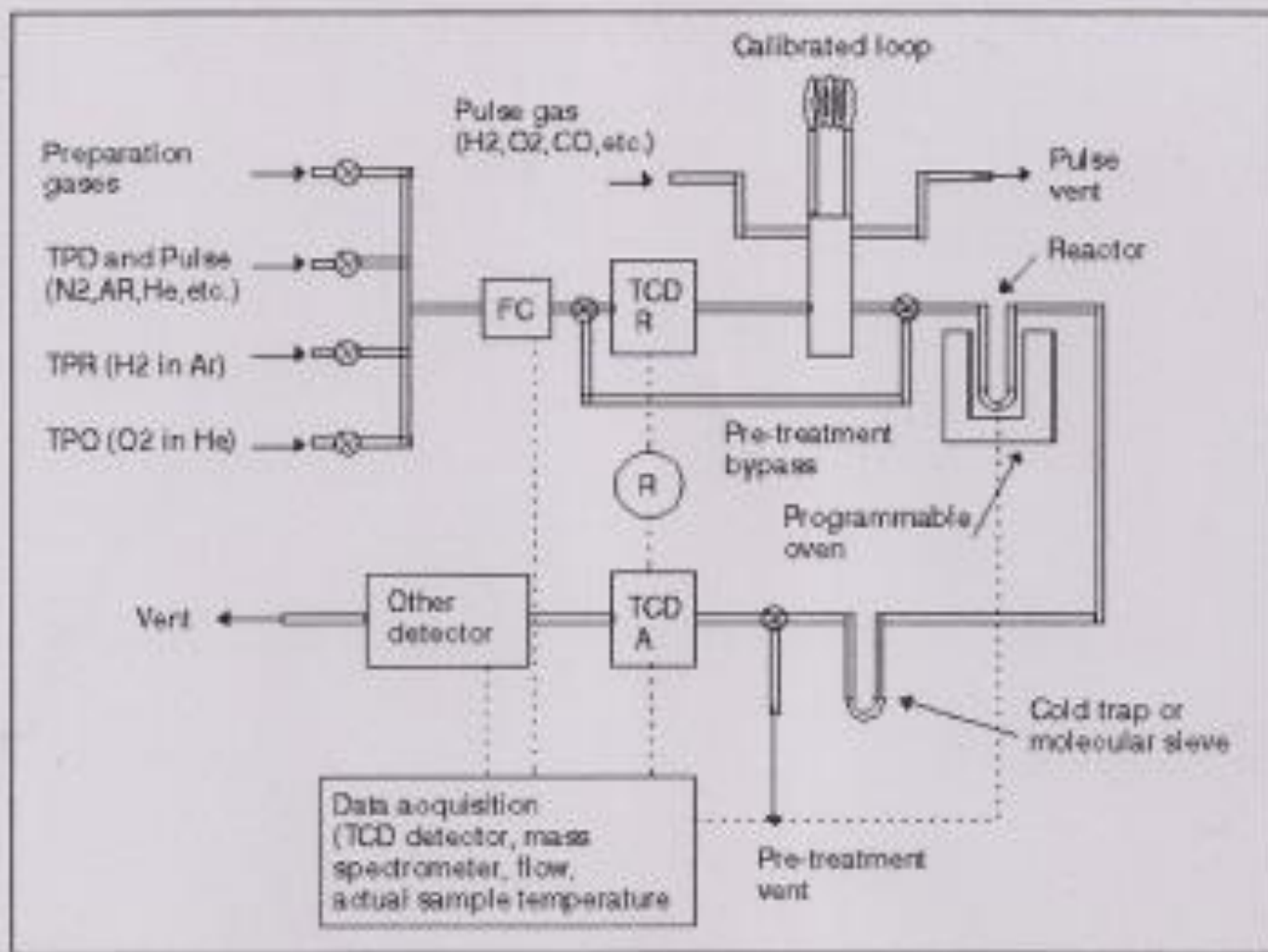
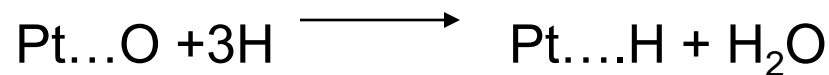
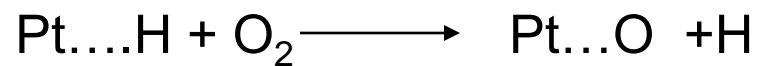
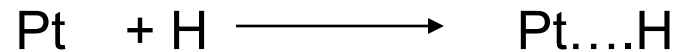


Figure 6. Diagram of a multipurpose apparatus for pulse chemisorption, TPD, TPR and TPO.



# Chemisorptive titration

- Pt adsorbs  $H_2$  &  $O_2$  reversibly at RT
- Titration cycles are possible



$O_2$  &  $H_2$  cycles to be repeated up to saturation

$H_2$  consumed in titration is 3 times higher than that in chemisorption

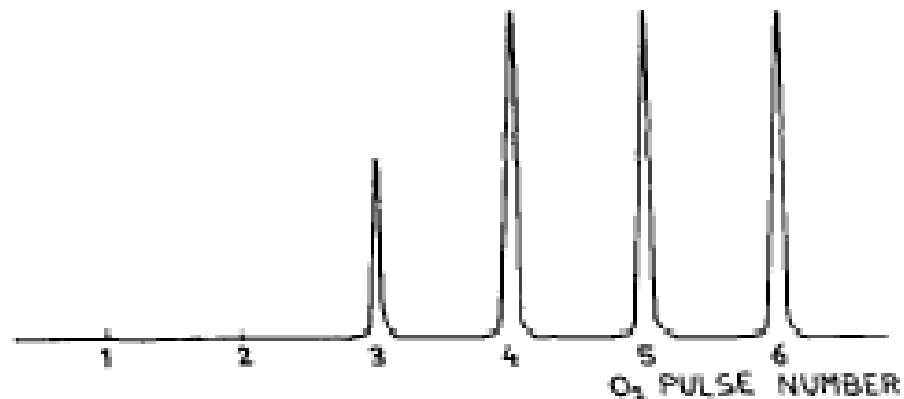


FIG. 2. Typical chromatogram for  $O_2$ -titration of a Pt- -H surface.

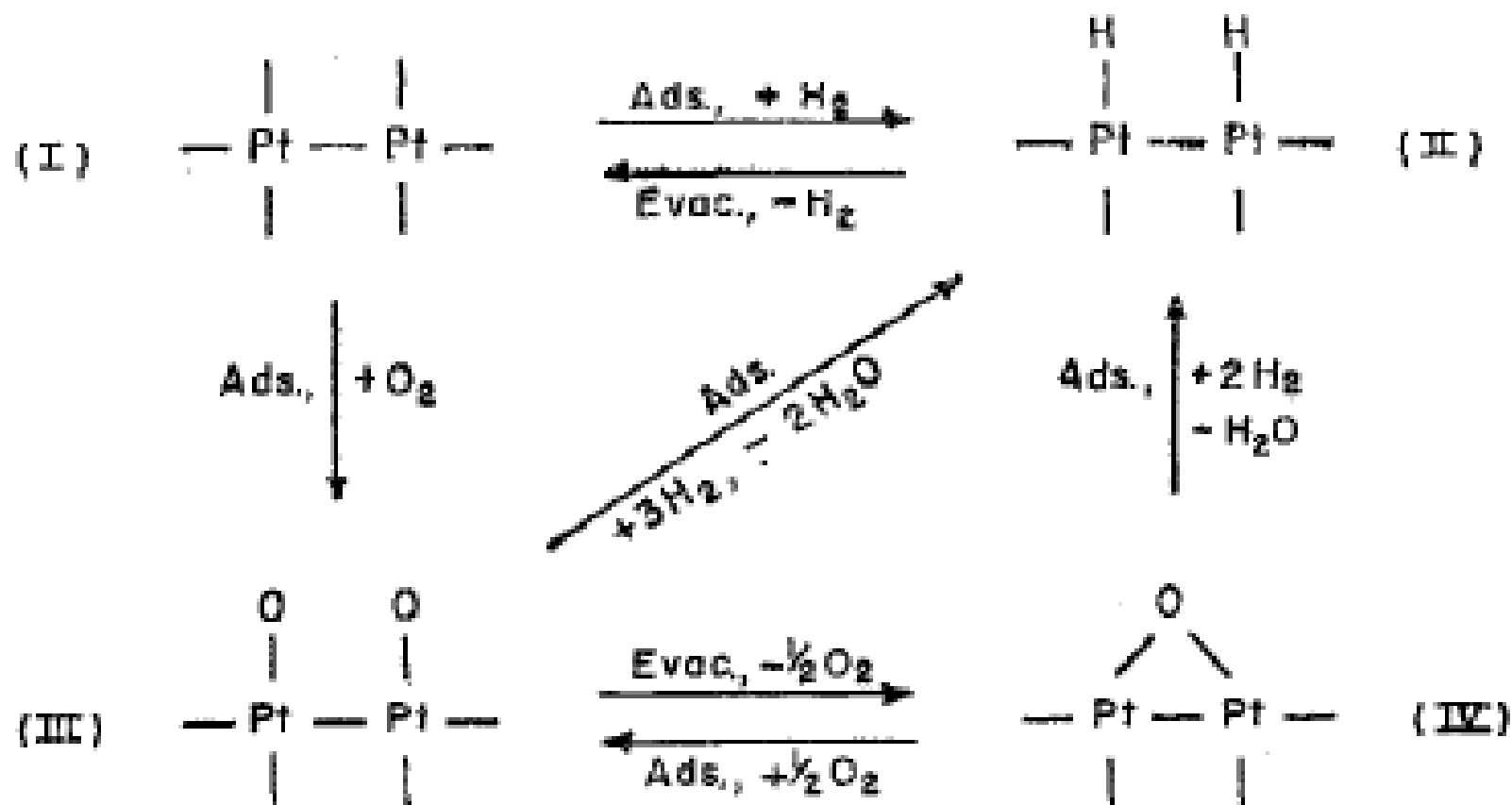


Fig. 4.—Reaction scheme for oxidation-reduction cycle.

# Mono metallic Pt- Dispersion

TABLE 1  
COMPARISON OF Pt DISPERSION VALUES  
FROM DIFFERENT METHODS<sup>a</sup>

Method	Measured by	Gas adsorbed, ml STP/g cat.	Dispersion, %
A	Goldstein	0.282	82
B	Boudart <i>et al.</i>		73
C	This work	0.278	81
D	This work	0.271	79

<sup>a</sup> Methods: A, volumetric chemisorption; B, H<sub>2</sub>-titration of Pt- -O surface volumetrically; C, H<sub>2</sub>-titration of Pt- -O surface gas chromatographically; D, O<sub>2</sub>-titration of Pt- -H surface gas chromatographically. Note that the pretreatments of the catalyst in A and B were extensive and more severe than those in C and D. Catalyst: Cyanamid-Ketjen reforming catalyst CK-306

Well established- Static & Dynamic methods

TABLE 7.5

A COMPARISON OF CRYSTALLITE DIAMETERS BY DIFFERENT METHODS OF MEASUREMENT

(Pt dispersed on an SiO<sub>2</sub> support by cationic exchange, calcined at the indicated temperatures, and reduced at 400 °C for 6 h).

Pt (%)	Calcination (3 h) (T, °C)	Diameter of crystallites (Φ, nm)			
		1	2	3	4
1.26	350	2.0	2.4	—	2.5
1.53	450	5.5	5.5	6	6.5
1.26	520	6.9	6.8	10	8.2
1.26	600	9.2	9.0	11	11.2
1.26	700	14.8	14.6	18	18.5

1. Φ is calculated from the volume of adsorbed CO, assuming cubic crystallites with one face resting on the support.

2. Φ is calculated by the formula:

$$\Phi = 6 V/S = \frac{6 \cdot (\% \text{ Pt})}{10^2 \cdot S \cdot d}$$

where Φ is in nm, S in m<sup>2</sup> · g<sup>-1</sup>, and d = 21.45 (the density of Pt).

3. The diameter is determined by X-ray diffraction.

4. Φ is calculated from the volume of adsorbed CO, assuming an octahedral shape more probable than a cubic one.

Brunelle, P., Sugier, A., Montarnal, R., Unpublished results.

TABLE 7.6  
COMPARING DIFFERENT METHODS OF CRYSTAL MEASUREMENT

(A catalyst of 2% Pd impregnated on SiO<sub>2</sub> by cation exchange is calcined at seven different temperatures; and the diameters of the crystallites are estimated by CO chemisorption, electron microscope (EM), and X-ray diffraction (XR). All catalysts were reduced at 150° C for 1.5 h).

$T$ (°C)	CO chemisorbed (cm <sup>3</sup> · g <sup>-1</sup> )	$\Phi$ by chemisorption <sup>(1)</sup> (nm)	$\Phi$ by EM (nm)	$\Phi$ by XR <sup>(2)</sup> (nm)
300	1.3	2.7	2	—
350	1.15	3.1	2.5	—
400	1	3.7	3	—
500	0.55	7.2	5	5.5
600	0.42	9.7	6	7
700	0.31	12.5	7	7.5
800	0.25	15.8	14	14

<sup>(1)</sup>  $\Phi$  is calculated by assuming that the crystallite is cubic with one face resting on the support.

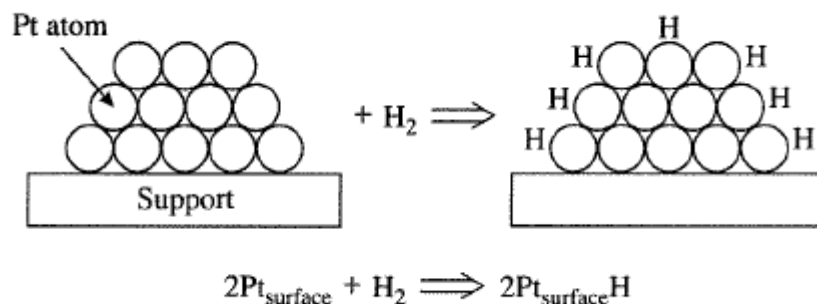
<sup>(2)</sup>  $\Phi$  is calculated with the Scherrer formula:

$$\Phi \text{ (nm)} = \frac{k\lambda}{b \cos \theta}$$

where  $b$  is the width of the line at mid-height,  $\lambda$  is the wave length (0.154 nm) of the  $K_{\alpha}$  line of copper, and  $\theta$  the corresponding Bragg angle.

Samanos, B., *L'acétoxydation de l'éthylène en phase gazeuse*. PhD. thesis, Paris, 1971, and Montarnal, R.





$$\text{Fraction exposed} = \text{Dispersion} = \frac{2 \times (\text{H}_2 \text{ molecules chemisorbed})}{\text{Total number of Pt atoms}}$$

**Table 5.1.1** | Determination of metal particle size on Pt/Al<sub>2</sub>O<sub>3</sub> catalysts by chemisorption of H<sub>2</sub> and CO, X-ray diffraction, and transmission electron microscopy.

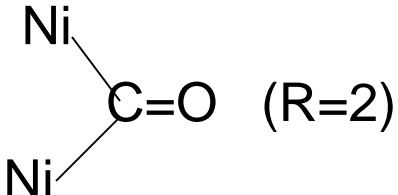
% Pt	Diameter of Pt particles (nm)			
	H <sub>2</sub>	CO	X-ray diffraction	Electron microscopy
0.6 <sup>a</sup>	1.2	1.3	1.3	1.6
2.0 <sup>a</sup>	1.6	1.8	2.2	1.8
3.7 <sup>a</sup>	2.7	2.9	2.7	2.4
3.7 <sup>b</sup>	3.9	—	4.6	5.3

<sup>a</sup>Pretreatment temperature of 500°C.

<sup>b</sup>Pretreatment temperature of 800°C.

Source: Renouprez et al., *J. Catal.*, **34** (1974) 411.

# Chemisorption- Limitations

- Metal- adsorbate stoichiometry
- Types of adsorbed species- CO, linear & bridged form & dependence on experimental conditions-Pressure &Temp.
- $\text{Ni}=\text{C}=\text{O}$  (R=1)  (R=2)
- $\text{N}_2\text{O} + 2\text{Cu} \longrightarrow (\text{Cu})_2\text{O} + \text{N}_2$  (R=2)
- Weakly adsorbed Vs strongly adsorbed
- Hydrogen spill-over to the support
- SMSI effects- Lower adsn- size- Direct observation by TEM
- To be supported by TEM data
- Bi-metallic clusters/alloys- Specific methods to be developed

# Chemisorption stoichiometry – Variations- Experimental conditions need to be defined

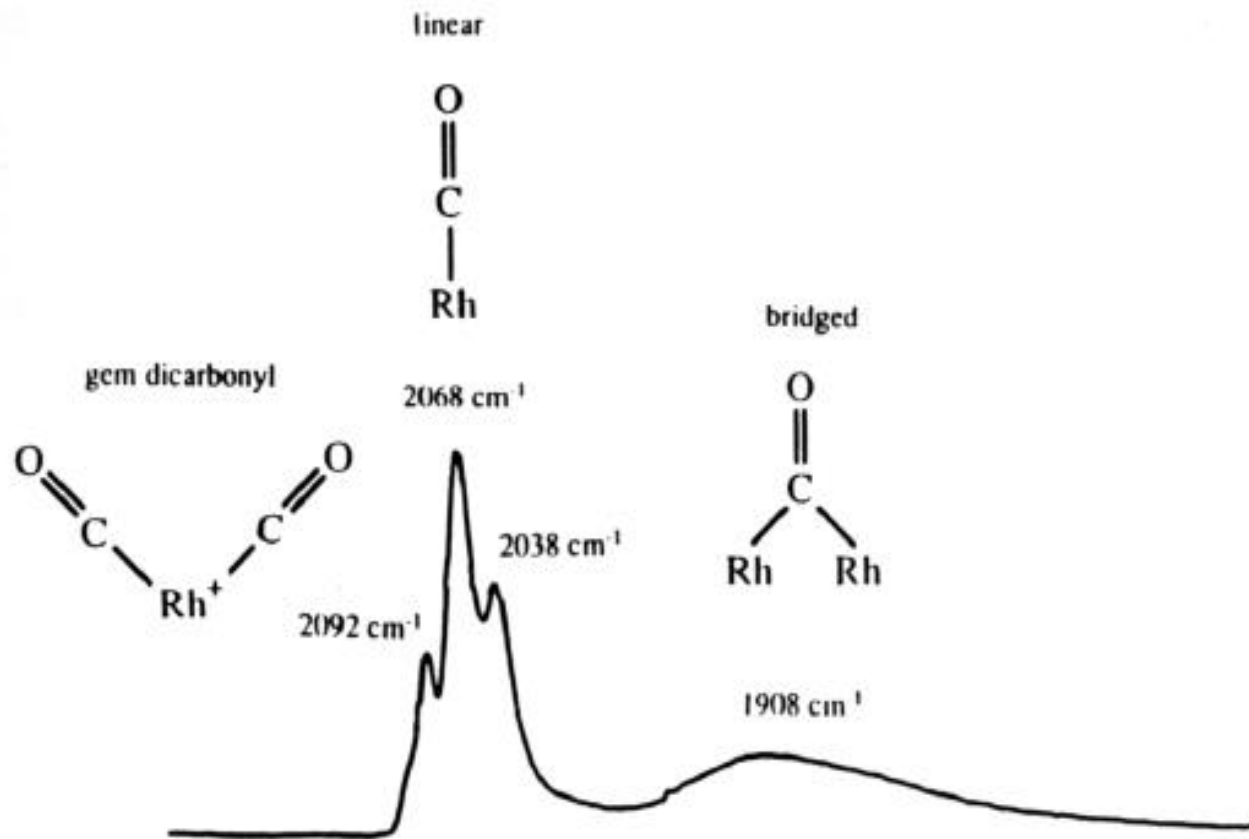


Fig.8. Transmission-absorption infrared spectrum of carbonyl species a  $\text{Rh}/\text{SiO}_2$  catalyst.

# Calculations

Metal surface area,  $S = (N_A \sigma / M) \times R$

$N_A$  Avogadro Number,  $\sigma$  –cross sectional area per metal atom in  $\text{\AA}^2$

$M$ - Mol. Weight of metal &  $R$ - ratio of adsorbate atoms adsorbed per metal atom

Crystallite size  $d = 5V/S = 5/(S \times \rho)$  where  $\rho$  –density of the metal &  $S$  metal area per gram

It is assumed that metal particle is a cube with 6 sides and one side/face rests on support and the remaining 5 faces exposed

Dispersion/Fraction of metal exposed =  $N_S / N_T$

$N_S$ - No.of metal atoms exposed as per the stoichiometry

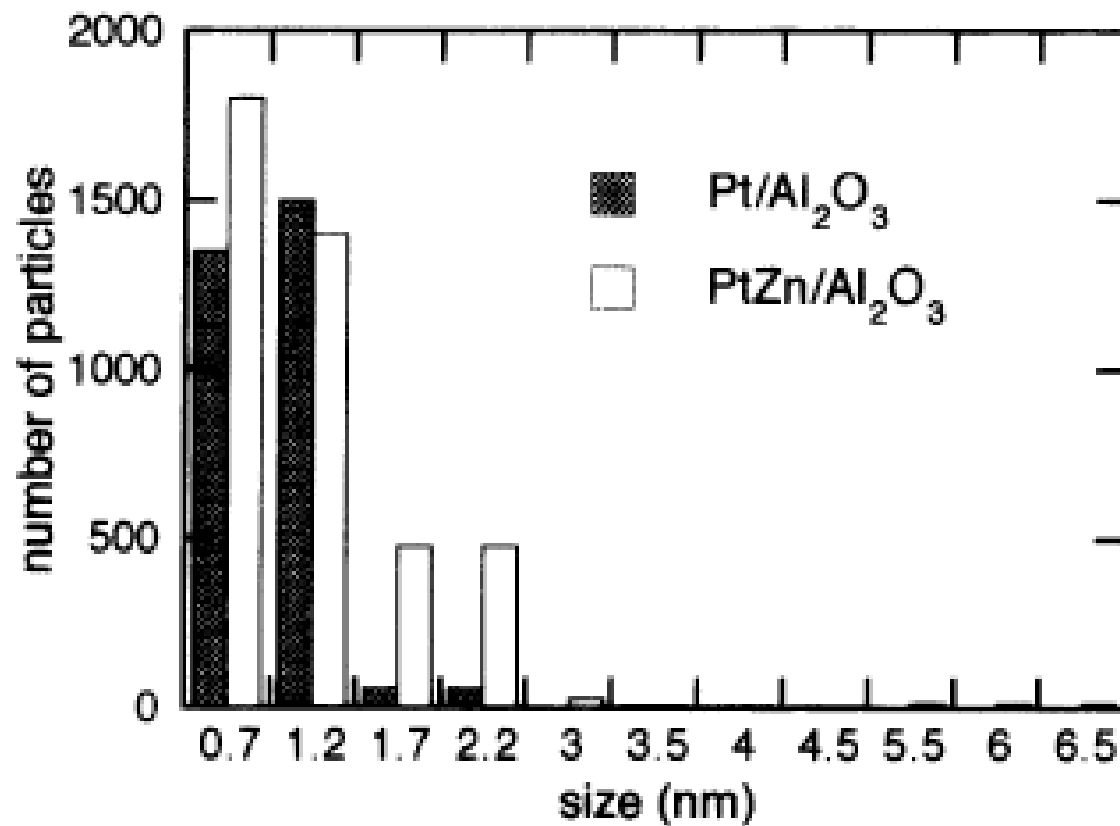
$N_T$ - No.of total metal atoms, as per loading

# Effect of promoter metals on Pt

Pt catalysts promoted by Re, Sn etc highly active and stable for catalytic reforming. Possible reasons are: (Pt-Sn, Pt-Re, Pt-Sn-Re)

- Increase the dispersion/activity of Pt- Geometric effect
- Form alloys and retard sintering of Pt
- Decrease the deep dehydrogenation capacity of Pt and thus decrease the formation of unsaturated coke precursors.
- They decrease the hydrogenolysis capacity and therefore also decrease the formation of light gases.
- They modify the concentration of surface hydrogen which has an effect on the relative production of different reaction intermediates and therefore on the final reaction selectivity.
- A portion of the additives remains oxidized on the surface and modifies the amount and strength of the acid sites of the support.

How do we measure the dispersion of bi- & trimetallic catalysts?



Distribution of particle sizes for a parent platinum catalyst and the same modified by addition of zinc.

*B. Coq, F. Figueras / Coordination Chemistry Reviews 178–180 (1998) 1753–1783*



# Pt-Re- Metal dispersion

- Pt adsorbs H<sub>2</sub> & O<sub>2</sub> reversibly
- Re does not adsorb H<sub>2</sub> ; but adsorbs O<sub>2</sub> irreversibly
- Saturate the surface with H<sub>2</sub> pulses
- Titrate with O<sub>2</sub>
- Go through next H<sub>2</sub> cycle- for Pt only
- 2 nd O<sub>2</sub> cycle- due to Pt only
- Difference in O<sub>2</sub> uptake is due to Re.
- Calculate dispersion of Pt & Re separately
- Total Oxygen uptake could be used for dispersion calculation

TABLE 2  
OXYGEN TITRATION OF Pt AND Re IN  
Pt-Re-Al<sub>2</sub>O<sub>3</sub> CATALYSTS AT 25°C<sup>a</sup>

	Re	0.0	0.1	0.3	0.6	1.0
Pt						
0.0				(0.06)	(0.24)	
0.1		0.06	0.03 (0.07)			
0.3		0.19	0.18 (0.12)	0.18 (0.20)	0.18 (0.39)	0.23 (0.39)
0.6		0.39			0.30 (0.47)	

JOURNAL OF CATALYSIS 29, 188-1~ (1973)

<sup>a</sup> Catalysts prepared by impregnation on  $\gamma$ -Al<sub>2</sub>O<sub>3</sub>. Metal contents in wt%. Titer values in ml STP/g catalyst. Titer values for Re are shown in brackets.

# Dispersion- bi metallics- Simple systems

TABLE 1  
SUMMARY OF BIMETALLIC CATALYSTS INVESTIGATED

Catalyst system <sup>a</sup>	Metal content wt%	Atomic ratio of metals	
		Cu/Ru	Cu/Os
Ru-Cu	1 Ru, 0 Cu	0	
	1 Ru, 0.126 Cu	0.20	
	1 Ru, 0.315 Cu	0.50	
	1 Ru, 0.63 Cu	1.00	
Os-Cu	1 Os, 0 Cu		0
	1 Os, 0.082 Cu		0.25
	1 Os, 0.166 Cu		0.50
	1 Os, 0.33 Cu		1.00

<sup>a</sup> All catalysts supported on silica.

# Dispersion- bi metallics- Simple systems

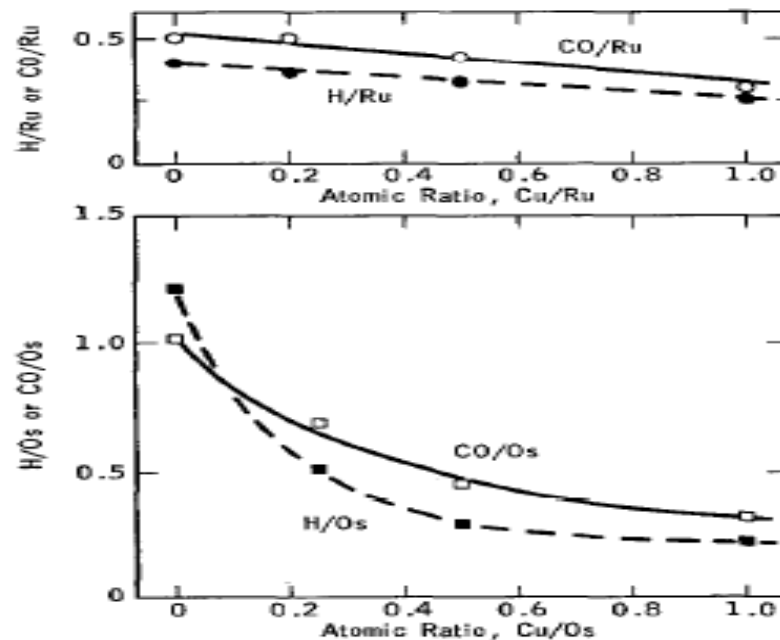


FIG. 2. The chemisorption of hydrogen and carbon monoxide at room temperature on silica-supported ruthenium-copper and osmium-copper catalysts. The catalysts all contain 1 wt% ruthenium or osmium, with varying amounts of copper. The adsorption data are expressed by the quantities  $H/Ru$ ,  $CO/Ru$ ,  $H/Os$ , and  $CO/Os$ , which refer respectively to the number of hydrogen atoms or carbon monoxide molecules chemisorbed per atom of ruthenium or osmium in the catalyst.

Expts on Cu/silica show that Cu does not adsorb  $H_2$  or CO

# Bimetallics- Chemisorption Vs Dispersion

Table 1

Fraction of Pt exposed to hydrogen (H/Pt) and mean metal particle size by TEM of some catalysts

Catalyst	H/Pt	Mean particle size (nm)
Pt	0.42	1.8
Pt-Re	0.19	1.5
Pt-Sn	0.00	1.8
Sn-Pt-Re	0.26	2.0
Re-Pt-Sn	0.08	1.9
Pt-Sn-Re	0.10	1.9
Pt-Re-Sn	0.21	2.0

# Bi & Tri metallic catalysts

## Dispersion measurements by hydrogen chemisorption

- Exhibit lower hydrogen uptakes, though , Pt crystallite sizes are smaller than Pt alone

## Possible reasons

- Alloy formation- electronic effect affecting the adsorption of H<sub>2</sub>
- Geometric effect- increasing dispersion- decreases no.of adjacent Pt atoms- essential for dissociative adsorption
  - Pt-Sn- H<sub>2</sub> uptake half of ethylene uptake
- Changes in electronic state of Pt<sup>0</sup> - Pt<sup>δ+</sup> or Pt<sup>δ-</sup> Both 2<sup>nd</sup> metal or support can change the electronic state of Pt
- Adsorption behavior of Re & Sn- Active for O<sub>2</sub> chemisorption, but not active for H<sub>2</sub>
- Do not get reduced completely
- Chemisorption data may not represent actual dispersion

# Metal dispersion- Bi & Tri metallics

Table 1

Chemisorption of CO and H<sub>2</sub> by a PVAI<sub>2</sub>O<sub>3</sub> catalyst subjected to different thermal treatments

Treatment	CO/Pt (dynamic method)	H <sub>2</sub> /Pt (static method)
None	54	52
600 °C, 2 h, air	40	44
600 °C, 6 h, air	10	11

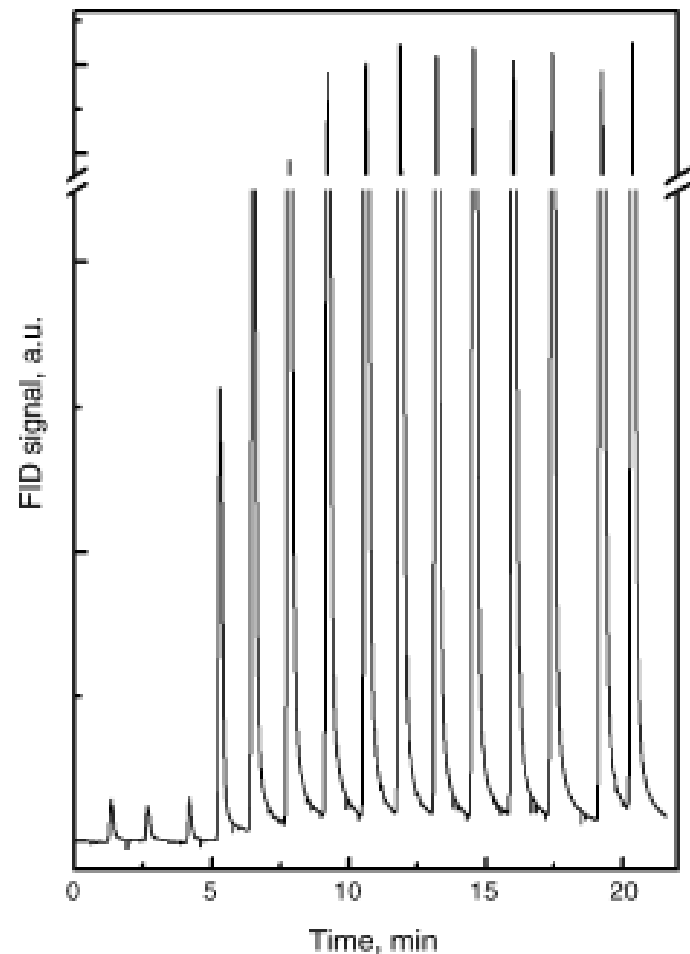


Fig. 2. CO chemisorption in the pulse chemisorption apparatus. FID signal evolution as a function of time (pulse number).



# Metal dispersion- Bi & Tri metallics

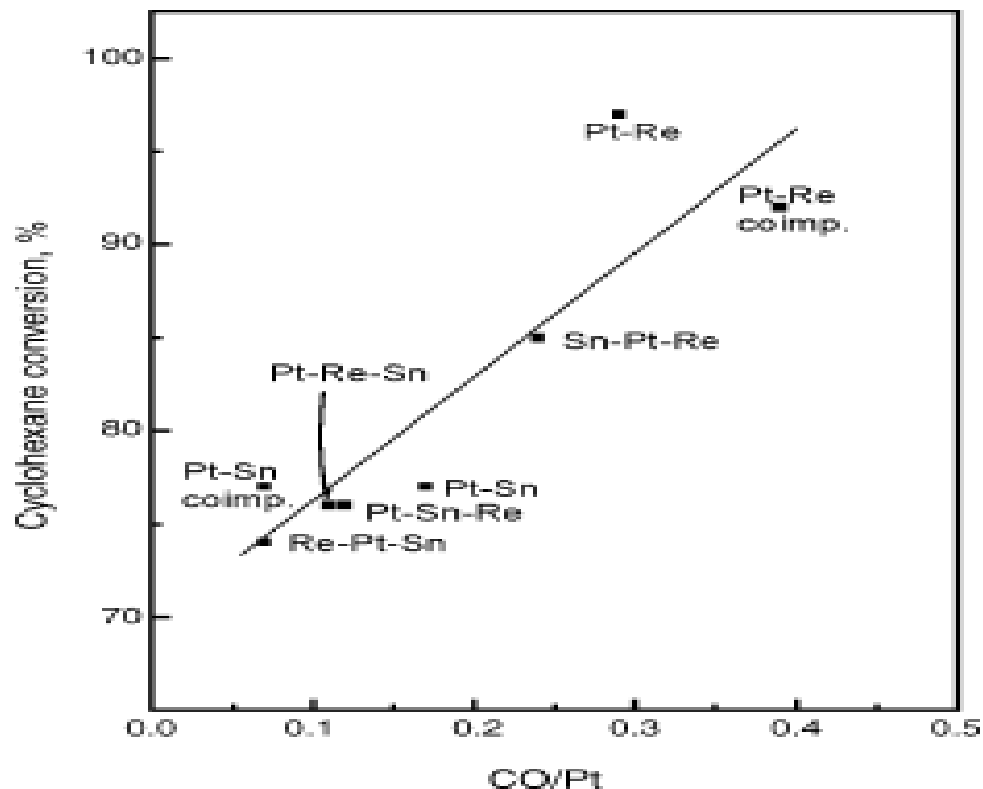
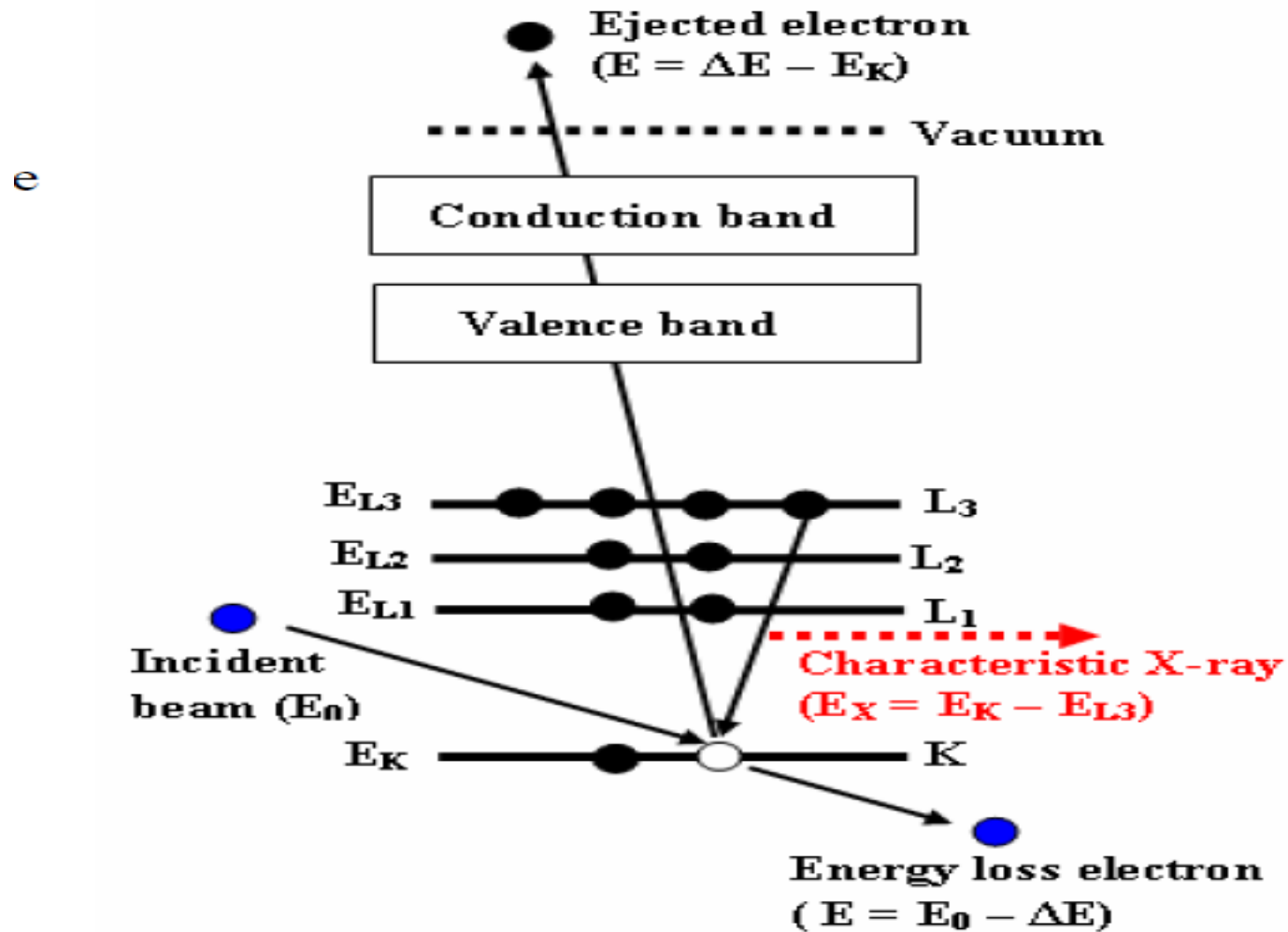


Fig. 3. Activity during dehydrogenation of cyclohexane as a function of the CO/Pt ratio. Stable conversion value all throughout the time span of the reaction. Regression coefficient,  $R^2 = 0.934$ . Coimp., catalysts prepared by coimpregnation of metal precursors; Suc., catalysts prepared by successive impregnations of metal precursors in the order indicated. Temperature = 400 °C, pressure = 0.1 Mpa,  $H_2/CH$  molar ratio = 30.

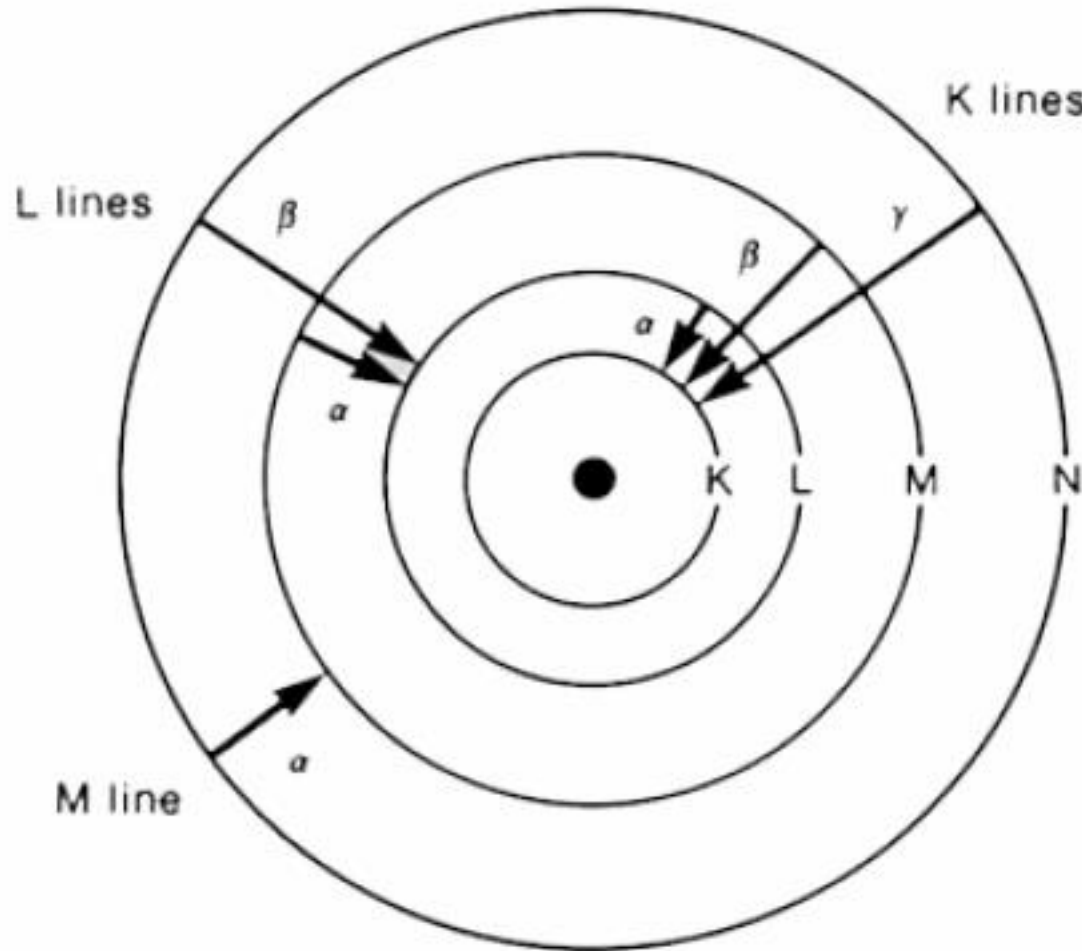
# Energy Dispersive X-ray Analysis-EDXA

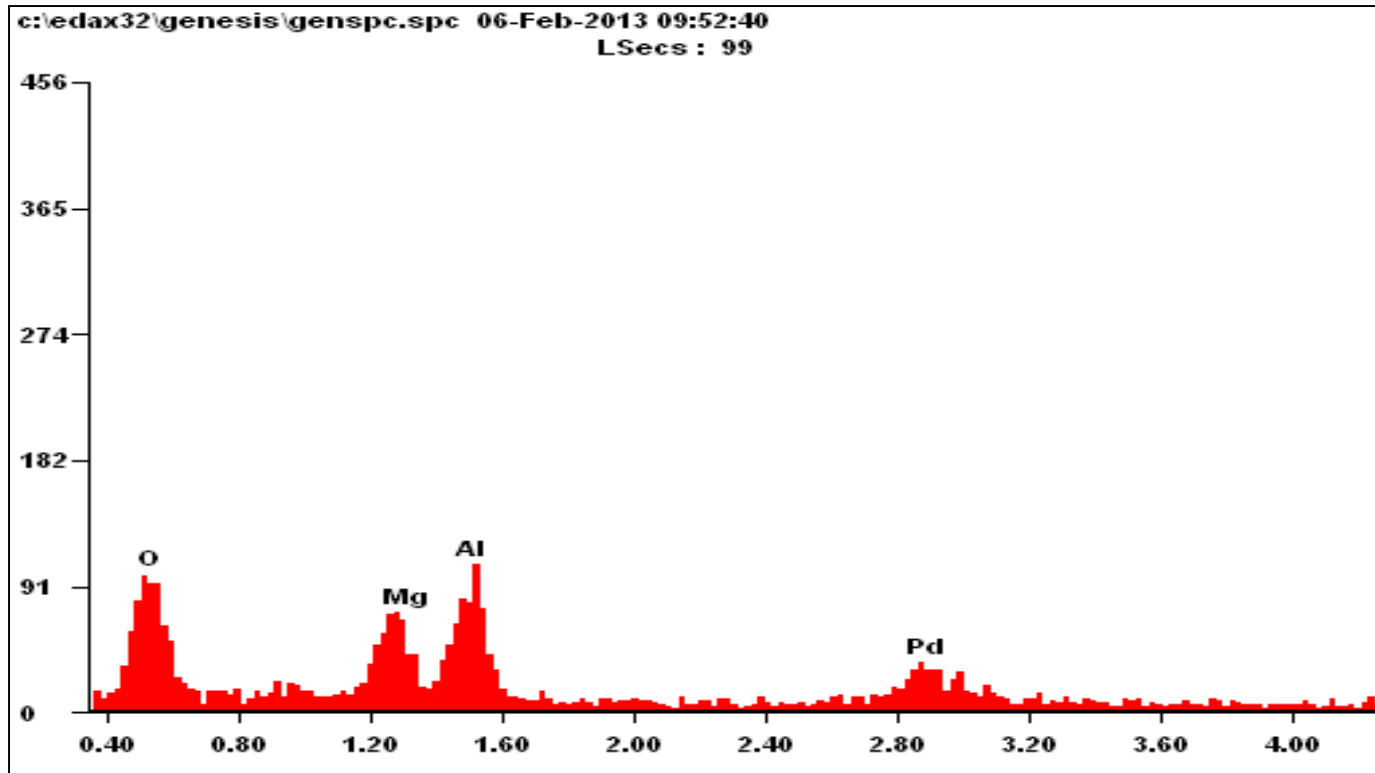
- Identification of elements based on their characteristic X-ray emission lines
- After due calibration concentration of elements can be measured
- EDXA is attached to SEM or TEM
- Qualitative as well as quantitative analysis can be done in a selected volume of  $1 \mu\text{m}^3$  of the sample
- Applications spread over several fields like metallurgy, materials and catalysis
- Applications in catalysis
  - Identification of impurities
  - Concentration profile of elements- preparation & manufacture
  - Characterization- fresh & spent catalysts – deactivation phenomenon

# Characteristic X-Rays



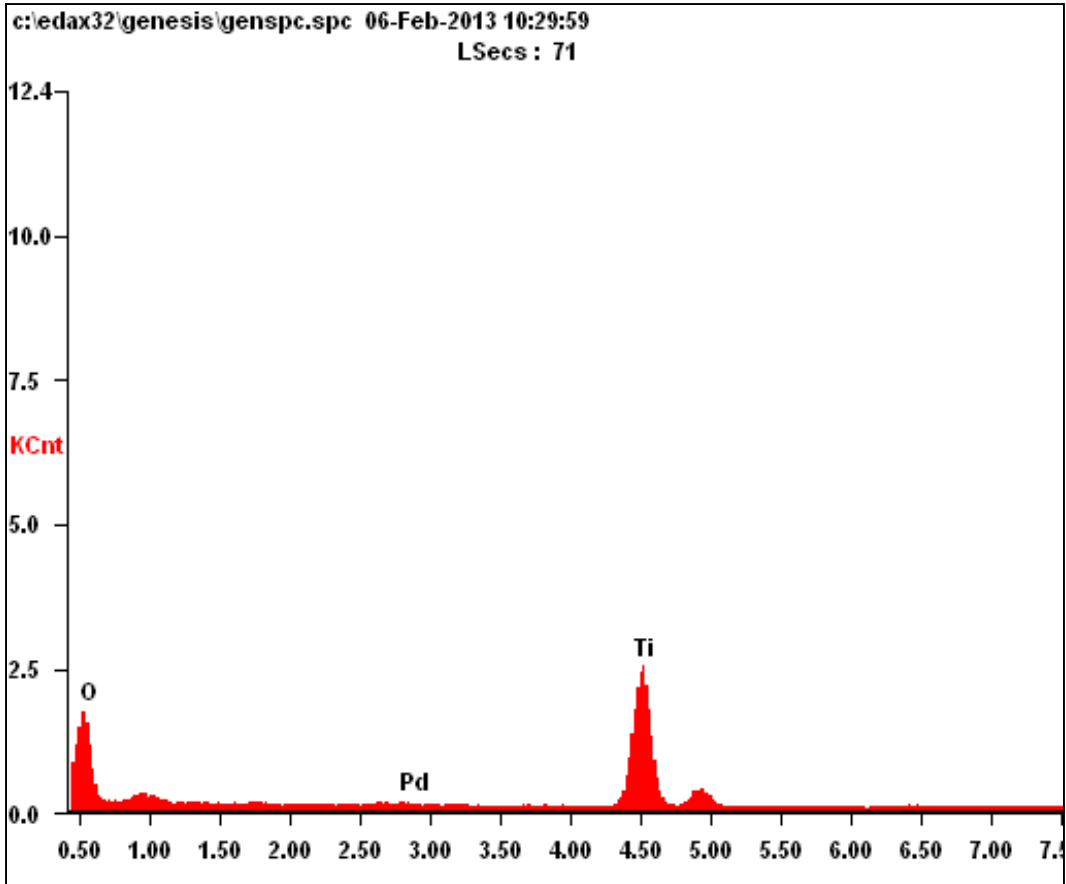
# Characteristic X-Ray lines





EDXA pattern for Pd-Mg-Al-O

<i>Elem</i>	<i>Weight %</i>	<i>Atomic %</i>
<i>O K</i>	20.90	36.80
<i>MgK</i>	26.50	30.80
<i>AlK</i>	23.80	24.80
<i>PdL</i>	28.90	07.70



EDAX pattern for Pd-TiO<sub>2</sub>

<i>Elem</i>	<i>Weight %</i>	<i>Atomic %</i>
<i>O K</i>	31.90	59.20
<i>PdL</i>	04.20	01.20
<i>TiK</i>	63.90	39.60



# Metal Impregnation- Concentration profile

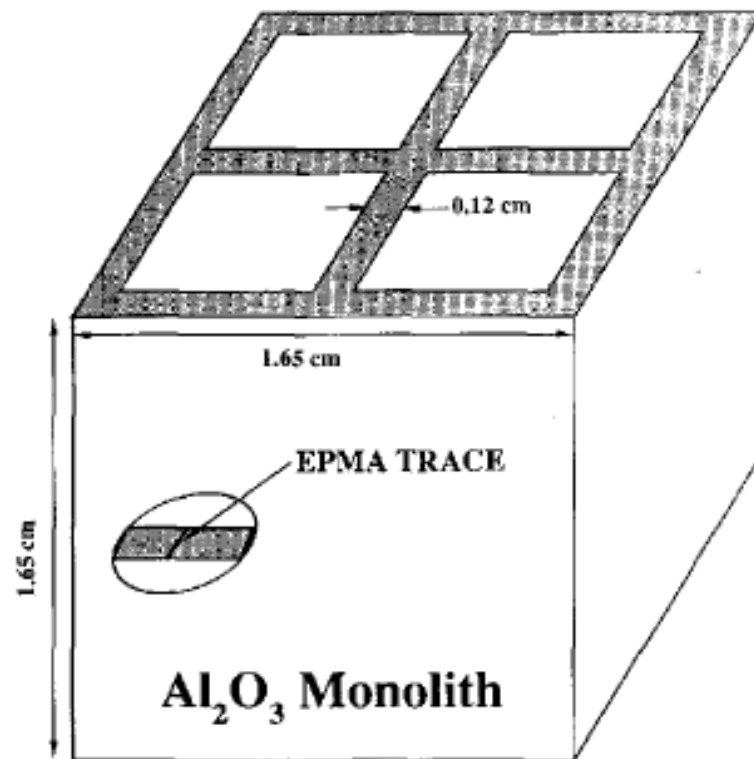
## Factors affecting the metal distribution

- (i) the method of impregnation- wet or dry,
- (ii) the duration of the impregnation,
- (iii) the nature of the precursor and support, , pH of impregn soln.  
precursor species in solution,  $\text{PtCl}_6^-$  or  $\text{Pt}(\text{NH}_3)_4^+$  - Alumina/Silica
- (iv) Added salts/acids as competing anions
- (v) the subsequent drying, calcination, and activation steps.

***Performance of the catalyst depends on the optimum distribution of active metal within the geometry of the support pellet***

### Concentration of impregnating solutions

Solution	Precursor conc. (mol/cm <sup>3</sup> )	HF conc. (mol/cm <sup>3</sup> )
1	$3.8 \cdot 10^{-5}$	0
2	$3.8 \cdot 10^{-5}$	$3.32 \cdot 10^{-3}$
3	$3.8 \cdot 10^{-5}$	$6.64 \cdot 10^{-3}$
4	$3.8 \cdot 10^{-5}$	$9.96 \cdot 10^{-3}$



JS Hepburn, Appl.Catal.55,271,1989;  
71,205,1991

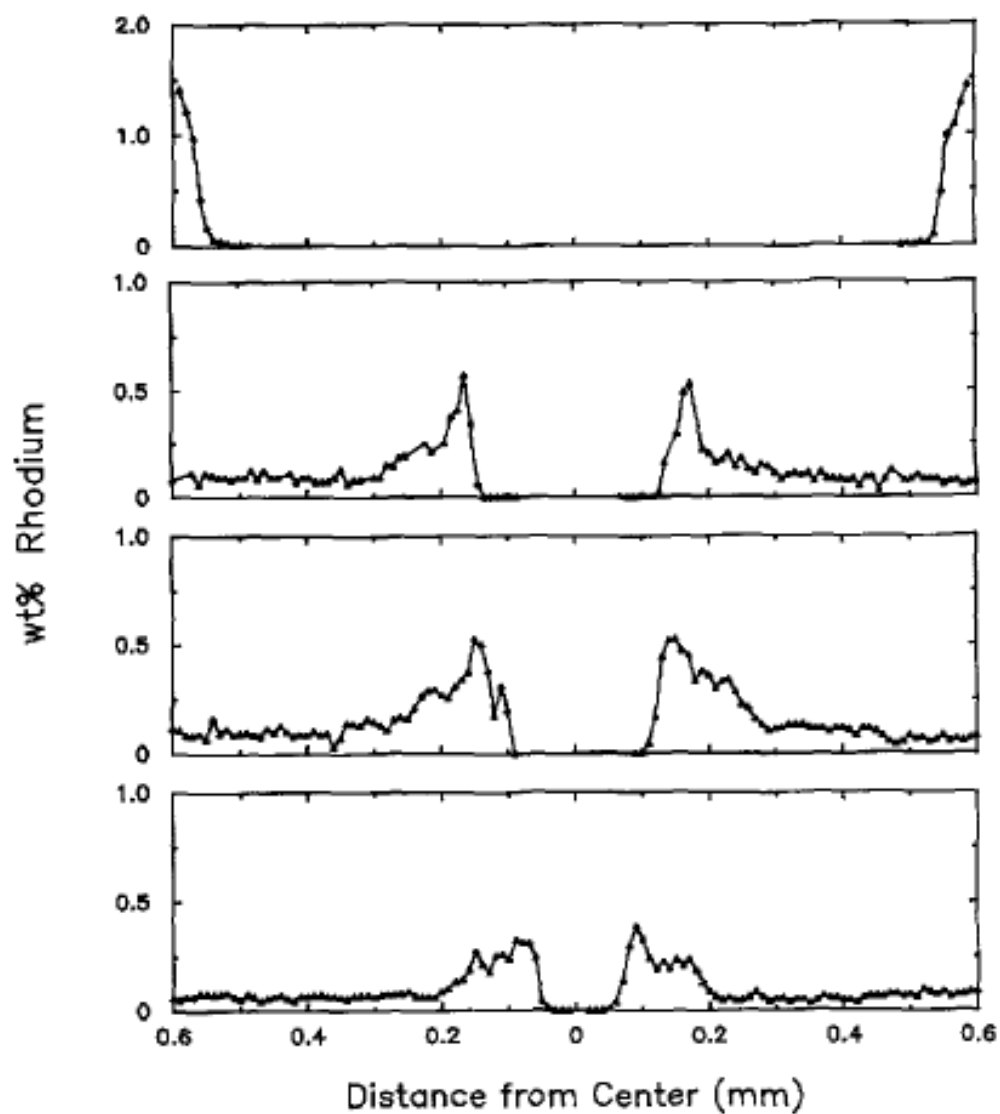


Fig. 4. Rhodium distributions. Top graph: solution 1, second graph: solution 2, third graph: solution 3, bottom graph: solution 4.

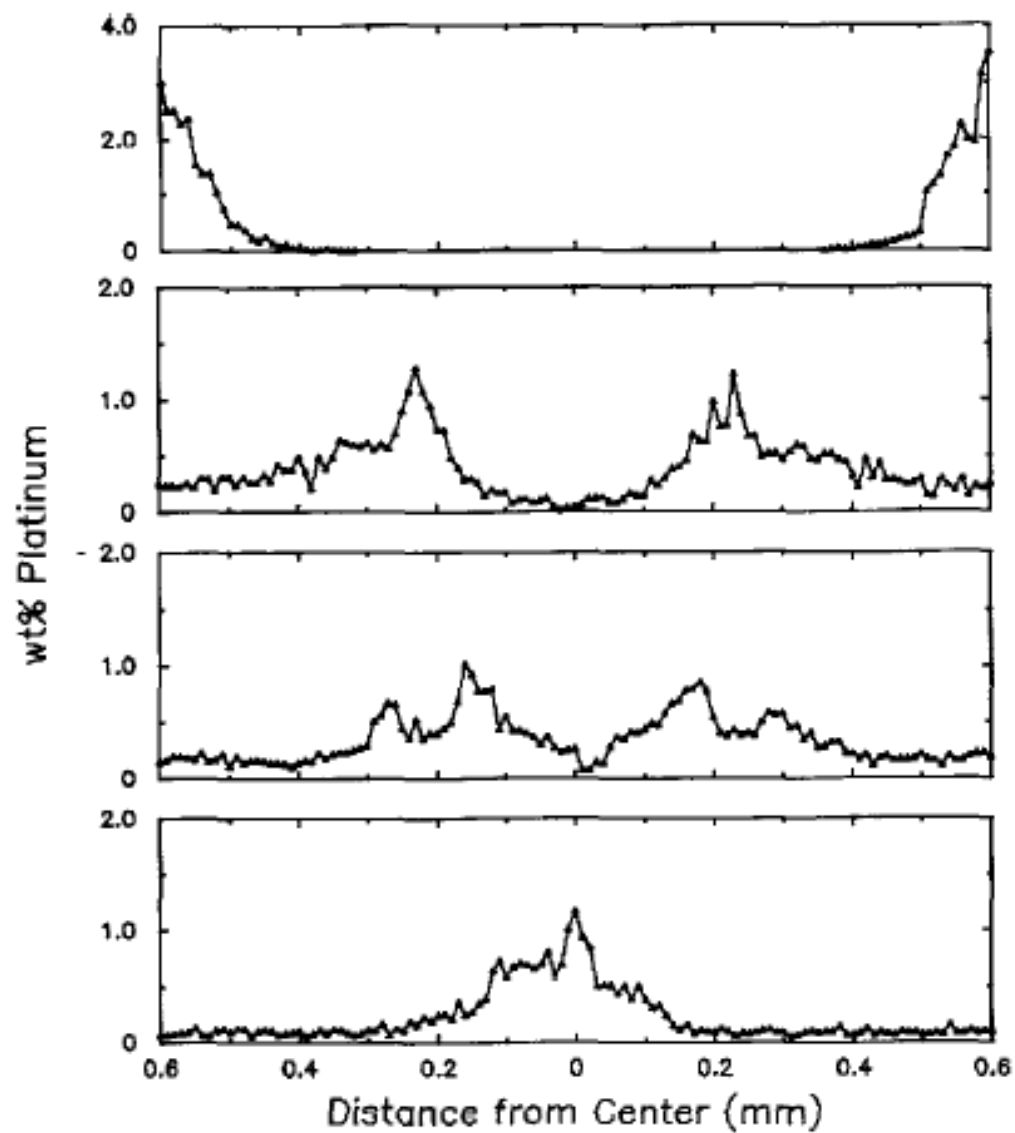


Fig. 5. Platinum distributions: Top graph: solution 1, second graph: solution 2, third graph: solution 3, bottom graph: solution 4.

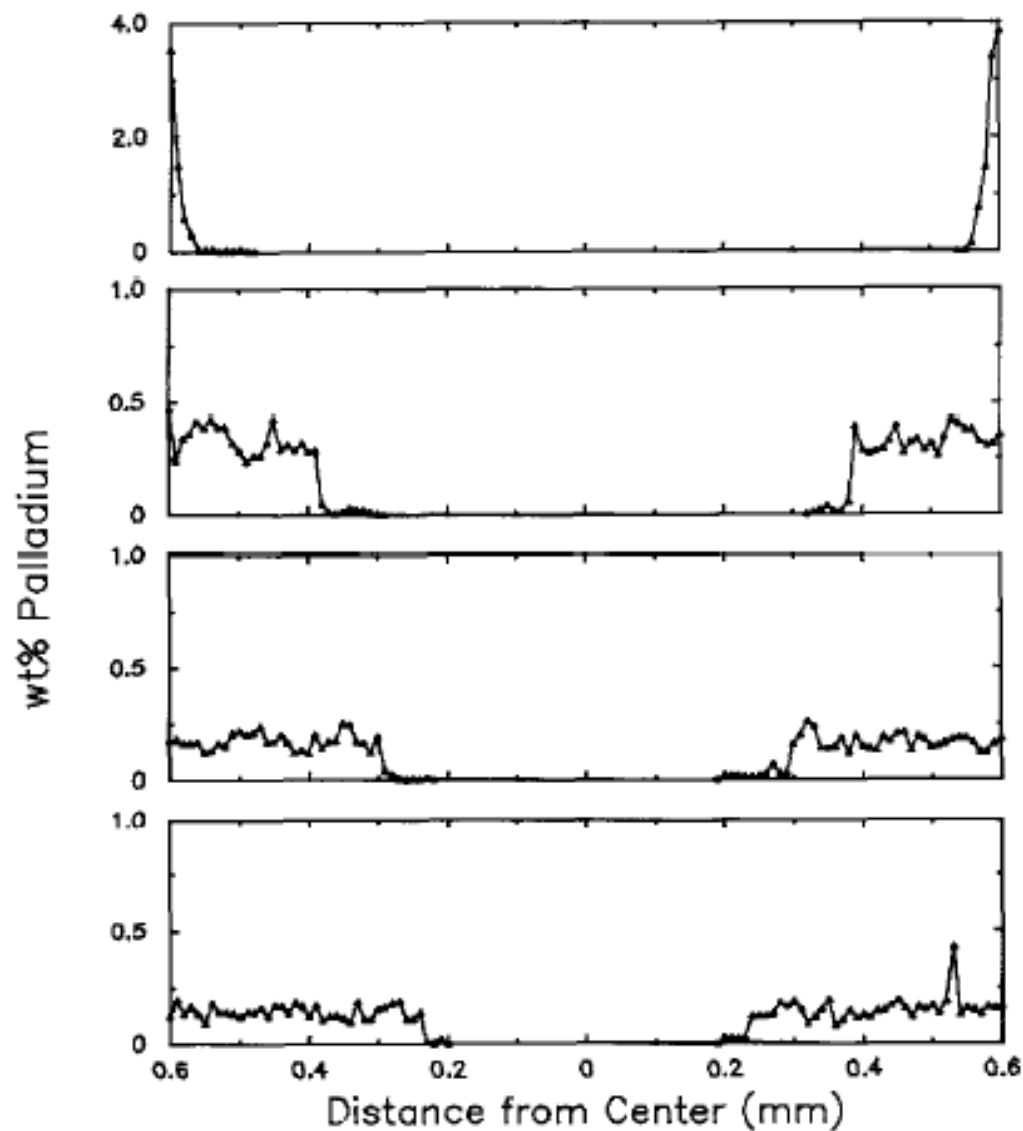


Fig. 6. Palladium distributions: Top graph: solution 1, second graph: solution 2, third graph: solution 3, bottom graph: solution 4.

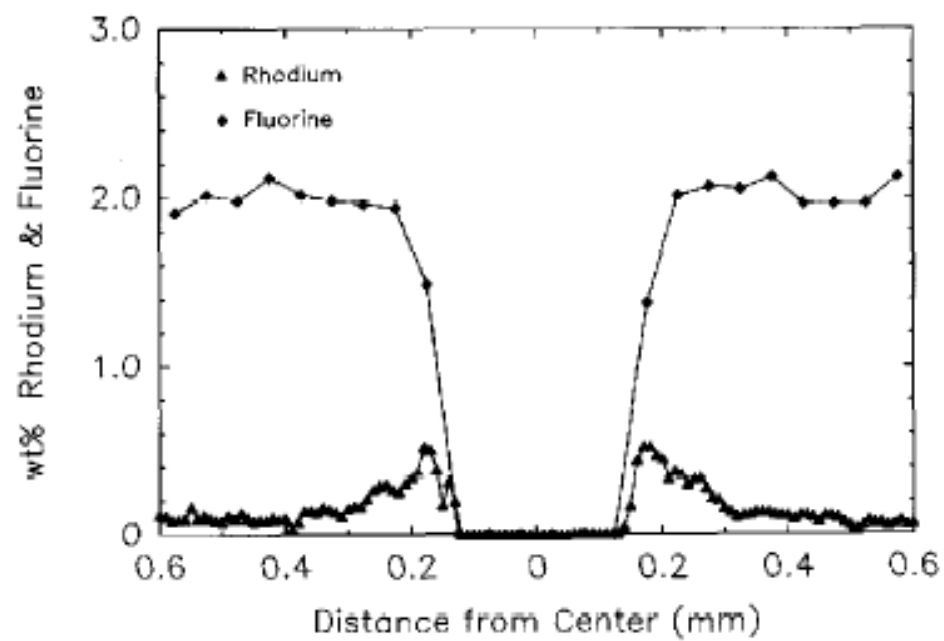
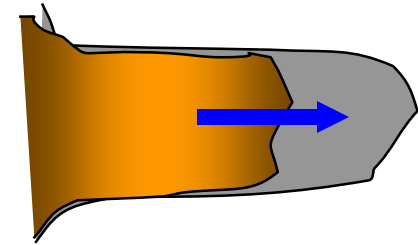


Fig. 7. Fluorine and rhodium distributions for solution 3.

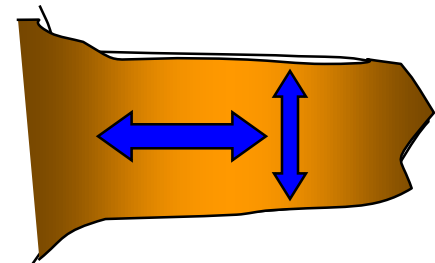


# Impregnation process

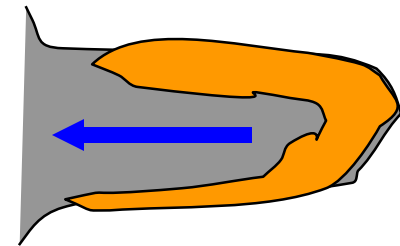
Solution flows  
Into the pores



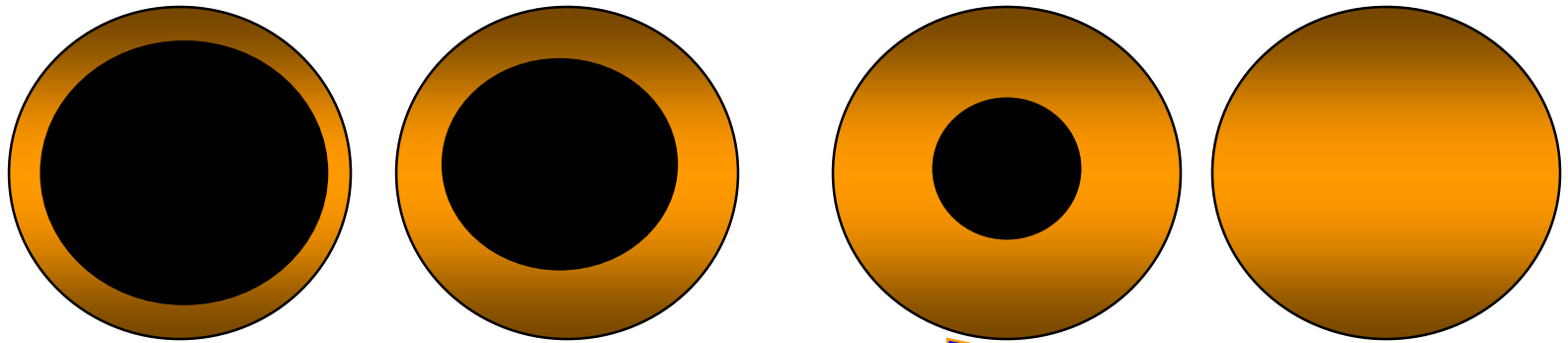
Adsorption  
Desorption  
Diffusion



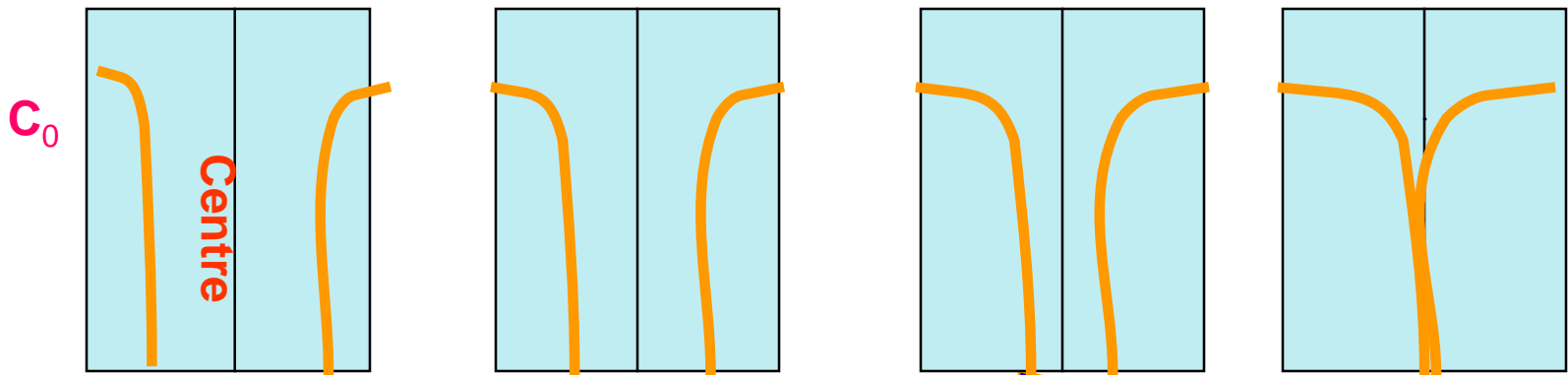
Evaporation



# Effect of Drying



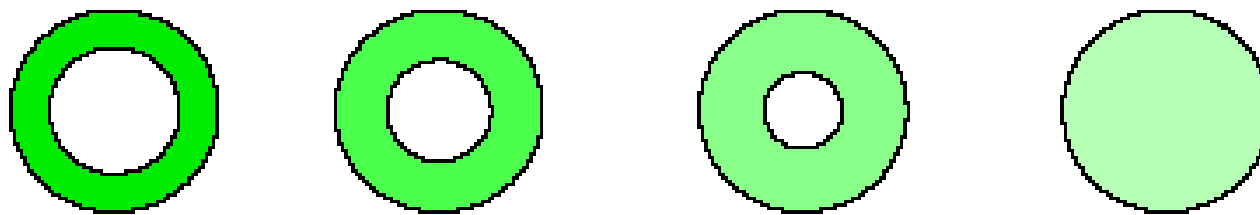
Drying time after impregnation



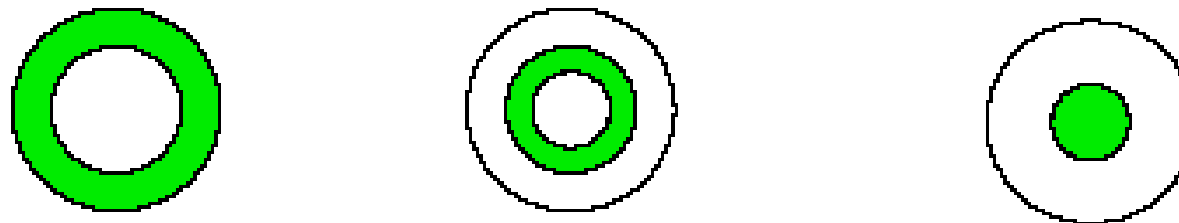
Concentration profile after Drying

# Active Phase Profiles

- Start from egg-shell catalyst Pt/Al<sub>2</sub>O<sub>3</sub> (from H<sub>2</sub>PtCl<sub>6</sub>)

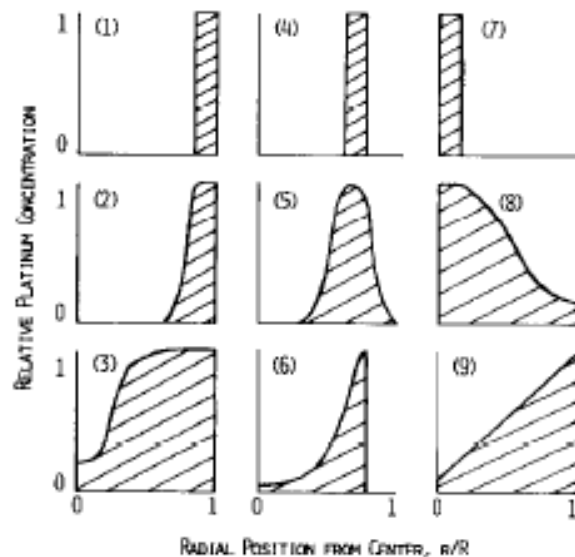


Increasing impregnation time



Increasing citric acid concentration

# Concentration profiles by EDXA



- Type 1—Outer shell, sharply defined
- Type 2—Outer shell, diffuse
- Type 3—Outer shell, diffuse to center
- Type 4—Inner shell, sharply defined
- Type 5—Inner shell, diffuse
- Type 6—Inner shell, diffuse to center
- Type 7—Core, sharply defined
- Type 8—Core, diffuse
- Type 9—Linearly increasing from center

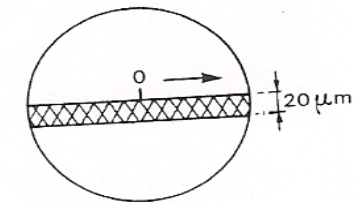
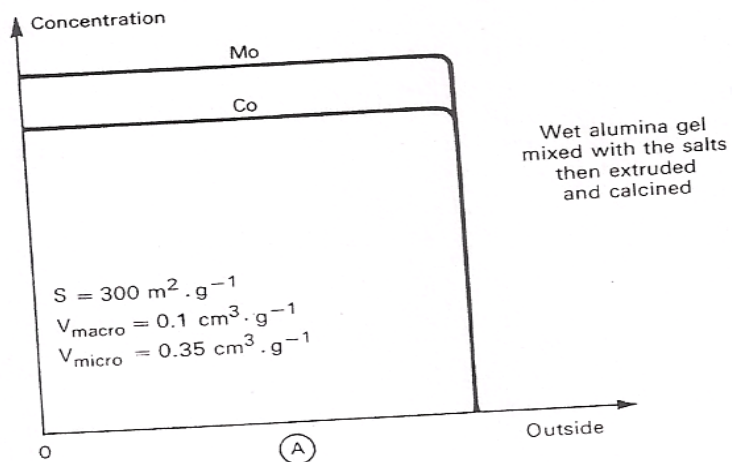
FIG. 4. Types of Pt profiles obtained in coimpregnation experiments.

# Concentration profiles by EDXA

TABLE 1  
Properties of Coimpregnated Catalysts

Acid or salt	Impregnation time, 1 hr					Impregnation time, 22 hr		
	Conc ( <i>M</i> )	Pt (wt%)	Pt band, <i>r/R</i>			Conc ( <i>M</i> )	Pt (wt%)	Pt band
			Begins at	Ends at	Type			
None	—	0.51	1	0.77	1	—	0.51	2
AlCl <sub>3</sub>	0.01	0.50	1	0.56	1	0.01	0.51	2
HCl	0.01	0.51	1	0.67	1	0.01	0.50	2
NaCl	0.01	0.49	1	0.81	1	0.01	0.51	2
HF	0.01	0.50	—	—	5	0.01	0.50	5
NaF	0.01	0.51	1	0.83	1	0.01	0.51	2
NaBr	0.01	0.50	1	0.77	1	0.01	0.50	9
HNO <sub>3</sub>	0.01	0.50	1	0.50	1	0.01	0.51	3
NaNO <sub>3</sub>	0.008	0.49	1	0.79	1	0.008	0.51	2
Na <sub>3</sub> PO <sub>4</sub> <sup>a</sup>	0.01	0.31	0.83	0	7	0.01	0.10	8
Na benzoate	0.01	0.48	1	0.78	1	0.01	0.50	2
Acetic acid	0.01	0.51	—	—	3	0.01	0.50	uniform
Citric acid	0.01	0.49	0.84	0.44	4	0.01	0.48	6
Na citrate <sup>a</sup>	0.02	0.19	0.33	0	7	0.01	0.14	8
Tartaric acid	0.01	0.49	—	—	6	0.01	0.51	7

<sup>a</sup> The 22-hr sample was prepared using a fresh solution of Na<sub>3</sub>PO<sub>4</sub> (or Na citrate) and H<sub>2</sub>PtCl<sub>6</sub> while the 1-hr sample was prepared using a portion of that same solution after it had been stored for 2 or 3 days.



Catalyst cross-section illustrating the path of the electron microprobe

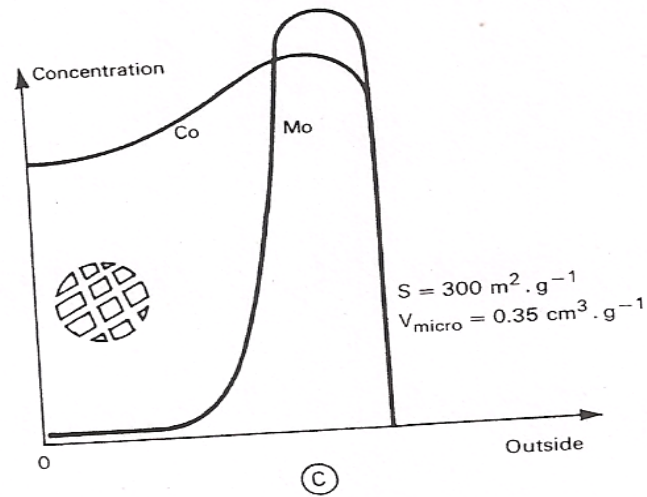
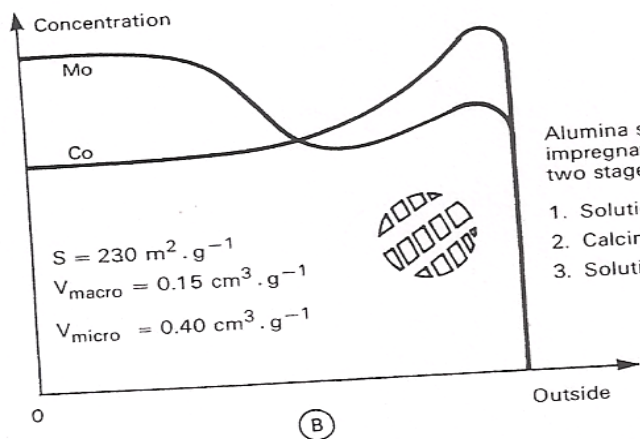
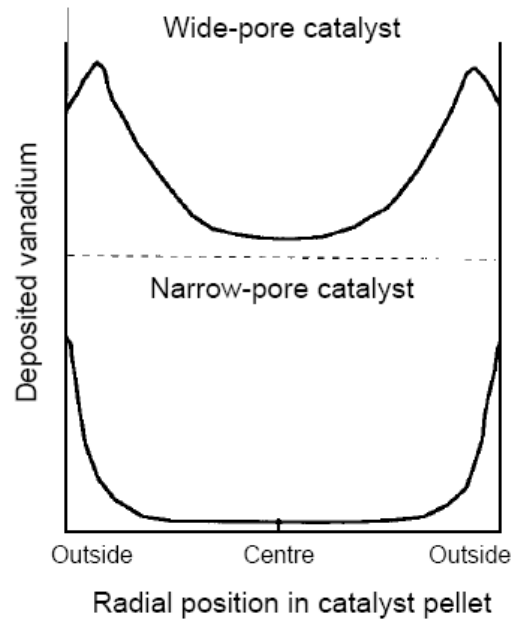


FIG. 7.23 Analysis of metal distribution from center to periphery in cobalt-molybdenum-alumina type catalysts.

(A) Homogeneous distribution such as is obtained by mixing salts with the wet gel before forming. (B) The distribution obtained by impregnating a catalyst with two pore systems,  $\varnothing < 15 \text{ nm}$  and  $\varnothing > 100 \text{ nm}$ . A fairly homogeneous distribution is obtained. (C) The distribution obtained by impregnating a microporous support (average  $\varnothing = 4.6 \text{ nm}$ ). The small diameter of the micropores and the absence of macropores block diffusion of the large highly adsorbed molybdate ion, and molybdenum is deposited in a layer at the exterior of the grain. (The curves for Mo and Co are drawn with different scales).

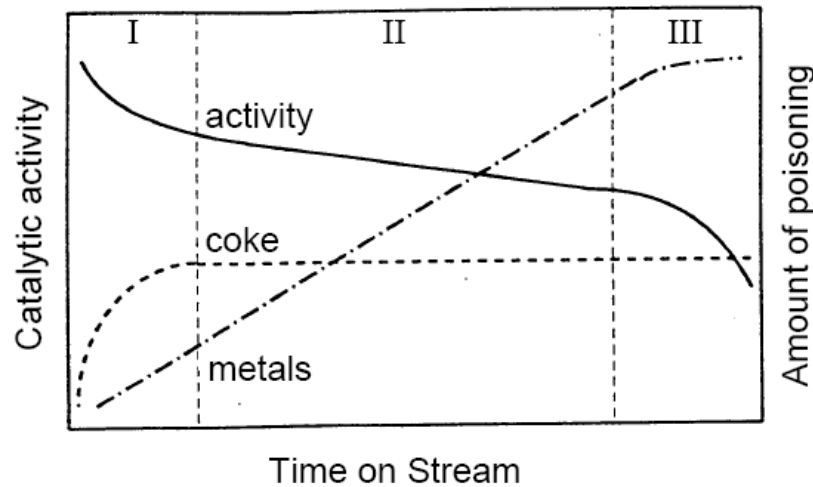
Jacquin, Y., Chenebaux, M. T., IFP unpublished results.

# Influence of Pore Size on Vanadium Deposition Hydrotreating of Heavy Feedstock





## Typical Stability Profiles in Hydrotreating



- Initially high rate of deactivation
  - mainly due to coke deposition
- Subsequently coke in equilibrium
  - metal deposition continues